DEVELOPMENT AND FUNCTIONS OF C-LOW-THRESHOLD MECHANORECEPTORS

DEVELOPMENT AND FUNCTIONS OF C-LOW-THRESHOLD MECHANORECEPTORS

A dissertation presented

by

Shan Lou

To

The Division of Medical Sciences

In partial fulfillment of the requirements

for the degree of

Doctor of Philosophy

In the subject of

Neuroscience

Harvard University

Cambridge, Massachusetts

April 2013

Abstract

Somatosensory neurons are essential for detecting diverse environmental stimuli, thus critical for survival of mammals. In order to achieve sensory modality specificity, many somatosensory subtypes emerge with various receptor and ion channel expression, as well as terminal morphologies. How the somatosensory system achieves such a high variety of neuronal subtypes is unknown. In this thesis, I used a newly discovered subtype, VGLUT3-expressing unmyelinated low-threshold mechanoreceptors (C-LTMRs), as a model to try to answer this question. C-LTMRs have been proposed to play a role in pleasant touch in humans or pain in mice. Previously, our lab has identified the Runt domain transcriptional factor Runx1 to be pivotal for the development of a cohort of sensory neurons such as pain related nociceptors, thermal receptors, as well as itch related pruriceptors. Here I found that Runx1 is also required to establish all known features associated with C-LTMRs. In search of the mechanism of how Runx1 controls C-LTMR development, I found that the zinc finger protein Zfp521 is predominantly expressed in C-LTMRs and its expression is Runx1 dependent. By generating and analyzing Zfp521 conditional knock out animals, I found Zfp521 is required for part of C-LTMR molecular identities and nerve terminal morphologies. Our studies suggest that Runx1 acts through Zfp521-dependent and Zfp521-independent pathways to specify C-LTMR identities. To study C-LTMR functions, we performed a series of behavioral analysis and found the loss of VGLUT3 and mechanosensitivities in C-LTMRs does not markedly affect acute or chronic mechanical pain measured from the hind paws, which argues against the proposed role of VGLUT3 in C-LTMRs in mediating mechanical

pain in mice. In the future, we will continue to use our mutant mice to study physiological functions of C-LTMRs.

Table of Contents

List of figures and tables

Number Page

Acknowledgments

I wish to express my sincere gratitude to Dr. Qiufu Ma and Dr. Bo Duan for their assistance in the preparation of this thesis. Dr. Ma has been dedicated in education and in sharing his wisdom with junior scientists. The projects depicted in this thesis will not happen without his generosity to provide the working environment, his wisdom and valuable advice.

We are very lucky to have the VGLUT3-Cre knock in mice from Dr. Brad Lowell from Beth Israel hospital, *Runx1* conditional knockout mice from Dr. Nancy Speck at University of Pennsylvania school of medicine, and Gary Gilliland at Brigham and Women's Hospital, and be able to use the electrophysiology recording facilities in professor David Corey's lab. In addition, special thanks to my DAC members, Rosalind Segal, Clifford Woolf and Jeff Macklis who sacrificed significant amount of their time to provide valuable information and advice to this project.

Thanks also to the members of the lab, Yang Liu, Fu-chia Yang, Omar Samad, Claudia Lopez, and Tari Tan, for teaching me the lab techniques when I first joined the lab, for their valuable inputs and help. I, too, enjoyed mentoring and teaching rising scientist. I need to thank my mentee Mulin Xiong for giving me the opportunity to bring her into the field of biological research. Special thanks to Zheng Wu from Catherine Dulac's lab for teaching me fluorescence *in situ* Hybridization, and my classmate collaborator Alex Wiltschko from program of neuroscience, who helped me to develop the animal behavior tracking software, which was not included in the thesis; Dr. Shu-Hsien Sheu from Children's Hospital, who did the confocal images of nerve

terminals mentioned in chapter III; Dr. Isaac Chiu from Children's Hospital, who taught me FACs sorting which is not included in this thesis; Dr. Michelle Ocana from department of neuroscience who helped with the confocal imaging facility and the Dana Farber FACs sorting facility.

I would not be able to finish my pursuit of PhD degree, if without my parents and grandparent, who have been extremely supportive and understanding. My sincere appreciation and admiration to my beloved fiancée, Oliver Holmes, for helping with nearly all of my manuscripts and being my source of joy.

Finally, endless thanks to Dr. Ma, who accepted me as a rotation student. He taught me how to do science and how to think about scientific problems. He is always extremely helpful and keeps himself available to the lab members. He showed great intelligence and diligence in the journey of pursuing academic excellence. His support carried me a long way in the sense of establishing collaborations and reaching out to the science community. He taught me that honesty is the most important character of a scientist. He once said, there is always something that you could learn from an experiment, whether successful or failed. He also said that a good scientist is the one who could see a forest while also able to paint a single tree in detail. Those are the lessons that I will find useful for my whole life.

Chapter I. Introduction

General introduction of somatosensory circuitry

The somatosensory system is essential for human beings in detecting the environment and making appropriate responses. The somatosensory system can only respond to a narrow range of sensory stimuli, called sensory modalities. The modalities can be generally divided into proprioception (sense of positioning), mechanoreception (touch, pressure, texture, *etc*.), nociception (pain, chemicals), thermal perception (temperature), and itch sensation. Each sensory modality has its own specific somatosensory pathways achieved by specialized receptors and circuitries.

Most somatic sensory neurons are located in the dorsal root ganglia (DRG) and the trigeminal ganglia (TG). DRG neurons are pseudo-unipolar neurons that have one neurite extending from the cell body which bifurcates into two neurites: one neurite is called the peripheral terminal and projects to the skin and other innervated organs (such as muscle, bone and internal organs *etc*.), and the other neurite is called the central terminal and projects to the dorsal horn of the spinal cord (Figure 1.1). This bipolar anatomical structure enables sensory neurons to receive the stimuli applied to sensory organs and transduce the action potentials generated by the sensors along the fibers and arrive at the central terminals in the spinal cord, which project to the secondary neurons.

The spinal cord is composed of neuron-enriched grey matter and neurite-enriched white matter. The grey matter in the spinal cord could be divided into 10 lamina. The nociceptors mainly project to the secondary neurons in the most superficial lamina including the marginal zone (Lamina I) and substantia gelatinosa (Lamina II). The second-order neurons send afferents contralaterally to the anterolateral column of the spinal cord. The fibers then segregate into three ascending pathways: the spinothalamic pathway goes to the ventral posterior lateral (VPL) nucleus of the brain thalamus, where it connects to third-order neurons. The spinaoreticular and spinomesencephalic pathways project to the third-order neurons in medulla and the pons, of which the third-order neurons further project to the thalamus or hypothalamus. Human brain imaging techniques show multiple places in the brain that respond to nociceptive stimuli, including primary somatosensory cortex (S1), secondary somatosensory cortex (S2), the insula, the anterior cingulate cortex (ACC), the amygdala, posterior parietal cortex (PPC), the prefrontal cortex (PFC), and supplementary motor area (SMA), all of which belong to the central network of transmission and procession of pain signals, called the pain matrix (Iannetti and Mouraux, 2010; Jones, 1998; May, 2009; Rainville et al., 1997; Talbot et al., 2008) (pathway shown in red line, Figure 1.1). The itch neurons project to medial lamina II and since it is a relatively newly discovered subtype, the projection in the central nervous system is not clear yet (Jessell, 2000; Nolte, 2002).

Mechanoreceptors in the lower thoracic, lumber and sacral levels partially project to the secondary neurons in Lamina III-IV of the spinal cord, but mostly ascend ipsilaterally and project to the gracile nucleus in the caudal medulla, while the secondary neurons that receive projections from mechanoreceptors locate in the upper thoracic and cervical levels project to the

cuneate nucleus. The secondary neurons cross contralaterally in the medulla from gracile or cuneate nuclei, forming medial lemniscus, and relaying to the thalamus; while the third-order neurons in the thalamus relay to S1, which is located in the postcentral gyrus of the parietal lobe, usually in area 3b and 1. The fourth-order neurons then project to S2 for information processing. Some of the neurons in S2 project to the insular cortex for tactile memory. The proprioceptors, which carry the information of joints and muscle, terminate in Lamina V-IX of the spinal cord, and share most of the pathways with the tactile sensory neurons.

The various sensory modalities that I mentioned earlier appear to be best explained by the population-coding model, in which most of the sensory afferents participate in corresponding circuitry (or labeled line), thus generating specific sensations, with the individual circuitries crosstalking with each other by connecting to interneurons. Since most of the sensory neurons are polymodal, an environmental stimulus can activate more than one labeled line. The specific sensation is achieved by the crosstalk and suppression. During pathological conditions, when the suppression is impaired, the normally suppressed lines can be unmasked, leading to allodynia and hyper-sensitizations (Ma, 2010, 2012).

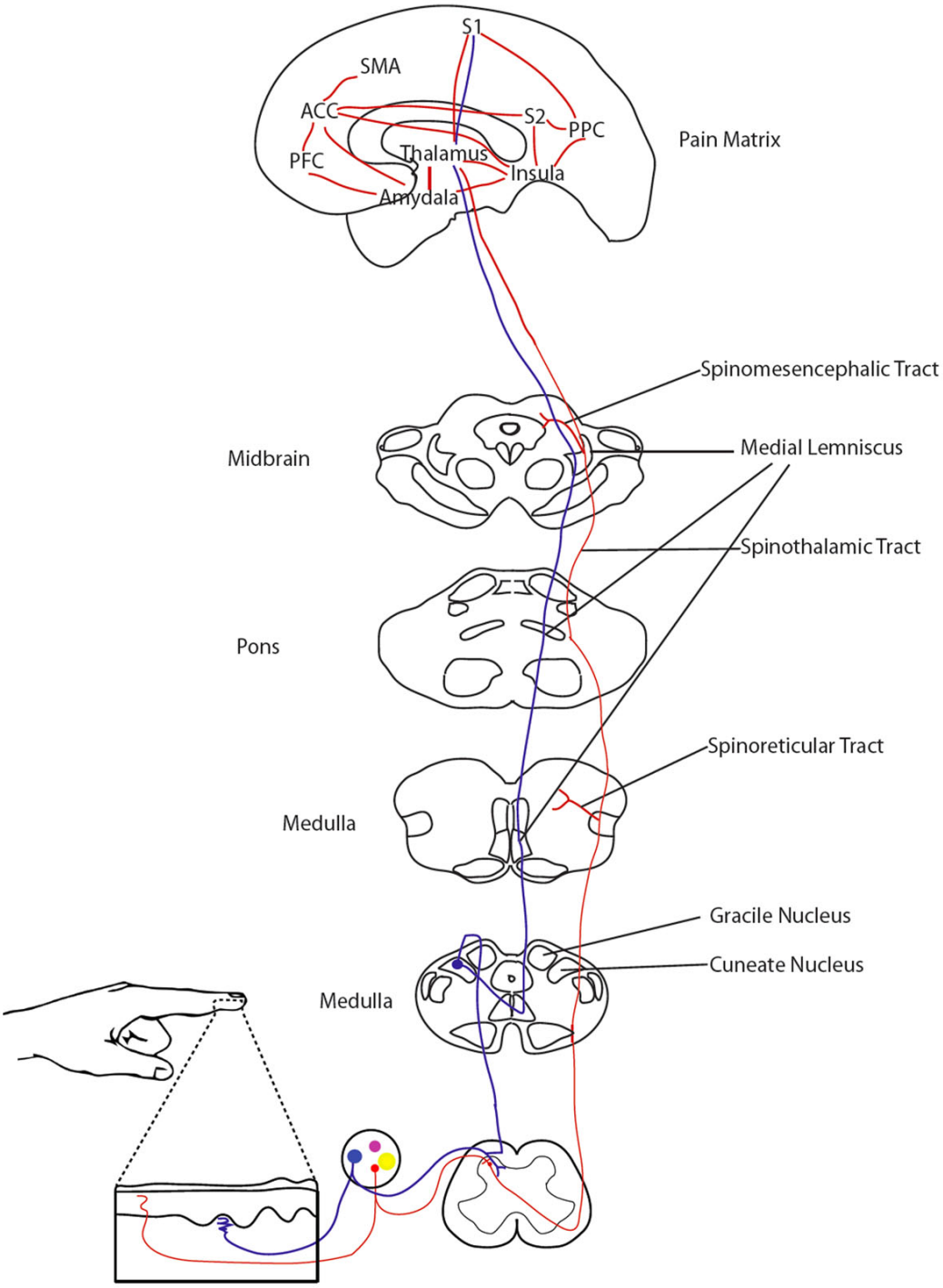

Figure 1.1 Somatosensory Circuitry

Categories of somatosensory neurons

To achieve the acuities of the sensory modalities, there are various subtypes of somatosensory neurons that have different molecular markers (such as peptides and ion channels), various fiber transmission speeds, and distinct target innervations. As a consequence, there are also different ways to categorize them.

According to their diameters and transmission speeds, there are four afferent fibers types: 1) A-alpha (Aα), thickly myelinated fibers that are 12-20μm in diameter, conducting signals at a speed of 72-120m/s; 2) A-beta (Aβ), medium myelinated fibers that are 6-12μm in diameter, conducting at 36-72m/s; 3) A-delta (Aδ), thinly myelinated fibers, that are 1-6μm in diameter, conducting at 4-36m/s; 4) C, unmyelinated fibers, with a diameter of 0.2-1.5 μm and conducting at 0.4-2.0m/s. The sizes of the neurons are controlled by neurofilaments, which are 10 nm intermediate filaments found specifically in the neurons. The large size DRG neurons are usually correlated to heavy neurofilament (NF-H, 200-220 KDa) that could be labeled by NF200 antibodies. The $NF200^+$ DRG neurons also express axon-myelin interaction protein Ncl-1, thus they are more likely to be myelinated. The small diameter neurons can usually be labeled by peripherin (Cojen Ho, 2011; Spiegel I, 2007). The Aα and Aβ nerve fibers are both $NF200^+$ and are wrapped by $S100^+$ Schwann cells; while Aδ fibers are rarely $NF200^+$ but $S100^+$ myelination is still visible in the neurites. Finally, C fibers are both S100 and NF200 negative. The myelination patterns and speed of signal transmission are closely correlated. Generally the heavier the myelination is, the bigger the cells are and the faster the transmission will be. Most of the proprioceptors are large in diameter and thickly myelinated Aα fibers, but also include Aβ

and Aδ fibers. Most of the mechanoreceptors are also myelinated fibers (with Aα, Aβ or Aδ fibers), with the exception of C-tactile low threshold mechanoreceptors (C-LTMRs) that I will discuss in this thesis. Nociceptors and thermo receptors are usually small in cell body and are mostly thinly and unmyelinated fiber neurons (Aδ and C). Itch sensitive neurons are mostly C fibers (Han et al., 2012; Liu et al., 2009).

According to the adaptation patterns, DRG neurons could be arbitrarily divided into rapidly adapting neurons (RAM) that have τ (half time current reduction) ≤ 10ms in response to constant stimuli, intermediate adapting neurons that have τ between 10ms and 20ms, and slowly adapting neurons (SAM) that exceed 20ms (Smith and Lewin, 2009).

Morphologically, proprioceptors are mostly distinct in their nerve innervation compares to other sensory neuron types. Proprioceptors innervate the muscle spindles to signal the muscle stretch and Golgi tendon organs to signal muscle tensions. Mechanoreceptors enjoy the largest varieties of nerve terminal morphologies and mostly innervate the skin. Nociceptors, itch receptors and thermal receptors also innervate the skin as well as internal organs, such as colon, bladder and muscles *etc*.

Mechanoreceptor subtypes

The categorization of mechanoreceptors is usually dependent on their specialized sensory terminal organs located in the skin. The skin is the biggest sensory organ in human body and could be divided into two general areas: hairy skin (that is covered by hair follicles) and glabrous

skin (with rare hair follicles). These two skin areas not only differ by the hair coverage, but also differ by types of nerve endings, which might be the mechanisms for distinct mechanical sensitivities (Hamalainen et al., 1985; Kakuda, 1992; Verrillo and Bolanowski, 1986).

Mechanoreceptors in the hairy skin include Merkel cell complexs, circumferential, and longitudinal hair follicle innervations. In the glabrous skin, there are slightly more dispersed Merkel cell complexes, Meissner's corpuscles, and occasionally, the dermal papillae epidermis (DPE), which is an ending that forms free nerve endings in the beginning, but changes to varicosities at the end of the nerve penetration entering the thick glabrous skin (Ridley, 1969). In the deep dermis of both hairy and glabrous skin, there are pacinian corpuscles as well as Ruffini's endings. (Figure 1.2. nerve terminals)(Lallemend and Ernfors, 2012).

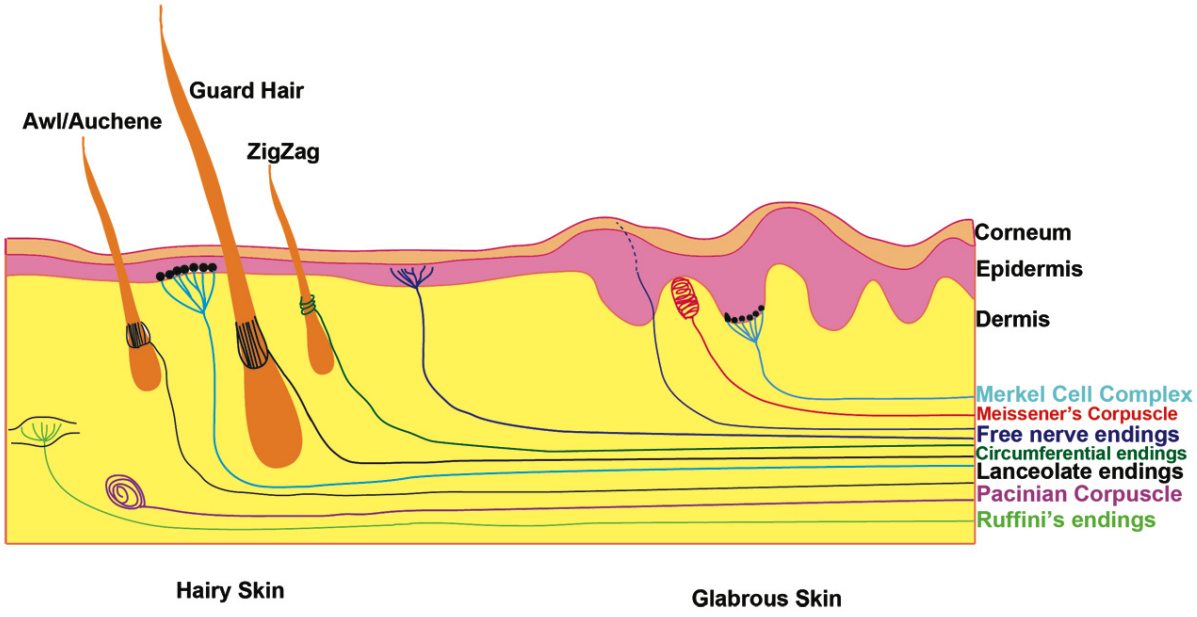

Figure 1.2 Sensory neuron innervations in the skin

Merkel cells (or Merkel disks) are located on the border between epidermis and dermis, with their cell bodies in the epidermal side (Figure 1.2 Light blue). In the superficial hairy skin, Merkel cells form a cluster of 30-70 Merkel cells, which is also called a touch dome. In the centers of glabrous skin papillary ridges, Merkel cells form a much smaller Merkel cell complex, with only 1-20 cells. Merkel cells are derived from epidermal lineage and their development is Atoh1 (Math1) dependent just like hair cells in the auditory system (Morrison and Maricich, 2009). It was also found that transcriptional factor Pax6 can regulate Merkel cell maturation (Parisi and Collinson, 2012). The Merkel cells are mechanically sensitive and are excitable cells. Innervation of Merkel cells happen at birth, much later than the formation of touch domes (Vielkind et al., 2010). Merkel cell complexes are innervated mainly by Aα and Aβ fibers. Electrophysiological recordings show that they belong to slow-adapting type I (SAI) subtype with small receptive fields (Haeberle and Lumpkin, 2004; Maricich et al., 2012; Maricich et al., 2009; Nunzi, 2004). It is suggested that Merkel cells could be activated mechanically and release ATP, glutamate or neuropeptide to activate the sensory nerves innervating them (Haeberle and Lumpkin, 2004). The loss of Merkel cells led to impairment of light touch in Atoh1 conditional knock out mice (Maricich et al., 2009). It is noticeable that there are some other specialized skin cells such as keratinocytes, melanocytes and Langerhans cells, which express sensor protein, neuropeptides and could activate surrounding nerve endings (Boulais and Misery, 2008). However it will not be discussed in detail in this thesis.

Meissner corpuscles are mainly found in the glabrous skin in mammals (Fig 1.2, red). They have a globular, fluid filled structure that encloses a stack of flattened epithelial cells, with the sensory nerve terminals entwined between the various layers of the corpuscles (Takahashi-

Iwanaga and Shimoda, 2004). Meissner corpuscles are innervated mainly by Aβ fibers and are RA-LTMRs (Gonzalez-Martinez et al., 2005; Gonzalez-Martinez et al., 2004; Kandel, 2006; Takahashi-Iwanaga and Shimoda, 2004). Functionally, they are coupled mechanically to the edge of the papillary ridge in primates and respond to grip and shape detection in humans (Westling and Johansson, 1987).

Pacinian corpuscles are located in the deep dermis (Fig 1.2, purple). They are abundant in human palms and fingers but cluster in periosteum (the membrane in the outer surface of the bones) in rodents (Zelená, 1976). Structurally, pacinian corpuscles have connective tissues called lamellae that surround the nerve endings. The large capsules flexibly attach to the skin, allowing the receptor to sense vibration occurring centimeters away. The deformation of the lamellar end organs initiates axon firing. Like Meissner corpuscles, pacinian corpuscles are also innervated by RA-LTMRs, but with large receptive fields instead of small receptive fields. They respond to rapid indentation of skin (but not to steady pressure) and are activated selectively by vibration generated by the common neurologist's test of holding a tuning fork (20-30hz) to the skin (Bell et al., 1994; Loewenstein and Mendelson, 1965).

Ruffini's endings are also found deep in the dermis (Fig1.2, light green). They link the subcutaneous tissues to folds in the skin at the joints and in the palm or to the finger nails (El-oteify and Mubarak, 2011). Ruffini's endings are innervated by SAII-LTMRs, and sense skin stretch or bending of the finger nails as they compress the nerve endings. The mechanical information sensed by Ruffini endings contributes to our perception of the shape of the grasped objects (Vallbo et al., 1999; Westling and Johansson, 1987).

The hair follicles in rodents can be divided into three types depending on the hair morphology: 1) Guard hairs compose 1% of all hairs, are the longest of all types and usually associated with touch domes; 2) awl/auchene hairs are shorter and contains several rows of medulla cells and constitute 23% of all hairs; 3) Zigzag hairs are the most abundant (76%) and have only a single row of medulla cells (Driskell et al., 2009). The hair follicles are developed from the thickening of the epithelial skin, at the embryonic day 14.5 (E14.5). The epithelial cells develop into dermal papilla (DP), which instruct the surrounding epithelial cells to proliferate and differentiate into hair shaft and inner root sheath (Driskell et al., 2011). The three different hair follicles develop at different stages: guard hairs develop the earliest around E14.5; Awl/Auchene hairs develop at E16.5; Zigzag hairs initiates development around E18.5 (Schlake, 2007). Noticeably, the sensory neuron innervation of the hair cells happens around the same time as the hair follicle development initiates (Chang and Nathans, 2013). In mice, loss of function in *Frizzled (Fz)6* or *Celsr1*, or the semidominant Loop-tail gain-of function in *Vangl2*, leads to aberrant hair follicle orientations. *Fz6* has been found to also affect the morphologies of the hair follicle sensory neuron innervations by changing the hair follicle orientations perinatally(Chang and Nathans, 2013). It is worth noting that a re-orientation happens during the first 3 postnatal weeks, which is not Fz6 dependent and can override the consequences of loss of *Fz6* in the perinatal stages (Chang and Nathans, 2013). Recently it was found that all three types of hair are innervated by lanceolate endings as well as circumferential endings (Fig 1.2 black and dark green). Guard hair lanceolate endings are mainly Aβ fibers that are RA-LTMR; Awl/auchene hairs are innervated by Aβ, Aδ and C fibers; and zigzag hairs are innervated by Aδ and C fibers (Li et al., 2011). Meanwhile, it was also found that some hair follicles are innervated by circular

endings, such as MrgB4$^+$ nerve endings and occasionally high threshold polymodal nociceptor MrgD$^+$ nerve endings (Liu et al., 2007; Zylka and Anderson, 2004).

There are also mechanoreceptors that form free nerve endings in the epidermis. However, not many myelinated conventional mechanoreceptors have been found to form free nerve endings in epidermis, instead they are mostly unmyelinated C-LTMRs (Fig 1.2, dark blue).

The molecular identities for each mechanosensory neuron subtypes was still unclear, despite some recent progress in identifying mechanosensory specific molecular markers. For example, TrkB has been used to label Aδ fibers lanceolate endings innervating the hair follicles; C-LTMRs with VGLUT3/TH expression specifically mark the lanceolate endings innervating the zigzag and Awl/Auchene hairs. And finally, the early wave of Ret$^+$/GFRα2$^+$ neurons could also mark Meissner corpuscles and pacinian corpuscles. The clear molecular identities for various mechanoreceptor subtypes will be helpful for further developmental and functional studies.

Table 1.1 Subtypes of cutaneous mechanoreceptors

Cutaneous Receptor type	Fiber innervation	Fiber adaptation type	Modality	Reference
Merkel cell complex	Aα, Aβ	SAI	Pressure, Texture, light touch	(Morrison and Maricich, 2009);(Vielkind et al., 2010);(Haeberle and Lumpkin, 2004);(Maricich et al., 2009);(Maricich et al., 2012);(Nunzi, 2004)
Meissner's Corpuscle	Aα, Aβ	RAI	Stroking, Fluttering, Grip, Shape detection	(Takahashi-Iwanaga and Shimoda, 2004); (Gonzalez-Martinez et al., 2005; Gonzalez-Martinez et al., 2004); (Westling and Johansson, 1987)
Pacinian Corpuscle	Aα, Aβ	PC, RAII	Vibration, indentation of skin	(Zelená, 1976);(Bell et al., 1994; Loewenstein and Mendelson, 1965)
Ruffini's ending	Aα, Aβ	SAII	Skin stretch, three dimensional force profile in the grip	(El-oteify and Mubarak, 2011);(Vallbo et al., 1999);(Westling and Johansson, 1987)
Guard hair	Aα, Aβ	RA	Stroking, Fluttering	(Driskell et al., 2009);(Li et al., 2011)
Awl/Auchene hair	Aβ, Aδ, C	D	Light stroking	(Driskell et al., 2009);(Li et al., 2011);(Liu et al., 2007; Zylka and Anderson, 2004)
Zigzag hair	Aδ, C	D	Light stroking	(Driskell et al., 2009);(Li et al., 2011; Liu et al., 2007; Zylka and Anderson, 2004)
Free nerve ending	Aδ, C	RA, SA and Intermediate Adapting	Skin stretch	(Iggo, 1960)

Modified from (Kandel, 2006) chapter 22

Mechanical channels in the DRG sensory neurons

Though many different subtypes of mechanosensory neurons have been identified, the mechanism of mechanical transduction is not well known(Árnadóttir and Chalfie, 2010; Chalfie, 2009; Christensen and Corey, 2007). There are four criteria for mechanical receptor/channels to be mechanical transducers (or mechanotransducers): 1) it needs to be expressed in mechanically sensitive neurons; 2) loss of the protein will lead to loss of mechanical sensitivity; 3) heterogeneously expressing the protein will confer non-mechanically sensitive neurons with mechanically sensitivities; 4) the protein should participate in forming the direct component for transducing cation.

Mechanical sensitivity appears at very early evolutionary stages. Ectopic expression of *E. coli.* MscL channels enables the transfected system to respond to osmolarity caused membrane tension (Sukharev et al., 1994). In invertebrates, several ion channels have been shown to play a role in mechanical transduction, such as no mechanoreceptor potential C (NOMPC) (Kang et al., 2010; Li et al., 2006; Walker et al., 2000; Yan et al., 2012) and degenerin/epithelial sodium channel (DEG/ENaC) (Árnadóttir and Chalfie, 2010; O'Hagan et al., 2005; Zhong et al., 2010). In vertebrates, two proteins in the Piezo family, Piezo1 and Piezo2, have been discovered and meet all four criteria for mechanical channels (Coste et al., 2010; Coste et al., 2012; Dubin et al., 2012; Kim et al., 2012). They are the only proteins discovered to belong to the vertebrate mechanical transducers so far. Piezo2 is found in a subset of DRG neurons. Later, I will discuss Piezo2 and its correlation with C-LTMRs.

Other mechanosensitive channels have been shown to play a role in modifying the eletrophysiological properties of mechanosensitive neurons, including their adaptation properties as well as firing frequencies. For example, the Kv1.1 channel encoded by Kcna1 gene has been shown to contribute to the high mechanical threshold in C mechano-nociceptors and tunes adaptation in rapid-adapting Aβ mechanoreceptors (Hao et al., 2013). Another example shows that TrpA1 mediates the slow-adapting mechanically activated $IB4^-$ small sensory neuron, but is not sufficient to confer the mechanical sensitivity (Vilceanu and Stucky, 2010). Changes of these modifying components could also affect mechanical allodynia in physiological conditions.

Other structures in the somatosensory circuitry in addition to DRG neurons also play important roles in mechanical transduction, such as Merkel cells and keratinocytes (Huang et al., 2008; Maricich et al., 2009; Vallbo et al., 1995). It is possible that some mechanoreceptors do not have mechanical channels expressed but function by connecting with the mechanically sensitive skin cells.

Molecular identifications of nociceptors, thermal receptors and itch sensitive neurons

Nociceptors, thermal receptors and itch receptors appear to have less variable terminal morphologies than the mechanoceptors, and they are more commonly categorized by molecular markers. These late-born sensory neurons can be classified into two categories: peptidergic and non-peptidergic neurons. Both peptidergic and non-peptidergic neurons are composed of highly heterogeneous subtypes that are distinguished by expression of different sensory

channels/receptors and that respond to noxious stimuli. Most channels/receptors have been shown to have specialized functions, which make the neurons expressing them have narrow modalities. Neurons expressing more than one of the channels and thus respond to multiple sensory stimuli are called poly-modal neurons. Channels/receptors can also sometimes respond to a wide range of sensory stimuli, though some of them are very specific. Many channels have not yet shown clear function, and it remains to be seen how they contribute to nociception (Dong and Anderson, 2001; Hjerling-Leffler et al., 2007; Story and Patapoutian, 2003; Zylka and Anderson, 2003).

There are 9 different voltage-gated sodium channels expressed in the mammalian muscle and nerve, of which Nav1.7, 1.8 and 1.9 were shown to be most physiologically relevant in sensory neurons. Nav1.7 (or PN1) is found to be expressed in nociceptors, Aδ fiber neurons, as well as LTMs (Djouhri et al., 2003). High-level expression of Nav1.7 was found in the growth cones of small diameter neurons (Toledo-Aral et al., 1997). Mutation of Nav1.7 in human leads to edema, redness, warmth and bilateral pain (Yang et al., 2004). Conditional knock out of Nav1.7 greatly affects all inflammatory pain responses evoked by formalin, carrageenan, CFA or NGF (Nassar and Wood, 2004). Both peptidergic and non-peptidergic small sensory neurons express sodium channel Nav1.8 (SNS/PN3). Nav1.8 is a Tetrodotoxin (TTX) insensitive sodium channel and produces slowly inactivating current when expressed ectopically (Aguayo and White, 1992). Nav1.8 expression in nociceptors is necessary for cold pain and pain in the cold (Zimmermann et al., 2007). Excitability of Nav1.8 was found to be altered after axonal injury and inflammation. Capsaicin treatment of the sensory neurons also led to loss of Nav1.8 transcripts (Anakopian et al., 1997). Because of Nav1.8 expression in most nociceptors, it has

been widely used as a nociceptor marker. Recently it was shown that Nav1.8 expression is not restricted in nociceptors, but also in C-LTMRs and Aβ LTMRs (Shields et al., 2012). Nav1.8^{Cre} transgenic mice are usually used to generate conditional knockout mice in nociceptors (Agarwal et al., 2004). Nav1.9 (or NaN) also produces TTX insensitive currents. Nav1.9 is preferentially expressed in small diameter neurons, while there are low levels of Nav1.9 in a small portion of large diameter neurons. Like Nav1.8, Nav1.9 expression is also downregulated after axotomy and has been indicated to play a role in inflammatory hyperalgesia (Dib-Hajj et al., 1998).

The peptidergic neurons make two additional peptide transmitters not present in non-peptidergic neurons: CGRP (Calcitonin gene-related peptide) and SP (substance P), and express the NGF (nerve growth factor) receptor TrkA (Neurotrophic Tyrosine Kinase, Receptor, type 1, also known as NTRK1) (Molliver and Snider, 1997; Snider and McMahon, 1998). These peptidergic nociceptors have their peripheral terminals in the skin, bones, joints and visceral organs, and their central terminals mainly in lamina I or outer lamina II (II_O) of the spinal cord (Christianson and Davis, 2006; Ivanavicius, 2004; Mach and Mantyh, 2002). There are several other molecular markers that are expressed exclusively within the peptidergic neurons, such as acid sensing channel DRASIC (or ASIC3) that respond to acid stimuli. DRASIC is also expressed in the large diameter RAM and SAMs such as Ruffini's Endings in Mouse incisors, in which DRASIC respond to cutaneous touch stimuli (Rahman et al., 2011). ASIC2, another family member of ASICs, also have similar expression patterns with DRASIC (Bassilana et al., 1997; Price et al., 2001; Waldmann et al., 1997a; Waldmann et al., 1997b; Waldmann and Lazdunski, 1998). Another important molecular marker is the Mu-Opioid receptor (MOR), which is found to be expressed in the majority of SP^+ and $CGRP^+$ peptidergic neurons, and has

been found to be in the axon terminal of the spinal cord innervation. It was proposed that endogenous opioids act through MOR to regulate the release of SP or CGRP (Li et al., 1998).

The non-peptidergic neurons can be labeled by Isolectin B4 (IB4: glycoprotein isolated from the seeds of the tropical African legume Griffonia simplicifolia). They predominantly innervate the skin epidermis and have their central terminals in the inner lamina II of the spinal cord (Christianson and Davis, 2006; Zylka, 2005).

Several gene families are expressed in non-peptidergic neurons in overlapping and non-overlapping ways. In Mas Related G protein coupled receptor (Mrgpr) family, member D, member A3, member B4, member B5 and member C11 are all found in non-peptidergic neurons (though the majority of MrgprA3^{+} and MrgprC11^{+} neurons are peptidergic neurons). MrgprD is expressed in polymodal nociceptors that respond to heat and mechanical pain (Mishra et al., 2010; Wang and Zylka, 2009; Zylka and Anderson, 2004). A proportion of MrgprD^{+} neurons also specifically responds to β-alanine, which induce itch sensations (Liu, 2012)(Shinohara, 2004). MrgprB4^{+} neurons innervate hairy skin, and were recently suggested to play a role in massage-like stroke (Vrontou et al., 2013). MrgprA3^{+} neurons innervate the hairy skin, and were found to contribute to itch sensation (Han et al., 2012). It is hard to distinguish MrgprA3 and MrgprB4 neurons, since MrgprB4^{+} neurons also express low levels of MrgprA3. Both MrgprB4 and A3 co-express with MrgprC11 (Liu et al., 2008). Recently, MrgprA3^{+} neurons have been found to express both IB4 and CGRP, using a MrgA3^{Cre}; Rosa-Tomato reporter line (Han et al., 2012). The function of MrgB5 remains unknown.

TRP (Transient receptor potential cation channel) channel class, TrpA1, TrpC3, TrpC6, TrpM8, TrpV1 and TrpV2 are polymodal sensors in DRG neurons. TrpA1 (TRP, subfamily A, member 1) is the integrator of noxious cold, diverse chemical and mechanical stimuli (Brierley et al., 2011; Knowlton et al., 2010; Kwan et al., 2009; Wilson et al., 2011). TrpC3 and TrpC6 are exclusively expressed in small diameter sensory neurons. TrpC3 is thought to contribute to cell excitability by interacting with K^+ channel activity (Crozier et al., 2007), while both TrpC3 and TrpC6 are suggested to be essential for mechanotransduction (Quick et al., 2012). TrpM8 (TRP, subfamily M, member 8) responds to cold, menthol and icilin (Story and Patapoutian, 2003), and has recently shown to be mechanically sensitive . Most $TrpM8^+$ neurons are not labeled by IB4 or CGRP, so belong to non-conventional nociceptors (Bautista et al., 2007; Dhaka et al., 2008; Knowlton et al., 2010). TrpV1 (Vanilloid receptor 1) is a receptor that opens in response to temperatures above 43^oC, low pH (Tominaga et al., 1998) and capsaicin (Caterina et al., 1997). Recently it was shown that TrpV1 channels are intrinsically heat sensitive and can be regulated by phosphoinositide lipids (Cao et al., 2013). It has been suggested that they play a role in injury or inflammation-induced hyperalgesia (Davis et al., 2000). TrpV1 has high and low expression levels in mouse DRG. TrpV1 immunostaining showed its expression in both peptidergic and non-peptidergic neurons, which respond to warm and mild heat. (Chen et al., 2006; Samad et al., 2010). TrpV2 responds to even higher temperatures than TrpV1 (53^oC), as well as to changes in osmolarity and to membrane stretch (Caterina et al., 1999; Muraki et al., 2003). However the function of TrpV2 in vivo is not known. TrpV4 is a calcium-permeable swell-activated channel and indicated to play a role in mechanosensation. It is found to be expressed in both small (low

threshold) and large (high threshold) DRG neurons, as well as keratinocytes and Merkel cells (Suzuki et al., 2003).

Ablation of $MrgD^+$ neurons led to significant reduction of mechanical nociception, while ablation of $TrpV1^+$ nerve endings in the spinal cord specifically affect noxious heat pain (Cavanaugh et al., 2009), suggesting the sensory modalities of nociception are transduced in labeled line (Ma, 2010, 2012).

The ATP cation dependent P2X purinoceptor P2X3 was found to be specifically expressed in $IB4^+$ non-peptidergic neurons (Bradbury et al., 1998; Chen et al., 1995). P2X3 expression was also reduced upon axotomy, which could be rescued by GDNF (Bradbury et al., 1998). In conclusion, this channel is enriched in non-peptidergic neurons and mediates ATP evoked nociceptor activation.

The classification and variety of sensory neuron subtypes makes sensory acuity possible and also plays the foundation for studying the differentiation of neuronal subtypes. Despite the advances in revealing molecular markers of the sensory neurons, there are several big questions to be answered: first of all, how are the sensory neuron progenitors specified into so many different types of sensory neuron? Second, how does one specific type of sensory neuron make the correct projections? And finally how does the system maintain the identities of the neurons after differentiation? To elucidate the development and maintenance of different subtypes of sensory neuron is the goal of this thesis. The large varieties of nociceptors, the accessibility of DRG, and the quantitative behavioral tests make nociceptors an ideal model to study the mechanism of neural development.

Somatosensory neuron development

The development of neurons generally undergoes several steps: early cell fate determination, neuronal migration, initial axon outgrowth, axon extension towards specific targets and target invasion, branching and synaptogenesis. During these processes, the neurons are instructed by both intrinsic and extrinsic signals.

Sensory neuron genesis

Somatic sensory neurons originate from neural crest stem cells (NCCs). Two basic helix-loop-helix transcription factors, neurogenin 1 (NGN1) and neurogenin 2 (NGN2), are required for neurogenesis and bias NCCs towards the sensory rather than autonomic lineage (which is dependent on Mash1) (Ma et al., 1998; Ma et al., 1999; Ma et al., 1996). The migration and neurogenesis of NCCs happens during embryonic day 8.5 (E8.5)- E11 (in mouse) in three waves to form the DRG (Kasemeier-Kulesa, 2005; Serbedzija and Bronner-Fraser, 2005). The Ngn2-dependent first wave mainly contributes to $TrkC^+$ proprioceptive precursors and $TrkB^+$, $TrkC^+$ and/or Ret^+ mechanoreceptors precursors (Zirlinger et al., 2002). The NGN1-dependent second wave, is the largest contributor to DRG neuron population, and develop into nociceptors, thermo-receptors and itch receptors, all of which initially express TrkA and respond to NGF (Marmigère and Ernfors, 2007). The third wave is the smallest contributor, which forms about 5% of all DRG neurons. These late born neurons come from the boundary cap, also express TrkA, and mostly become nociceptors, with 40% of them being $IB4^+$, and 47% being $CGRP^+$(Maro et al., 2004). NGN1 and NGN2 are required for neurogenesis of all DRG neurons, since *NGN1* and *NGN2*

knock out mice do not form DRG (Bertrand et al., 2002; Lo et al., 2002; Ma et al., 1999; Perez et al., 1999). In the absence of NGN2, $NGN1^{+}$ cells can still give rise to all neuronal subtypes. However, in the absence of NGN1, the small TrkA neurons are missing (Ma et al., 1999).

Before and during NCC migration, sensory neuron precursors express the multipotent marker, the high-mobility group transcription factor SRY (sex determining region Y) box 10 (Sox10). Sox10 is downregulated after proliferation finishes and specification initiates. Brn3a, Foxs1 and Isl1 are among the earliest markers and functional transcriptional factors for sensory neurons. Isl1 acts together with Brn3a to drive the transition from sensory neurogenesis to terminal differentiation (Lanier et al., 2009; Montelius et al., 2007) (Dykes et al., 2011; Sun et al., 2008).

Neurotrophin Receptors

During the sensory subtype specification, the first class of molecular markers present are the trk signaling receptor family TrkA/B/C, which binds to different neurotrophins: TrkA responds to NGF, TrkB to BDNF and NT4, and TrkC to NT3 (Ginty, 2002; Philips and Armanini, 2008; Postigo, 2002). TrkC (1^{st} wave) is the earliest expressing subtype marker, followed by TrkB (also 1^{st} wave) and later TrkA (the 2^{nd} and 3^{rd} waves) in the sensory neurons. During the process of specification, all three markers experience dynamic expression patterns and segregations. In the adult DRG neurons, most of TrkC and TrkB expressing neurons become proprioceptors and/or mechanoreceptors, while the TrkA lineage neurons become nociceptors, thermal receptors and itch receptors. Trk receptors are more than mere markers, but also functional during development. Trk signaling is important for neuronal survival, maturation, and target innervation

(Pezet and McMahon, 2006). The genetic replacement of TrkA with TrkC switches the cell fate from unmyelinated sensory neurons to proprioceptors (Moqrich et al., 2004).

From E11.5 to E14.5, several distinct populations arise within $TrkC^+$ precursors: the $TrkC^+$ only, $TrkB^+/TrkC^+$, $TrkB^+$ only, $TrkB^+/Ret^+$ and Ret^+ only populations. The $TrkC^+$ population maintains TrkC expression and later become proprioceptors. Between E11.5-E12.5, $TrkB^+/TrkC^+$ population neurons experience downregulation of $TrkC^+$ and become a $TrkB^+$ only population. Between E12.5-E14.5, $TrkB^+/Ret^+$ population neurons also downregulate TrkB expression and become exclusively Ret^+ (Kramer et al., 2006). These two populations later turn into mechanoreceptors. The specification of the first wave of molecular markers happens before terminal target innervation and thus might be a consequence of local signals or of innate developmental programs.

TrkA expression was found in most sensory neurons at E12. From E16, a subset of $TrkA^+$ neurons starts expressing RET. The RET expression has been found to be NGF/TrkA signaling dependent. Between P0 –P14, the $RET^+/TrkA^+$ neurons experience gradual downregulation of TrkA and turn into RET^+ only, non-peptidergic neurons. Meanwhile, $TrkA^+$ only neurons become peptidergic neurons. The distinction of TrkA within $RET^+/TrkA^+$ neurons is RET dependent. Loss of RET signaling was found to lead to disruption of non-peptidergic neuron differentiation and also influence peripheral but not central projections of the non-peptidergic sensory neurons (Luo et al., 2007).

Specification of Proprioceptors

As mentioned before, the development of proprioceptors is Runx3 dependent. From E11.5-E14.5, the $TrkC^+$ neurons that remain Runx3 expression during differentiation become proprioceptors. Runx3 suppresses mechanoreceptor identities by inhibiting transcriptional factor Shox2, biasing sensory neurons towards proprioceptor fate. Without Runx3, Shox2 controls the development of $NGN2^+$ neurons and biases them toward the mechanoreceptor specifications (Abdo et al., 2011). Loss of Runx3 leads to disruption of proprioceptor markers, such as TrkC and Parvalbumin, proprioception circuit formation, as well as proprioceptive function (Inoue et al., 2003; Inoue et al., 2002; Levanon and Groner, 2002).

Specification of myelinated Mechanoreceptors

The development of mechanoreceptors seems more complicated as there are multiple subtypes of mechanoreceptors. Both intrinsic and extrinsic factors have been found to play important roles in mechanoreceptor specification.

Mice lacking BDNF-TrkB signaling completely lose the Meissner corpuscles and have modest morphological disorganization of lanceolate endings (Gonzalez-Martinez et al., 2005; Gonzalez-Martinez et al., 2004; Perez-Pinera et al., 2008; Rice et al., 1998). Using the temporal specific Ret reporter line, it was shown that early Ret^+ neurons that co-express GFRα2 are mostly rapidly adapting mechanoreceptors (RAM) and form the termination of Meissner Corpuscles of the glabrous skin, lanceolate endings in the hairy skin as well as the pacinian corpuscles in deep tissues (Luo et al., 2009). The development of early RET RAM is mostly dependent on NRTN-GFRα2/Ret signaling, as shown with a conditional knockout of RET

leading to disorganization of Meissner corpuscles and lanceolate endings, while the pacinian corpuscles are totally lost (although the signaling is not required to maintain pacinian corpuscles once they are formed) (Luo et al., 2009).

MafA was found to exclusively express within the early RET/GFR$\alpha 2^+$ population. Upon loss of MafA, there is a disruption of development in a subtype of MafA and Ret only neurons, changes of Merkel Cell complex and lanceolate endings, as well as changes of the terminal innervations in the spinal cord. Loss of MafA also impairs the downregulation of TrkB expression within the Ret^+ only population (Bourane et al., 2009; Luo et al., 2007). C-Maf is another transcriptional factor in the same family as MafA. Early c-Maf is found to be expressed in $RET^+/MafA^+$ RAMs. Loss of c-Maf leads to elongation of adaptation of RAMs while the SAM and D-hair receptor functions remain unchanged. Meanwhile, a disruption of terminal morphologies of heavily-myelinated and guard-hair-innervating lanceolate endings, circumferential endings, Meissner's corpuscles and Pacinian corpuscles was observed. This is consistent with human c-Maf mutations, as the Pacinian corpuscle dependent high frequency vibration sensation was affected (Wende et al., 2012). There are no other detailed reports about how each individual mechanoreceptor subtype differentiates. It is possible that the specification of Meissner corpuscles, Ruffini corpuscles, lanceolate endings, Merkel cell complex and pacinian corpuscles are determined by target-derived signals (Rice et al., 1998).

Segregation of TrkA lineage neurons

The TrkA lineage neurons form nociceptors, thermoreceptors, pruritic receptors *et al*. Between E12.5-E14.5, most $TrkA^+$ neurons co-express with Runx1. After sensory neuron genesis, a

segregation of peptidergic versus non-peptidergic nociceptor phenotype happens, with some DRG neurons extinguishing TrkA expression and up-regulating Ret expression while the rest retain TrkA expression (Molliver and Snider, 1997). This segregation takes place around perinatal stages and finishes at postnatal day 14 (P14). It was found that the transcription factor Runx1 plays a pivotal role in this segregation. Runx1 is a runt domain transcription factor with an activation domain and a repression domain (Dhaka et al., 2006). In wild-type mice, Runx1 is first detected at the age of E12.5. From E12.5-E14.5, Runx1 is found in almost all nociceptors and is co-expressed with TrkA. From E14.5 to P14, some of the nociceptors that maintain TrkA expression extinguish Runx1 expression. The other subset of nociceptors maintains Runx1 expression, switch off TrkA and turn on Ret. It was found that hepatocyte growth factor (HGF)-Met signaling acts synergistically with TrkA to promote peptidergic identity and to suppress Runx1 expression in the peptidergic neurons (Gascon et al., 2010).

To determine the function of Runx1 in peptidergic versus non-peptidergic cell fate segregation, a conditional Runx1 knockout mouse line was generated by crossing Runx1f/f mice with Wnt1-Cre mice, which eliminates Runx1 expression in DRG neurons (Chen et al., 2006). In these *Runx1* conditional knock out mice (*Runx1*$^{f/f}$; *Wnt*$^{Cre/+}$, Cre initiates at E8.5), at P60, the percentage of TrkA^{+} neurons in lumbar DRG is doubled compared to control mice, while the percentage of Ret^{+} DRG neurons decreases to half of the controls, many remaining Ret^{+} neurons are early born mechanoceptors. CGRP, which is expressed only in TrkA^{+} neurons, also shows significantly increased expression. By examining central projections, IB4^{+} non-peptidergic terminals are seen shifted to the outer lamina layer, where CGRP^{+} peptidergic projections usually terminate. These results indicate that Runx1 promotes a non-peptidergic over a peptidergic

nociceptor identity. Meanwhile, expression of many sensory channels/receptors is eliminated or greatly reduced in the Runx1 mutant, including Trp channels (TrpM8, TrpV2, TRPC3, and TrpV1 highly expressing channel ($TpV1^{High}$)), the ATP-gated P2X3 receptor, the sodium channel Nav 1.9 and a dozen of the Mrgpr class GPCRs. This suggests the requirement of Runx1 expression for sensory modality specification. Accompanying the molecular and morphological abnormalities in the Runx1 knockout mice, behavioral studies showed impairment in thermal, neuropathic and inflammatory pain.

Like many other molecular markers and transcriptional factors expressed in the DRG neurons, the Runx1 expression pattern is quite dynamic. Not only was it switched off in adult Runx1-independent $TrkA^{+}$ peptidergic neurons, Runx1-dependent neurons can also be divided into Runx1 persistent and Runx1 transient populations. Using *Runx1* late knockout (SNS^{Cre} ; $Runx1^{f/f}$, in which Runx1 is knocked out between E16-E17), the Runx1 persistent and Runx1 transient populations were segregated. MrgD, MrgB5, GluR5, PKCq, TrpC3, TrpM8 and most of $TrpV1^{High}$ are expressed in Runx1-persistent neurons that are lost in both early and late Runx1 knockout mouse. MrgA3, MrgB4 and MrgC11 belong to the second population of markers that are expressed in Runx1-transient neurons and are lost in the early *Runx1* knockout but unaffected in late *Runx1* knockout mouse (Samad et al., 2010).

Recently, another transcriptional factor Tlx3 has been found to be required to establish most of the Runx1 dependent phenotypes, including the segregation of peptidergic and non-peptidergic neuronal fates as well as dozens of the sensory channels and receptors mentioned above. Tlx3 is expressed more widely than Runx1 (in both peptidergic and non-peptidergic neurons) in adult mice DRG neurons. The expression of Tlx3 and Runx1 are independent with

each other; and co-expression of these two transcriptional factors is sufficient to drive several channel/receptor expressions in the open book assay of spinal cord. (Lopes et al., 2012).

Other studies showed that Runx1 first acts as an activator of MrgA3, B4 and C11, but later switches to become a repressor for these genes. As a result, expression of A3, B4 and C11 can only be sustained in Runx1-transient neurons. To explain the transition of Runx1 functions, it was found that the dynamic expression and functions of Runx1 might be due to the activation and inhibition domain of this transcriptional factor. Mutation of the Runx1 inhibition domain led to expansion of MrgA3, B4 and C11 into the MrgD population (Liu et al., 2008) (Figure 1.3 B).

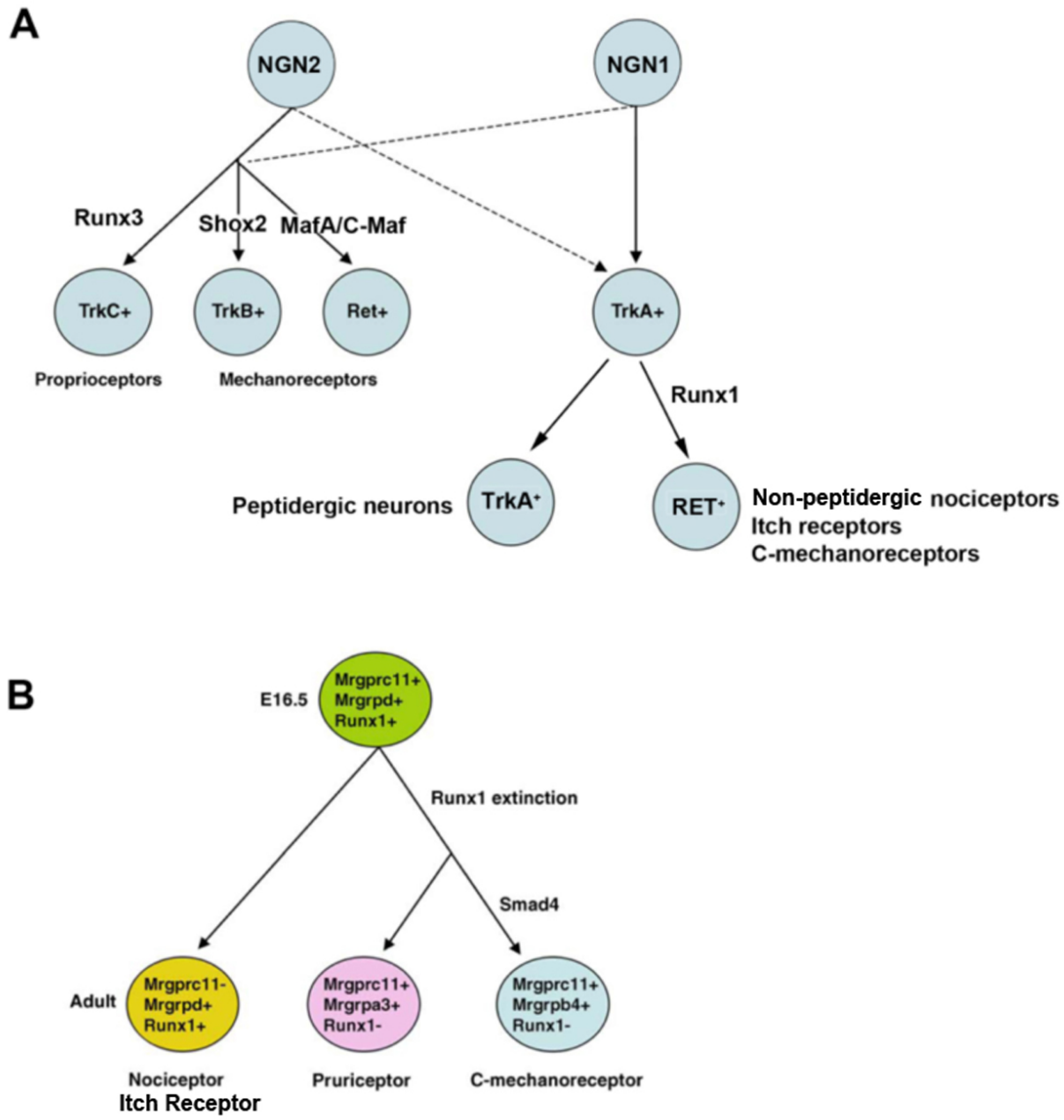

Figure 1.3 Scheme of DRG neuron diversification during development

Modified from (Liu and Ma, 2011)

Target derived signals and subtype specification

It is widely acknowledged that the cellular survival, specification as well as circuit formation are closely related with target-derived signals (da Silva and Wang, 2011; Ginty, 2002; Hippenmeyer et al., 2004). Within Runx1 dependent subtypes, neurons have wide range of target innervation patterns. MrgD neurons form free nerve endings in the epidermis throughout the skin (Zylka and Anderson, 2004); MrgA3/MrgB4^{+} neurons form free nerve endings only in the hairy skin epidermis (Han et al., 2012); MrgB4^{+} neurons were also found to form circular endings in the neck of hair follicles (Liu et al., 2007); VGLUT3^{+} C-LTMRs, which we will talk about in this thesis, form longitudinal lanceolate endings in the zigzag and Awl/Auchene hair follicles (Li et al., 2011). These evidence suggest that target derived signals might play an important role in sensory neuron subtype specifications.

Here we use the example of BMP signaling to explain the mechanism of how target derived signals control the specification of individual sensory neuron subtypes. BMP signaling has been shown to be important for cellular identity specification in many animal models and multiple tissue development. In Drosophila, target derived BMPs homologs Glass Bottom Boat (Gbb) signaling induces the phosphorylation of Smad homolog Mothers against decapentaplegic (Mad), which eventually directs the Tv neurons that target on the Gbb secreting neurohemal organ (NHO) to take up neuropeptidergic character that expresses FMRFamide (Allan et al., 2003; Eade and Allan, 2009; Marqués et al., 2003; Miguel-Aliaga et al., 2004).

In mammals, BMP family derived from the dorsal aorta induces expression of several transcriptional factors, such as mouse achaete-scute homologue 1(Mash1) and paired-like homeodomain transcriptional factor Phox2a/b, which control autonomic neuron-

specifications(Guillemot et al., 1993; Pattyn et al., 1999; Schneider et al., 1999; Stanke et al., 1999).

In the mouse sensory system, BMP signaling has been shown to be critical both for the subtype identity establishment, as well as circuit formation. BMP signaling from the peripheral innervation of the whisker hair follicle is required to maintain the topographic map of the trigeminal ganglia projection. Deletion of Smad4 at late embryonic stages led to loss of topography of the barrelettes (da Silva et al., 2011). For trigeminal ganglia, BMP4 signals act through Onset 2 to determine trigeminal sensory neuron specification and formation of somatosensory map (Liberty K. Hodge, 2007). In Smad4 conditional knockout mice, MrgB4 expression is lost, suggesting the role of BMP signaling in specifying $MrgB4^{+}$ neurons (Liu et al., 2008).

However, it was unknown what the downstream effector of BMP signaling is. Using trigeminal ganglia *in vitro* cell culture, it was found that neuron specification requires two sequential actions: BDNF induces axonal translation of SMAD1/5/8 and that BMP4 induces phosphorylation of SMAD1/5/8 (Ji and Jaffrey, 2012; Takatoh and Wang, 2012). This suggests that the retrograde signals can interact with each other to achieve a more precise subtype specification.

Central innervations of sensory neurons

Extrinsic cues such as semaphorin Sema3A are responsible for sensory neuron lamina formation in the spinal cord. Sema3A acts as a diffusive chemorepulsive cue to the axon projections by interacting with neuropilin 1 (NRP1) plexinA3 or plexinA4. During sensory neuron projection into the spinal cord, Sema3a is concentrated in the ventral horn of the spinal cord. Since $TrkC^{+}$ proprioceptors express lower level of NRP1, while the $TrkA^{+}$ small neurons express higher level of NRP1, $TrkC^{+}$ neuron afferents could enter and synapse in the ventral horn, whereas $TrkA^{+}$ nerve afferents are repelled and innervate the dorsal horn of the spinal cord (Behar et al., 1996; Bron et al., 2004; Gu et al., 2003; Messersmith et al., 1995). Developing muscles release NT3 and GDNF. NT3 promotes the expression of ER81, which is important for TrkC expression in the proprioceptors; while GDNF promotes the expression of PEA3 in the motor neurons. It was shown by removal of the target derived signals (GDNF and NT3) using limb ablation, that the proprioceptor central projections and target innervations are greatly compromised (Lin et al., 1998). Using $NT3^{-/-}$; $Bax^{-/-}$ mice, it was shown that $TrkC^{+}$ proprioceptors could no longer project to the ventral horn of the spinal cord, and failed to synapse with the motor neurons to form the circuitry (Arber et al., 2000; Ernfors et al., 1995; Ernfors et al., 1994; Levanon and Groner, 2002; Patel et al., 2003). Other local cues such as cell adhesion molecules axonin 1 and transient axonal glycoprotein for the axons of small neurons, and coagulation factor 11 (F11) were all shown to contribute to proprioceptor longitudinal and retrocaudal axonal trajectory (Perrin et al., 2001).

In conclusion, intrinsic and extrinsic factors reciprocally function to regulate the survival, specification and initiation of circuitry formation of the sensory neurons. However, little is known about the further specification and synaptogenesis of specific subtypes of sensory neuron. The working model is that subtype sensory neurons acquire distinct expression of neurotrophic receptor combinations after the initial differentiation, and that the temporal and spatial differences of their target innervations leads to differences in target-derived signals. The distinct receptors, the innate transcriptional program status, as well as the different signals will trigger expression of downstream transcriptional factors necessary for differentiation events to turn on various ion channels and ligand receptors.

Discovery of C-LTMRs

Traditionally, it was believed that all the low-threshold mechanoreceptors are myelinated. Unmyelinated low threshold mechanoreceptors (C-LTMR) were first discovered by Zotterman in cats over 70 years ago (Zotterman, 1939), and were subsequently found in all tested mammals, including humans (Björnsdotter et al., 2010; Brown and Hayden, 1971; Brown and Iggo, 1967; Olausson et al., 2010; Vallbo et al., 1993). The C-LTMRs were mostly found in the face and forearm skin (hairy skin).

Functionally, Zotterman proposed that human C-LTMRs might be involved with ticklish sensation (Zotterman, 1939). More recent studies in humans suggested that C-LTMRs signal pleasant touch associated with affiliative social body contact (Björnsdotter et al., 2010; Olausson et al., 2010). Microneurography recording showed that C-LTMR exhibit bell-shape responses to the speed of moving stimuli, whose peak activity correlates well with the perception of touch-evoked pleasantness (Löken et al., 2009). Consistently, human patients lacking myelinated A-fibers were still able to sense pleasant touch (Björnsdotter et al., 2010; Löken et al., 2009; Morrison et al., 2011). It was also found that human C-LTMRs project to the dorsal posterior part of the insular, bypassing SI, as shown by a lack of activation in SI when stroking the patient without Aβ fiber (Olausson et al., 2002). The dorsal posterior insular, interesting, has been shown to involve in pain, itch and other sensory related emotions (Bartels and Zeki, 2000; Brooks et al., 2002; Craig et al., 2000; Stoleru et al., 2000).

Since the studies of human C-LTMRs, two types of C-LTMRs have been discovered in mice: the VGLUT3$^+$ C-LTMRs discovered by Seal *et al* (Seal et al., 2009) and the MrgB4$^+$ C-

LTMRs discovered by Liu and Vrontou *et al*. more recently (Liu et al., 2007; Vrontou et al., 2013).

VGLUT3$^+$ C-LTMRs represent ~10% of total DRG neurons in mice, can be marked by the expression of VGLUT3, a vesicular glutamate transporter (Seal et al., 2009). A large subset of VGLUT3$^+$ neurons are TH$^+$. Li et al. showed that TH$^+$ C-LTMRs form longitudinal lanceolate endings exclusively around zigzag, Awl/Auchene hairs (Li et al., 2011). Each TH$^+$ C-LTMR seems to innervate 18±1.7 hair follicles. Centrally VGLUT3$^+$ C-LTMRs project to inner lamina II in the spinal cord and the afferents overlap with interneurons expressing the γ isoform of protein kinase C (PKCγ) (Seal et al., 2009).

Ex-vivo recordings showed that VGLUT3$^+$ C-LTMRs have a slow conduction velocity (0.58±0.02m/s), a small receptive field (0.2-0.4mm^2) and respond to as low as 0.07mN of Von Frey stimuli in the rodents. C-LTMRs have the trend to fire higher in respond to stronger stimuli than lower stimuli and exhibit after discharges following mechanical stimuli and have an intermediate adaptation to stationery stimuli. They also respond to cooling with a threshold of 25 ^{o}C, but no response to heat. And finally, they respond to slow motion across the skin better than fast moving stimuli (Bessou and Taylor, 2003; Iggo, 1960; Li et al., 2011; Seal et al., 2009).

Seal et al. further proposed that mouse C-LTMRs are required for the expression of mechanical allodynia (pain evoked by innocuous mechanical stimuli) induced by inflammation, tissue injury, chemicals (capsaicin), and nerve injury, based on behavioral analyses in *VGLUT3* complete null mice (Seal et al., 2009). A number of questions remained to be addressed, which became the focus of this study. Firstly, the mechanical pain defects were measured from the glabrous skin in the hindpaw plantar. However it was shown that C-LTMRs exclusively

innervate the hairy skin rather than the glabrous skin. Furthermore, VGLUT3 has been shown to express in the spinal cord as well as the brain, with which the somatosensory circuitry is closely related (see this chapter). Conventional knockout of VGLUT3 will lead to disruption of the other parts of the sensory circuitry. As a result more extensive characterization and specific conditional ablation of VGLUT3$^+$ C-LTMR in the sensory neurons are required and the physiological functions of VGLUT3$^+$ C-LTMRs are unknown.

MrgB4$^+$ C-LTMRs represent ~2% of total DRG neurons, and most MrgB4$^+$ neurons also express MrgC11 and low levels of MrgA3 (Liu et al., 2007; Liu et al., 2008; Vrontou et al., 2013). Peripherally, MrgB4$^+$ neurons innervate the epidermis of the hairy skin in the form of free nerve endings, as well as circular nerve endings in the neck of hair follicles. The anatomic analysis of peripheral innervations showed that MrgB4$^+$ neurons have large dendritic arborization mimicking the receptive field features of C-LTMRs in human (Liu et al., 2007). Centrally, MrgB4$^+$ neurons project to the IB4$^+$ lamina II. Electrophysiological recordings of MrgB4$^+$ sensory neurons in vitro and ex vivo fail to show any response to thermal or mechanical stimuli. However, in vivo calcium imaging analysis of MrgB4$^+$ neurons showed that they respond to massage-like strokes. Using conditioned place preference (CPP), it was shown that pharmacological activation of MrgB4$^+$ neurons could promote the coupling of the place preferences with the neuronal activations (Vrontou et al., 2013). However, since MrgB4 does not have close homologs in human, it raises the question what is the MrgB4 comparable sensory neurons in human being and if there are such kind of neurons, if they will function as C-LTMRs as they do in mice.

Chapter II. Runx1 controls terminal morphology and mechanosensitivity of C-LTMRs[1]

Chapter II is modified from the paper that is published in Journal of Neuroscience Jan 2013 Volume 33, page 870, entitled "Runx1 Controls Terminal Morphology and Mechanosensitivity of VGLUT3-expressing C-Mechanoreceptors". It is co-authored by Shan Lou, Bo Duan, Linh Vong, Bradford B. Lowell, and Qiufu Ma. The electrophysiology experiments as well as the behavior experiments are mainly carried out by Bo Duan.

[1] 'C-LTMR(s)' in this chapter all refers to VGLUT3$^+$ C-LTMRs, unless indicated otherwise.

Chapter II. Abstract

VGLUT3-expressing unmyelinated low-threshold mechanoreceptors (C-LTMR) are proposed to mediate pleasant touch and/or pain, but the molecular programs controlling C-LTMR development are unknown. Here, we performed genetic fate mapping, showing that VGLUT3 lineage sensory neurons are divided into two groups, based on transient or persistent VGLUT3 expression. VGLUT3-transient neurons are large- or medium-diameter myelinated mechanoreceptors that form the Merkel cell-neurite complex. VGLUT3-persistent neurons are small-diameter unmyelinated neurons that are further divided into two subtypes: (1) tyrosine hydroxylase (TH)-positive C-LTMRs that form the longitudinal lanceolate endings around hairs, and (2) TH-negative neurons that form free nerve endings in the skin epidermis. We then found that VGLUT3-persistent neurons express the runt domain transcription factor Runx1. Analyses of mice with a conditional knockout of Runx1 in VGLUT3 lineage neurons demonstrate that Runx1 is pivotal to the development of VGLUT3-persistent neurons, such as the expression of VGLUT3 and TH and the formation of longitudinal lanceolate endings. Furthermore, Runx1 is required to establish mechanosensitivity in C-LTMRs, by controlling the expression of the mechanically gated ion channel Piezo2. Surprisingly, both acute and chronic mechanical pain were largely unaffected in these Runx1 mutants. These findings appear to argue against the recently proposed role of VGLUT3 in C-LTMRs in mediating mechanical hypersensitivity induced by nerve injury or inflammation. Thus, our studies provide new insight into the genetic program controlling C-LTMR development and call for a revisit to the physiological functions of C-LTMRs.

Introduction

Unmyelinated low threshold mechanoreceptors (C-LTMRs) were first discovered by Zotterman in cats over 70 years ago (Zotterman, 1939), and were subsequently found in all tested mammals, including humans (Björnsdotter et al., 2010; Olausson et al., 2010). Zotterman initially proposed that C-LTMRs might be involved with ticklish sensation (Zotterman, 1939). More recent studies in humans suggested that C-LTMRs signal pleasant touch associated with affiliative social body contact (Björnsdotter et al., 2010; Löken et al., 2009; Olausson et al., 2010). In mice, C-LTMRs in the dorsal root ganglia (DRG) are marked by the expression of VGLUT3, a vesicular glutamate transporter (Seal et al., 2009), and by the expression of the tyrosine hydroxylase (TH) (Li et al., 2011). The TH^+ subset of C-LTMRs form longitudinal lanceolate endings around hairs (Li et al., 2011). Mice lacking VGLUT3 showed marked deficits in mechanical allodynia (pain evoked by innocuous mechanical stimuli) induced by inflammation, tissue injury, chemicals (capsaicin), and nerve injury (Seal et al., 2009). Based on these behavioral phenotypes, C-LTMRs were proposed to mediate mechanical pain under pathological conditions (Seal et al., 2009). However, this interpretation is complicated by VGLUT3 expression in many parts of the nervous system besides C-LTMRs (Boulland et al., 2004; El Mestikawy, 2011).

In recent years, a number of transcription factors have been identified that control the development of myelinated low threshold mechanoreceptors, including the formation of specialized mechanoreceptor nerve endings and end organs (Abdo et al., 2011; Arber et al., 2000; Inoue et al., 2002; Kucera, 2002; Levanon and Groner, 2002; Scott et al., 2011; Sedý,

2006; Senzaki K, 2010; Wende et al., 2012). However, the genetic program controlling C-LTMR development is entirely unknown. The runt domain transcription factor Runx1 is known to play a pivotal role in controlling the development of a diverse array of unmyelinated sensory neurons, such as pain-related nociceptors, itch-related pruriceptors, and thermoceptors (Lallemend and Ernfors, 2012; Liu et al., 2011). Runx1 is initially expressed in most embryonic neurons marked by the expression of the nerve growth factor receptor TrkA (Chen et al., 2006; Kramer et al., 2006; Levanon and Groner, 2002; Marmigere et al., 2006; Yoshikawa, 2007). In adult mice, persistent Runx1 expression is confined to those sensory neurons that have switched off TrkA and activated the expression of the Ret receptor tyrosine kinase (Chen et al., 2006; Kramer et al., 2006). Since C-LTMRs belong to the unmyelinated sensory neuron population, we hypothesized that the development of C-LTMRs is also Runx1 dependent. Here we demonstrate that Runx1 indeed coordinates C-LTMR development. Furthermore, by creating mice with selective defects in C-LTMRs, we were able to reassess the physiological functions of C-LTMRs.

Results

Genetic marking of VGLUT3 lineage sensory neurons

To mark VGLUT3 lineage DRG neurons, we crossed Vglut3-Cre mice, in which an IRES-Cre cassette was inserted into the 3' end of the Vglut3 locus, with ROSA26-CAG-LSL-tdTomato reporter mice (Madisen et al., 2010), with the resulting double heterozygous mice referred to as $ROSA^{Tomato/+};Vglut3^{Cre/+}$ mice (Figure 2.1 A). In $ROSA^{Tomato/+};Vglut3^{Cre/+}$ mice, VGLUT3 lineage neurons are permanently marked by red fluorescent Tomato expression, irrespective of persistent or transient VGLUT3 expression. We found that 18.9% (674/3574) of adult lumbar DRG neurons, visualized with the expression of the pan neuronal marker SCG10, were Tomato-positive (data not shown). All neurons with detectable VGLUT3 mRNA coexpressed Tomato (Figure 2.1 B), suggesting that VGLUT3-Cre faithfully marks VGLUT3-expressing ($VGLUT3^+$) sensory neurons in the DRG. However, we did note that only 85.4% of $Tomato^+$ neurons showed detectable VGLUT3 mRNA (Fig.2.1B, arrow). VGLUT3-positive $Tomato^+$ neurons belong predominantly to small-diameter DRG neurons (Fig. 2.1B, arrow), whereas the remaining 14.6% of VGLUT3-negative $Tomato^+$ neurons represent medium- (Fig. 2.1B, arrowhead) or large- (Fig. 1B, dashed circle) diameter neurons. At P0.5, some large neurons did show detectable VGLUT3 expression (Fig. 2.1C, dashed circle), indicating that adult VGLUT3-negative $Tomato^+$ neurons represent neurons with transient VGLUT3 expression. It should also be noted that at P0.5, Tomato expression had not yet established in some neurons with detectable VGLUT3 mRNA (Fig. 2.1C, arrowhead), suggesting that VGLUT3 expression was initiated at prenatal or neonatal

stages. Thus, adult Tomato$^+$ neurons are divided into two groups: small VGLUT3-persistent versus large/medium VGLUT3-transient.

VGLUT3-persistent neurons are unmyelinated (Seal et al., 2009). Consistently, NF200, a marker for myelinated DRG neurons, was not expressed in small Tomato$^+$ neurons (Fig. 2.1D, arrows). In contrast, NF200 expression was detected in medium/large Tomato$^+$ neurons (Fig. 2.1D, arrowheads and dashed circles). Thus, VGLUT3-persistent and VGLUT3-transient Tomato$^+$ neurons represent unmyelinated and myelinated neurons, respectively.

A subset of VGLUT3-persistent neurons can also be marked by the expression of TH, and electrophysiological recording shows that they represent C-LTMRs (Li et al., 2011; Seal et al., 2009). We found that in adult lumbar DRG of *ROSA*$^{Tomato/+}$*; Vglut3*$^{Cre/+}$ mice, TH mRNA was detected in 57.9% of small diameter Tomato$^+$ neurons (Fig. 2.1E, arrow). Thus, VGLUT3-persistent neurons (representing 85.4% of total Tomato+ neurons) are divided into TH+ C-LTMRs (~58%) and TH-negative (TH$^-$) neurons (~27%).

Thus, the genetic fate mapping experiments reveal four subsets of VGLUT3 lineage neurons in DRG (Fig. 2.1F): medium- and large-diameter subsets of VGLUT3-transient myelinated A-mechanoreceptors (for mechanosensitivity, see below), TH$^+$ VGLUT3-persistent C-LTMRs, and TH$^-$ VGLUT3-persistent neurons.

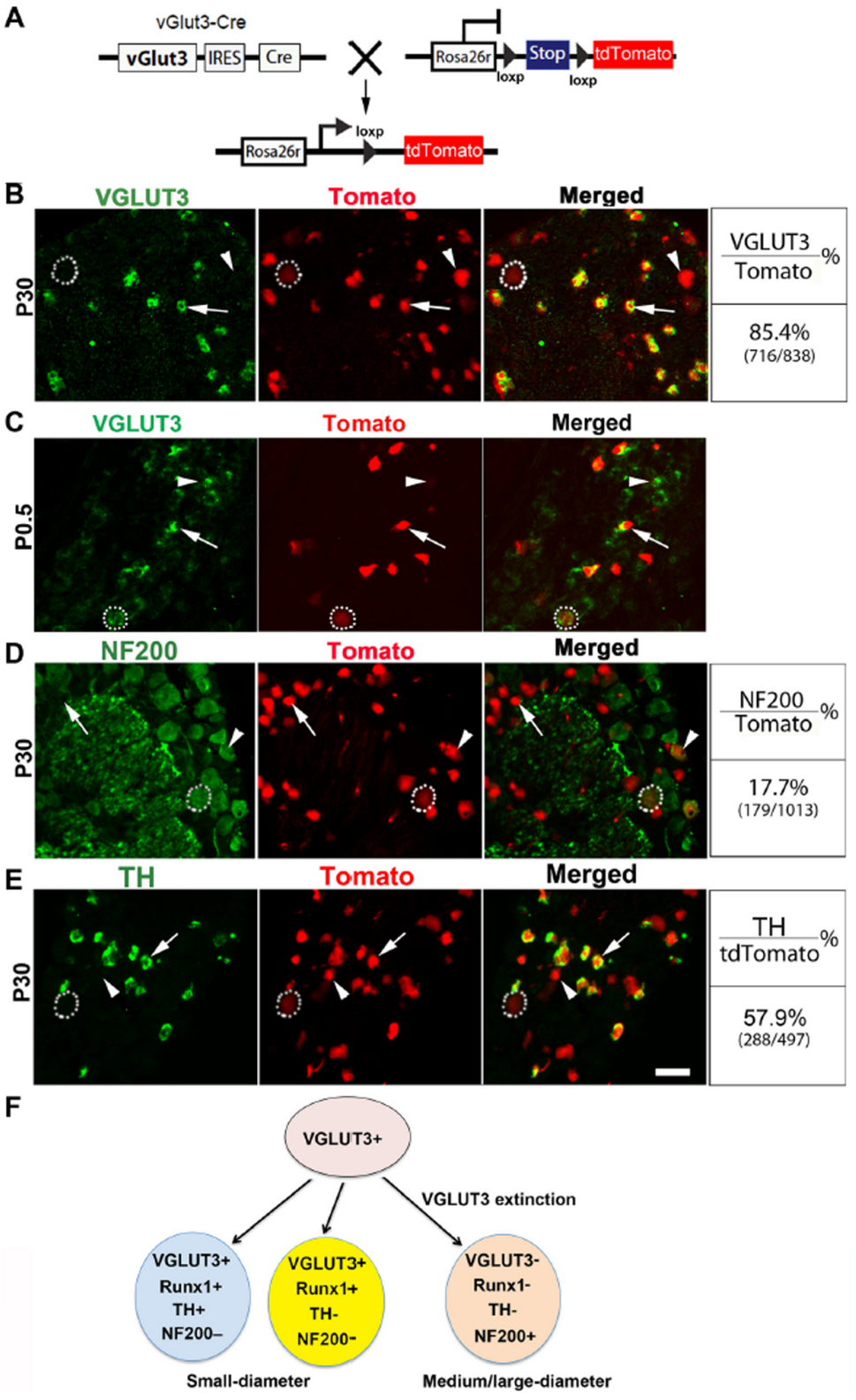

Figure 2.1 Genetic Marking of VGLUT3 lineage neurons

Figure 2.1 (Continued)

Figure 2.1 Genetic marking of VGLUT3 lineage sensory neurons. ***A***, Scheme of making *ROSA*$^{Tomato/+}$*; Vglut3*$^{Cre/+}$ mice. ***B, D, E***, Double staining of Tomato with VGLUT3 mRNA, NF200 protein, or TH mRNA on sections through lumbar DRG of adult *ROSA*$^{Tomato/+}$*; Vglut3*$^{Cre/+}$ mice. (***B-E***) Arrow, arrowhead, and dashed circle indicate the small-, medium-, and large-diameter Tomato$^+$ neurons, respectively. ***(C)*** Double staining of VGLUT3 mRNA on sections at P0.5 of *ROSA*$^{Tomato/+}$*; Vglut3*$^{Cre/+}$ mice. ***(E)*** Arrow and arrowhead indicating TH-positive and TH-negative small Tomato$^+$ cells, respectively. Dashed circles indicate large TH-negative Tomato$^+$ neurons. ***F,*** Summary of distinct molecular identities of VGLUT3-persistent versus VGLUT3-transient DRG neurons, based on data shown here and Fig. 3. That all VGLUT3-persistent neurons function as C-LTMR is based on a previous report (Seal et al., 2009). Scale bars, 50 μm.

Skin innervations by VGLUT3 lineage sensory neurons

To examine peripheral innervations, we took advantage of *ROSA*$^{Tomato/+}$*; Vglut3*$^{Cre/+}$ mice, in which Tomato expression can be used to directly visualize axonal endings. From transverse sections through hairy back skin, we sampled 266 hair follicles from 5 different mice and found that Tomato$^+$ fibers innervated 64.2% (171/266) of these hair follicles (Fig. 2.2A, arrow). The actual percentage of hairs with Tomato$^+$ fibers is likely higher since transverse sections may cut through parts of the hairs that do not contain Tomato$^+$ fibers. Most of these Tomato$^+$ fibers form longitudinal lanceolate endings (Fig. 2.2A, 2.2B). A double staining with NF200, a marker for myelinated fibers, showed that these Tomato$^+$ lanceolate endings were NF200-negative (Fig.

2.2A, 2.2B, arrows), and were wrapped with $NF200^+$ circumferential endings (Fig. 2.2A, arrowheads) and in some cases intertwined with $NF200^+$ longitudinal lanceolate endings (Fig. 2.2B, arrowheads). These unmyelinated $Tomato^+$ lanceolate endings are most likely derived from the TH^+ subset of VGLUT3-persistent C-LTMRs, as reported previously (Li et al., 2011).

We also observed two other types of unmyelinated Tomato+ nerve endings. In the hairy skin, $NF200^-$ (thereby unmyelinated) $Tomato^+$ free nerve endings were observed in the epidermis adjacent to hair follicles (Fig. 2.2C, arrow). In the glabrous skin, we observed another type of Tomato+ epidermal free nerve (Fig. 2.2D, arrow). These fibers entered the epidermis through the dermal papillae and extended all the way to the stratum corneum (or the cornified layer) of skin (Fig. 2.2D). Within the dermal papillae, $Tomato^+$ fibers were continuous and sometimes intertwined with NF200+ Meissner's corpuscles (Fig. 2.2D, arrowhead). However, in the outer layers of the epidermis, we observed strings of varicosities (Fig. 2.2D, arrow). The resolution of our microscope failed to distinguish if these varicosities were linked with nerve segments, or represented fibers dying back from the cornified layer. We referred to these previously un-described nerve fibers as "Dermal Papillae-Epidermis " or "D.P.E." nerve endings. Because TH^+ C-LTMRs only innervate hairs (Li et al., 2011), these unmyelinated epidermal nerve endings are most likely derived from the TH^- subset of VGLUT3-persistent neurons.

VGLUT3-transient A-mechanoreceptors appear to form Merkel-cell neurite complex. First of all, VGLUT3 itself was expressed in Merkel cells, as indicated by the co-expression of Tomato with the Merkel cell marker CK20 in the touch dome of the hairy skin (Fig. 2.2E, arrowheads). This VGLUT3 expression was further confirmed by immunostaining (see below) and is consistent with previous reports (Haeberle and Lumpkin, 2004; Nunzi, 2004). Whole

mount preparation of the hairy skin from *ROSA*$^{Tomato/+}$*; Vglut3*$^{Cre/+}$ mice revealed Tomato+ fibers innervating the touch domes (Fig. 2.2E, arrow). These Tomato+ fibers were myelinated, as suggested by the association of S100+ Schwann cells (Fig. 2.2F, arrow) and by the coexpression of NF200 (data not shown). Thus, these myelinated Tomato+ fibers are most likely derived from medium/large VGLUT3-transient A-mechanoreceptors.

To conclude this section of the results, each type of VGLUT3 lineage neurons has its specific terminal morphology (summarized in Fig. 2.2G). TH^+ VGLUT3-persistent C-LTMRs form longitudinal lanceolate endings around hairs. TH^- VGLUT3-persistent neurons form epidermal free nerve endings adjacent to hairs or the "D.P.E." ending passing through the dermal papillae in the thick glabrous skin. VGLUT3-transient A-mechanoreceptors form the Merkel cell-neurite complex.

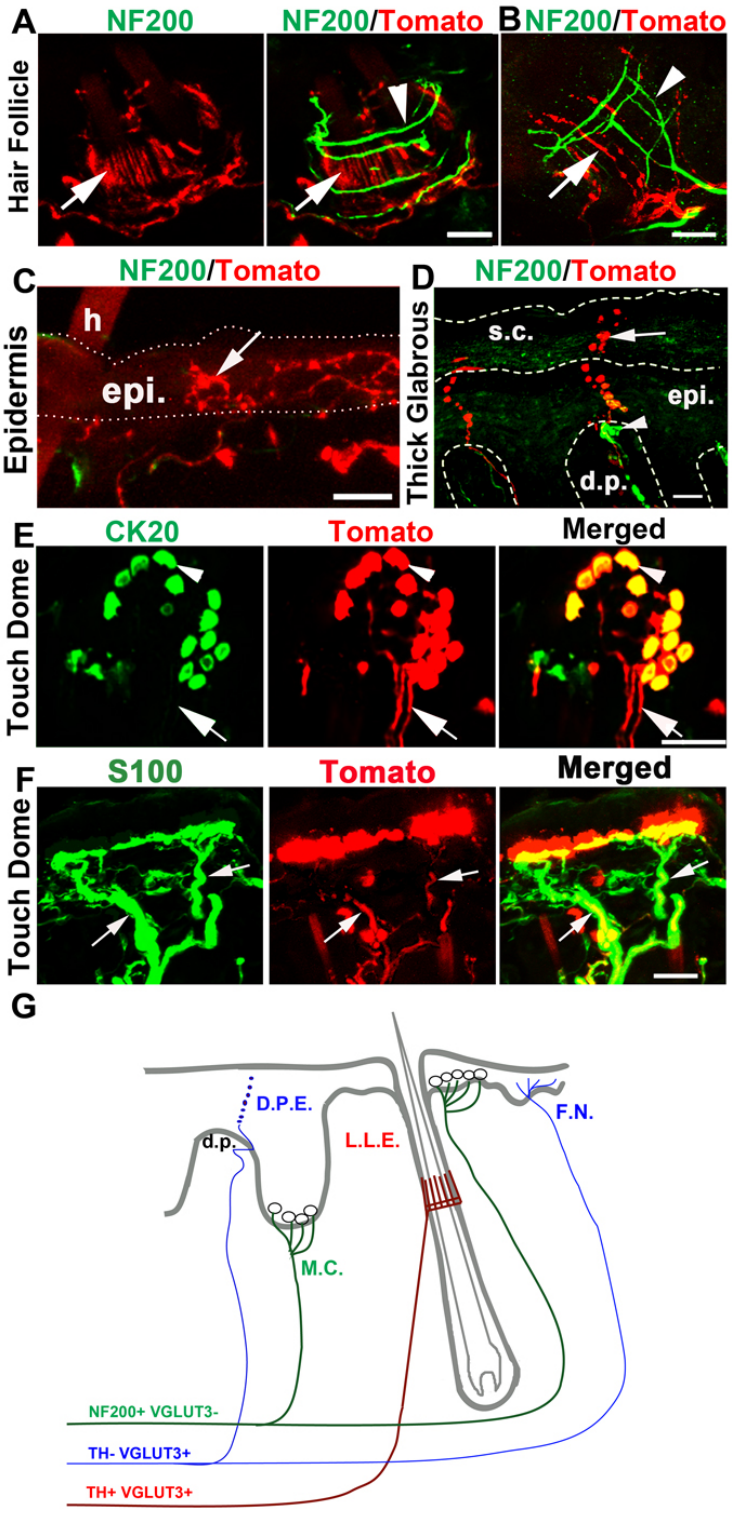

Figure 2.2 Skin innervations by VGLUT3 lineage sensory neurons

Figure 2.2 (Continued)

Figure 2.2 Skin innervations by VGLUT3 lineage sensory neurons. ***A-D***, Double staining of Tomato with NF200 on sections through the hairy skin (***A-C***) or the glabrous skin (***D***). (***A,B***), Arrow indicating Tomato^{+}; NF200^{-} longitudinal lanceolate endings wrapped by NF200^{+} circumferential ending (***A***, arrowhead) or intertwined with NF200^{+} longitudinal lanceolate endings (***B*****,** arrowhead). (***C)***, Arrow indicating NF200^{-};Tomato^{+} free nerve endings in the epidermis ("epi.") adjacent to a hair ("h"). (***D***), Arrow indicating a Tomato^{+} fiber passing through the dermal pappilae ("d.p.") and then entering the epidermis ("epi.") and the stratum corneum ("s.c"), referred to as the "D.P.E" ending (summarized in **G**). Arrowhead in (***D***) indicating a NF200^{+} Meissner's corpuscle. ***E***, Whole mount double staining of Tomato with the Merkel cell marker CK20 within a touch dome around a guard hair. Arrowhead indicating Merkel cells in the touch dome. ***F***, Arrows indicating Tomato^{+} fibers innervating the touch dome of the hairy skin are wrapped by S100^{+} Schwann cells (green). ***G***, Schematic summary of nerve endings from VGLUT3 lineage sensory neurons. "F.N.": free nerve endings. "L.L.E": longitudinal lanceolate endings. "M.C.": Merkel Cell complex. Red and blue indicating fibers derived from TH^{+} and TH^{-} VGLUT3-persistent neurons, respectively; Green indicates fibers derived from myelinated VGLUT3-transient mechanoreceptors. Scale bars, 20 μm.

Runx1 controls VGLUT3 expression and other molecular identities in C-LTMRs

We next asked how C-LTMRs are specified during development. Runx1 is a transcriptional factor that coordinates the development of a large cohort of unmyelinated DRG neurons (Liu et al.,

2011). We found that Runx1 mRNA was detected in most, if not all, small-diameter Tomato^{+} neurons in lumbar DRG of adult *ROSA$^{Tomato/+}$; Vglut3$^{Cre/+}$* mice (Fig. 2.3A, arrows). In contrast, Runx1 expression was not detected in medium/large Tomato^{+} neurons (Fig. 2.3A, arrowheads and dashed circles). In other words, Runx1 is associated exclusively with C-LTMRs within VGLUT3 lineage DRG neurons (summarized in Fig. 2.1F).

To determine the role of Runx1 in controlling C-LTMR development, we crossed Vglut3$^{Cre/+}$ mice with mice carrying a floxed allele of Runx1 (Runx1$^{F/+}$) (Growney, 2005), with the resulting conditional null mice referred to as *Runx1$^{F/F}$; Vglut3$^{Cre/+}$*. In these mutants, Cre-mediated recombination selectively removed Runx1 from VGLUT3 lineage sensory neurons. To monitor VGLUT3 lineage neurons by Tomato expression, we further created mutants carrying the ROSA26-CAG-LSTOPL-tdTomato reporter allele, referred to as *Runx1$^{F/F}$;ROSA$^{Tomato/+}$;Vglut3$^{Cre/+}$*. In situ hybridization showed that VGLUT3 mRNA, detected in adult lumbar DRG from control mice, was not detected in DRG from *Runx1$^{F/F}$;ROSA$^{Tomato/+}$; Vglut3$^{Cre/+}$* mice (Fig 2.3B). Mutant sensory neurons survived, as indicated by similar percentages of lumbar DRG neurons that were Tomato^{+} in mutant mice (20.8%) versus control mice (18.9%). Because Vglut3$^{Cre/+}$ mice were used to make Runx1 (in other words, Runx1 knockout occurred after onset of VGLUT3 expression), VGLUT3 expression was observed in some DRG neurons at P4.5, but not after P7 (data not shown). Thus, Runx1 is required to maintain VGLUT3 expression. TH expression was also eliminated (Fig. 2.3C and data not shown), further indicating an impairment of C-LTMRs in *Runx1$^{F/F}$;ROSA$^{Tomato/+}$; Vglut3$^{Cre/+}$* mice.

Other than DRG neurons, Runx1 expression is rarely detected in the nervous system (Levanon and Groner, 2002; Zagami, 2010). Consistently, we have not yet detected a loss of

VGLUT3 expression in other neural cells in Runx1 knockouts. Firstly, the VGLUT3 protein detected by immunostaining was still present in $CK20^{+}$ Merkel cells in the thick glabrous skin of $Runx1^{F/F};ROSA^{Tomato/+};\ Vglut3^{Cre/+}$ mice (Fig. 2.3D). Secondly, VGLUT3 is expressed transiently in the dorsal spinal cord in wild type mice, detectable at P4 and downregulated at P56 (Allen mouse spinal cord atlas, http:// mousespinal.brain-map.org). We found that at P7, normal VGLUT3 expression was still detected in the dorsal spinal cord of $Runx1^{F/F};ROSA^{Tomato/+};\ Vglut3^{Cre/+}$ mice (Fig. 2.3E), despite that VGLUT3 expression was already lost in lumbar DRG at this stage (data not shown). Finally, normal VGLUT3 expression was detected in serotonergic neurons in the adult hindbrain raphe nuclei (Fig. 2.3F) and in many other parts of the brain (data not shown). Thus, in $Runx1^{F/F};ROSA^{Tomato/+};\ Vglut3^{Cre/+}$ mice, VGLUT3 expression appears to be selectively eliminated in VGLUT3-expressing DRG neurons.

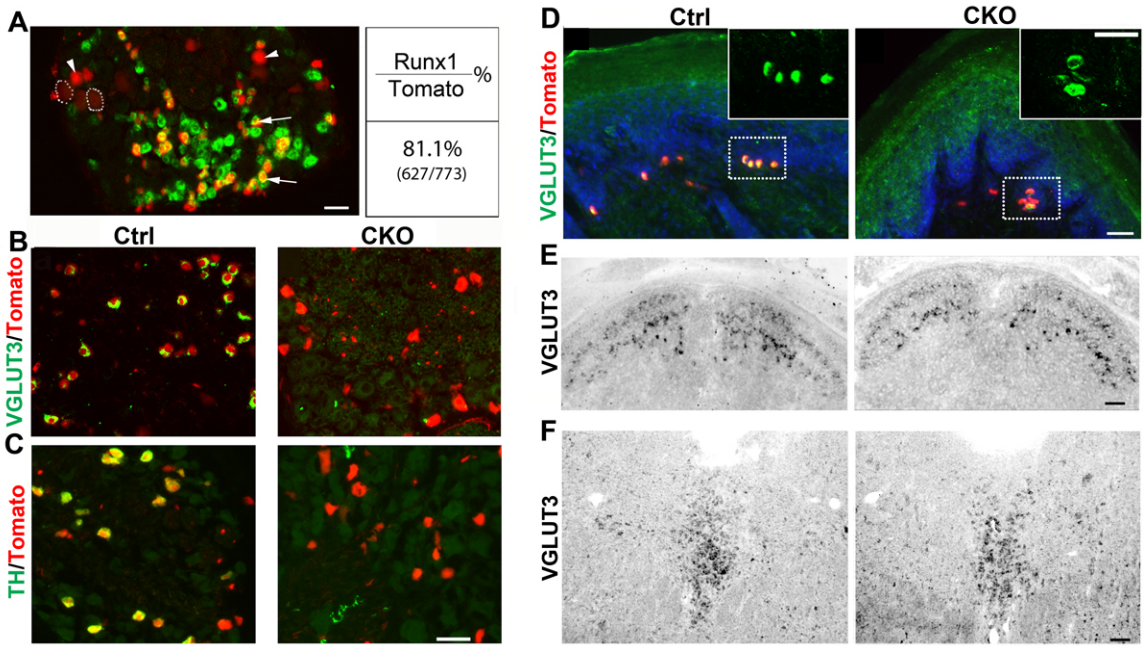

Figure 2. 3 Runx1 controls VGLUT3 and TH expression in C-LTMRs

Figure 2.3 Runx1 controls VGLUT3 and TH expression in C-LTMRs. A, Runx1 in situ hybridization on a lumbar DRG section from a *ROSA*$^{Tomato/+;}$ *Vglut3*$^{Cre/+}$ mouse. Runx1 mRNA was detected in small (arrows), but not medium (arrowheads) or large (dashed circles) Tomato+ neurons. B, C, Double staining of Tomato with VGLUT3 mRNA (B) or TH mRNA (C) detected by in situ hybridization on lumbar DRG sections from the *ROSA*$^{Tomato/+}$*; Vglut3Cre/+* control mice ("Ctrl") or *Runx1*$^{F/F}$*;ROSA*$^{Tomato/+}$*; Vglut3Cre/+* mutant mice ("CKO"). D, Double staining of Tomato with VGLUT3 immunostaining on sections through the thick glabrous skin from Ctrl and CKO mice. Red indicates Merkel cells, and the inserts are the higher magnification of the dashed boxes. E, F, VGLUT3 in situ hybridization on sections through P7 spinal dorsal horn (E) or the adult dorsal raphe nuclei of the brainstem (F) of the Ctrl and CKO mice. Scale bars, 50μm.

Runx1 controls the formation of lanceolate endings by C-LTMR

We next examined how peripheral terminal morphologies of VGLUT3 lineage neurons were affected in *Runx1*$^{F/F}$*;ROSA*$^{Tomato/+}$*; Vglut3*$^{Cre/+}$ mutant mice, using *ROSA*$^{Tomato/+}$*; Vglut3*$^{Cre/+}$ littermates as the control. A whole mount view on the hairy skin showed that in control mice, most Tomato^{+} fibers innervating hair follicles showed clear longitudinal lanceolate endings (Fig. 4A, B, left column, arrows). In contrast, while Tomato^{+} fibers in *Runx1*$^{F/F}$*;ROSA*$^{Tomato/+}$*; Vglut3*$^{Cre/+}$ mutant mice still innervated hair follicles, most of them did not form longitudinal lanceolate endings (Fig. 2.4A, B, right column), and instead circumferential Tomato^{+} endings were observed (Fig. 2.4A, B, right column, arrowheads). Thus, either the loss of longitudinal lanceolate endings unmasks Tomato^{+} circumferential endings, or a transformation from longitudinal to circumferential endings had occurred (Fig 2.4C). A double staining with NF200 further showed that these Tomato^{+} circumferential endings (Fig. 2.4B, small arrowheads) were located ventral to Tomato-negative NF200^{+} myelinated circumferential endings (Fig. 2.4B, big arrowheads).

In the epidermis around hairs, no obvious reduction of Tomato^{+} free nerve endings was observed (data not shown). The morphology of the unmyelinated D.P.E endings in the thick glabrous skin was also unchanged (data not shown). Also unchanged was the innervation of the touch dome by Tomato^{+} myelinated mechanoreceptors (data not shown), consistent with a lack of Runx1 expression in VGLUT3-transient A-mechanoreceptors. Thus, despite Runx1 controlling VGLUT3 expression in both TH^{+} and TH^{-} neurons, Runx1 is required selectively for TH^{+} C-LTMRs to form unmyelinated lanceolate endings.

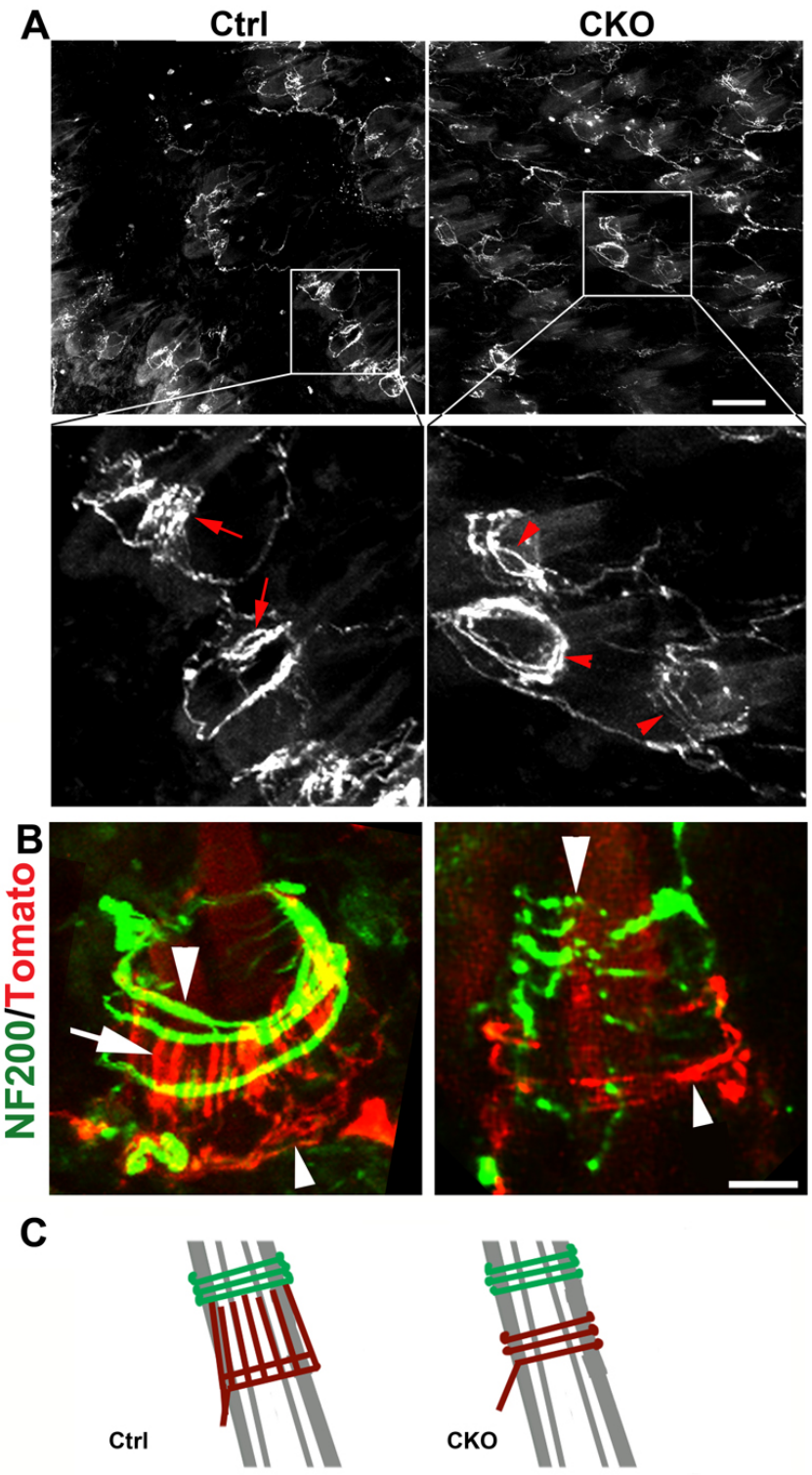

Figure 2. 4 Runx1 controls the formation of C-LTMR lanceolate endings

Figure 2.4 (Continued) Runx1 controls the formation of C-LTMR lanceolate endings. ***A,*** Wholemount view of Tomato^{+} nerve endings innervating hair follicles in the back skin of adult *ROSA$^{Tomato/+}$; Vglut3$^{Cre/+}$* control ("Ctrl"), and *Runx1$^{F/F}$;ROSA$^{Tomato/+}$; Vglut3$^{Cre/+}$* mutant ("CKO") mice. Arrows indicating longitudinal lanceolate endings and arrowheads for circumferential endings. ***B***, A double staining of Tomato and NF200 on transverse skin sections. Arrowheads indicating NF200^{+} circumferential endings. Arrow in the left panel indicating lanceolate endings in wild type control mice, while arrowheads in the right panel indicating a Tomato^{+} circumferential ending in mutant mice. ***C***, Schematic diagrams illustrating the change from the lanceolate to the circumferential ending in mutant mice.

Runx1 controls mechanosensitivity in VGLUT3^{+} C-LTMRs

To examine mechanosensitivity, we performed whole-cell patch recordings on cultured DRG neurons (Coste et al., 2010; Drew, 2002; Hu, 2006; McCarter, 1999; Vilceanu and Stucky, 2010). We first tried *ROSA$^{Tomato/+}$; Vglut3$^{Cre/+}$* control mice, by applying mechanical forces to the cell surface of Tomato^{+} neurons (visualized under a fluorescent microscope) via a piezo-electrically driven glass probe, while another pipette was used for patch-clamp recording of mechanically evoked currents (Fig. 2.5A). First, we determined activation curves for each mechanosensitive current by applying incremental mechanical forces (Fig. 2.5B) and found that membrane displacement evoking half of the maximum mechanical current ($Stim_{50}$) was 6.9 μm (Fig. 2.5C). We then grouped currents on the basis of half-inactivation times (τ_{inac}) during 8 μm-displacement stimulation, and revealed three classes of currents (Fig. 2.5D): rapidly adapting ($\tau_{inac} < 10$ ms),

slowly adapting (τ_{inac} >10 ms, including intermediate and ultra-slow) and mixed adapting. The mixed adapting current was well fitted by two exponentials, instead of one exponential fitting (Drew, 2004): τ_{inac1} < 10 ms and τ_{inac2} >10 ms (Fig. 2.5D). In other words, mixed adapting neurons are composed of both slowly and rapidly adapting mechanical currents. In contrast, some neurons did not respond to mechanical probing and were referred to as non-responders.

For 51 recorded small-diameter (<25 μm) Tomato^{+} neurons from 4 individual mice, corresponding to VGLUT3-persistent neruons, rapidly adapting (35.8 ± 2.4%) and mixed adapting (31.8 ± 4.8%) currents are predominant, followed by slowly adapting (7.8 ± 2.8%) and non-responders (24.5 ± 3.4%) (Fig. 2.5E). For 13 recorded medium/large-diameter (>35 μm) Tomato^{+} neurons (representing VGLUT3-transient neurons) from 3 individual mice, mixed adapting currents are predominant, followed by slowly adapting rapidly adapting, and non-responders (data not shown). Thus, different subtypes of VGLUT3 lineage neurons may contain distinct mechanical channel components.

We next asked if mechanosensitivity was affected in Runx1 conditional knockouts. Recording from 55 cultured small-diameter (<25 μm) Tomato^{+} neurons from 5 individual *Runx1$^{F/F}$;ROSA$^{Tomato/+}$; Vglut3$^{Cre/+}$* mutant mice showed a marked loss of mechanosensitive neurons in comparison with *ROSA$^{Tomato/+}$; Vglut3$^{Cre/+}$* control mice, with rapidly adapting neurons reduced from 35.8 ± 2.4% to 7.7 ± 5.6%, and mixed adapting neurons reduced from 31.8 ± 4.8% to 2.0 ± 2.0% (Fig. 2.5E). Because of the rarity of neurons expressing slowly adapting currents, it remains uncertain if these neurons were significantly reduced (Fig. 2.5E). Accordingly, there was a marked increase in non-responders, from 24.5 ± 3.4% in control mice to 88.3 ± 5.6% in mutants (Fig. 2.5E). Moreover, the average current density in the remaining 7 (out of 55) mechanosensitive

small Tomato^{+} neurons was significantly reduced in comparison with that in control mice (from 31.8 ± 5.3 pA/pF to 12.8 ± 4.2 pA/pF, $P < 0.01$). In contrast, no change in average current density was detected in medium/large (>35 μm) Tomato^{+} neurons (data not shown), consistent with a lack of Runx1 expression in medium/large VGLUT3-transient A-mechanoreceptors. Thus, Runx1 is selectively required to establish mechanosensitivity in small-diameter VGLUT3-persistent neurons.

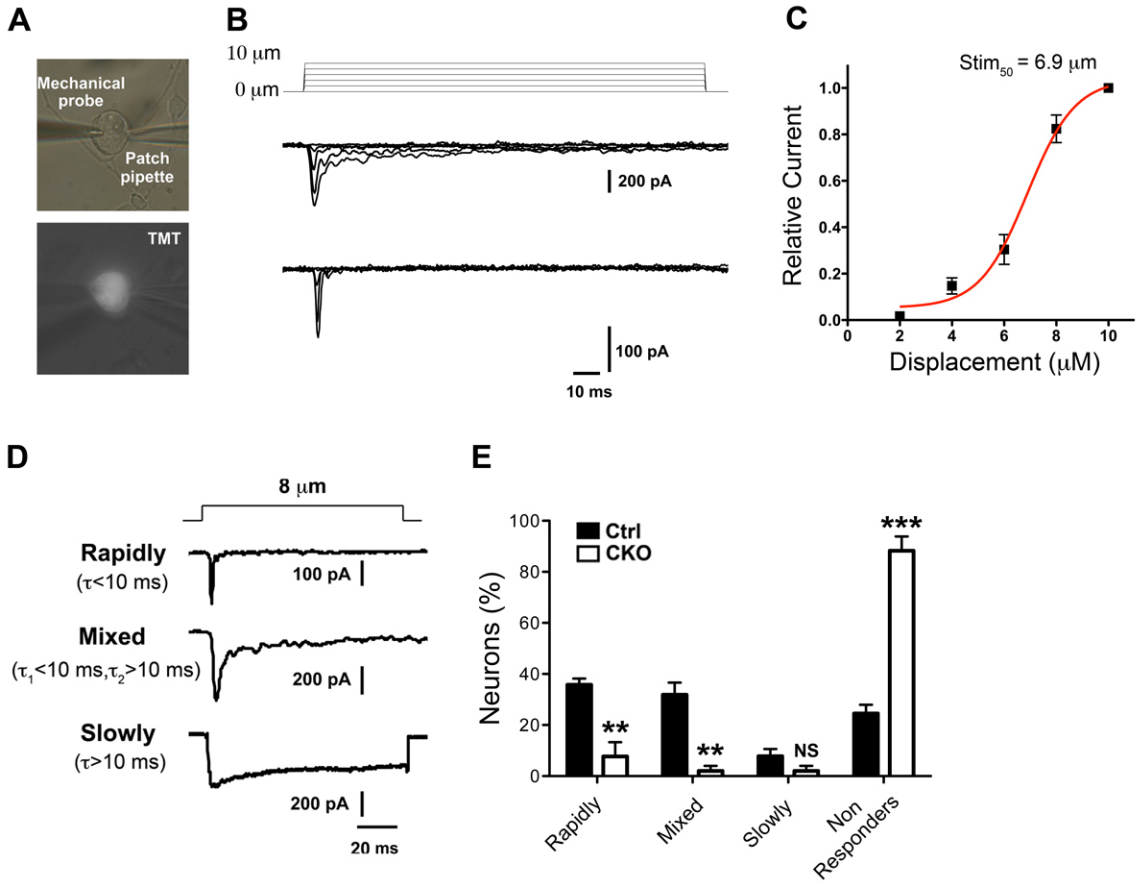

Figure 2. 5 Runx1 controls mechanosensitivity in VGLUT3-expressing C-LTMRs

Figure 2.5. Runx1 controls mechanosensitivity in VGLUT3^{+} C-LTMRs. ***A***, photograph showing mechanical stimulation of a patch-clamped Tomato^{+} DRG neuron from *ROSA$^{Tomato/+}$; Vglut3$^{Cre/+}$* control ("Ctrl") mice. ***B***, Families of rapidly adapting mechanosensitive current traces evoked by a

(Figure 2.5 continued) series of mechanical steps in 2 μm increments for the DRG cells from Ctrl mice. ***C***. Relationship between stimulation displacement and relative currents from ***B*** (n = 6). ***D***, Representative traces of rapidly adapting, mixed adapting and slowly adapting currents evoked by a short mechanical stimulus of 8 μm. ***E,*** Histograms showing the proportions of distinct mechanosensitive currents observed in small-diameter VGLUT3 neurons from control "Ctrl" (n = 4 mice, 51 neurons totally) and *Runx1*$^{F/F}$*;ROSA*$^{Tomato/+}$*; Vglut3*$^{Cre/+}$ mutant ("CKO") mice (n = 5 mice, 55 neurons totally), respectively. **, $P < 0.01$, ***, $P < 0.001$. Ctrl vs. CKO, Student's unpaired *t* test. "NS": non-significant.

Runx1 controls mechanosensitivity by regulating piezo2 expression

Piezo2 mediates mechanically evoked currents in a subset of cultured DRG neurons in mice (Coste et al., 2010). In situ hybridization on lumbar DRG sections from *ROSA*$^{Tomato/+}$*; Vglut3*$^{Cre/+}$ fate-mapping mice showed that 83.7 ± 1.9% of Tomato^{+} neurons expressed Piezo2 at a relatively high level (Piezo2^{high}) (Fig. 2.6A). Most small-diameter and medium-diameter Tomato^{+} neurons expressed Piezo2^{high} (Fig. 2.6A), and only large Tomato^{+} neurons showed Piezo2^{low} expression (Fig. 2.6A).

We next examined Piezo2 expression in lumbar DRGs of Runx1 mutant and control mice. Double staining showed that the percentage of Tomato^{+} neurons with detectable Piezo2 was markedly reduced in mutants (Fig. 2.6A), from 83.7 ± 1.9% in control mice to 13.6 ± 2.9% in *Runx1*$^{F/F}$*;ROSA*$^{Tomato/+}$*; Vglut3*$^{Cre/+}$ mice ($P < 0.001$). Most small-diameter Tomato^{+} neurons, representing VGLUT3-persistent neurons, lost Piezo2 expression (Fig. 2.6A). In contrast, medium-

diameter Tomato^{+} neurons retained Piezo2^{high} expression in mutant mice (Fig. 2.6A), consistent with the lack of Runx1 expression in these neurons (Fig. 2.3A).

To determine if Piezo2 is required to mediate mechanical responses in VGLUT3 lineage neurons, we used the same set of siRNAs (a mixture of four) used by Coste et al. (Coste et al., 2010) to knock down Piezo2 expression in cultured DRG neurons from *ROSA*$^{Tomato/+}$*; Vglut3*$^{Cre/+}$ mice. By solution electroporation, we found that nearly 98.3% of Tomato^{+} neurons were transfected with siRNAs, monitored by the inclusion of a fluorescence-conjugated scrambled siRNA (data not shown). In 4 paired mice, compared with the results from 33 small Tomato^{+} neurons transfected with control siRNA, transfection with Piezo2 siRNAs in 38 neurons led to a marked reduction of small Tomato^{+} neurons expressing rapidly adapting currents (from 35.8 ± 6.3% with control siRNA to 4.4 ± 2.6% with Piezo2 siRNAs), which in turn resulted in a marked increase in non-responders (from 29.2 ± 3.2% to 74.0 ± 6.3%) (Fig. 2.6B). Piezo2 knockdown appeared to lead to a reduction of mixed adapting neurons (from 28.8 ± 12.3% to 6.9 ± 4.2%), and an increase of slowly adapting neurons (from 6.2 ± 4.0% to 14.6 ± 6.4%), but these changes did not reach statistical significance (Fig. 2.6B). These findings suggest that Runx1-dependent Piezo2 is required to mediate mechanosensitivity in small-diameter Tomato^{+} neurons.

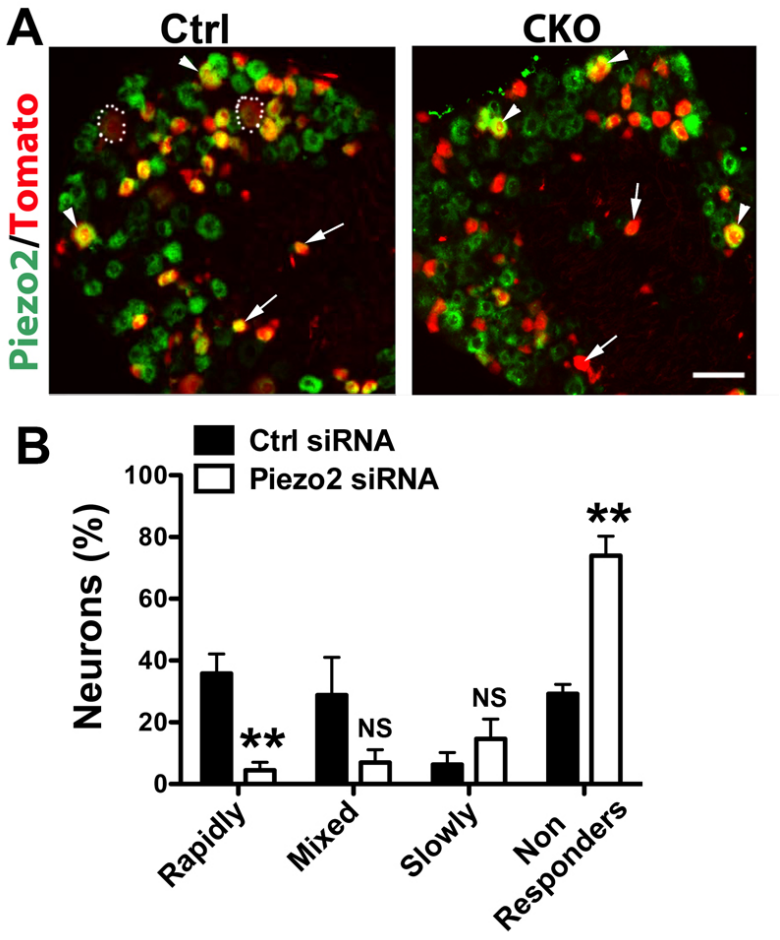

Figure 2. 6 Runx1 controls C-LTMR mechanosensitivity

Figure 2.6 Runx1 controls C-LTMR mechanosensitivity by regulating Piezo2 expression. ***A,*** Piezo2 in situ hybridization on lumbar DRG sections from $ROSA^{Tomato/+}$; $Vglut3^{Cre/+}$ control ("Ctrl") mice or $Runx1^{F/F}$;$ROSA^{Tomato/+}$; $Vglut3^{Cre/+}$ mutant ("CKO") mice. Arrows, arrowheads, and dashed circles indicating small, medium, and large $Tomato^{+}$ neurons, respectively. ***B***, Histograms showing the percentages of neurons exhibiting different types of mechanosensitive currents upon transfection with scrambled control siRNA (Ctrl, n = 4 mice, 33 neurons totally) or Piezo2 siRNAs (n = 4 mice, 38 neurons totally). **, $P < 0.01$. Ctrl vs. Piezo2 siRNAs, Student's unpaired *t* test.

Mechanical pain from glabrous skin was largely unaffected in Runx1f/f; Vglut3cre/+ mutant mice.

The selective impairment in C-LTMRs in *Runx1*$^{F/F}$*; Vglut3*$^{Cre/+}$ mutant mice offered a unique opportunity to reassess the physiological functions of these mechanoreceptors. We therefore performed a series of acute and chronic pain assays in *Runx1*$^{F/F}$*; Vglut3*$^{Cre/+}$ mutant mice, using Runx1$^{F/F}$ or Runx1$^{F/+}$ littermates as control. The thresholds in response to light and intense mechanical stimuli delivered by Randall-Selitto apparatus and the von Frey filaments, respectively, were unchanged between mutant and control mice (Fig. 2.7A,B). Similarly, *Runx1*$^{F/F}$*; Vglut3*$^{Cre/+}$ mutant mice showed no difference in paw withdrawal latencies in response to radiation heat stimuli, in comparison with control littermates (Fig. 2.7C). Thus, acute mechanical and heat pain remains intact in *Runx1*$^{F/F}$*; Vglut3*$^{Cre/+}$ mutant mice.

Intradermal injection of capsaicin into the plantar of the hindpaw induces not only acute nociception but also secondary mechanical allodynia (Campbell, 2006; LaMotte, 1991; Torebjörk, 1992). We found that duration of licking following capsaicin injections, a measurement of acute chemical pain, was comparable between *Runx1*$^{F/F}$*; Vglut3*$^{Cre/+}$ mutant mice and control littermates (Fig. 2.7D). Capsaicin also induced similar degrees of secondary mechanical hypersensitivity on the adjacent plantar area, as indicated by similar reduction in withdrawal thresholds in response to von Frey stimuli (Fig. 2.7D). Thus, capsaicin-induced secondary mechanical allodynia in the glabrous skin also remained intact in mutants.

To assess neuropathic pain, we used the spared nerve injury (SNI) model (Decosterd and Woolf, 2000b). We found that both control and mutant mice showed indistinguishable mechanical

hypersensitivity following SNI (Fig. 2.7E), indicating that neuropathic mechanical pain is unaffected in mutant mice.

To assess inflammatory pain, we first performed intraplantar injection of the Complete Freund's Adjuvant (CFA). Three day after intraplantar injection of CFA, both thermal hypersensitivity (measured by the radiant heat assay) and mechanical allodynia (measured by the von Frey assay) remained intact in *Runx1*$^{F/F}$*; Vglut3*$^{Cre/+}$ mice in comparison with control mice (Fig. 2.7F). We next performed intraplantar injection of carrageenan (Kayser, 1987). Thermal hypersensitivity was again unchanged in mutant mice (Fig. 2.7G). However, although mechanical hypersensitivity induced by carrageenan still developed in mutants, the mutants showed a modest, yet significant, increase in mechanical thresholds, in comparison with control littermates (Fig. 2.7G), suggesting a minor impairment of inflammatory mechanical pain. Collectively, these studies suggest that developmental impairment of VGLUT3-persistent neurons in *Runx1*$^{F/F}$*; Vglut3*$^{Cre/+}$ mice does not markedly affect acute or chronic mechanical pain measured from the glabrous skin.

Since TH^{+} C-LTMRs only innervate the hairy skin (Li et al., 2011), we further examined mechanical allodynia following capsaicin injection into the hairy skin of the dorsal hindpaw. We again did not find any difference between *Runx1*$^{F/F}$*; Vglut3*$^{Cre/+}$ mice versus control mice (data not shown). All together, we conclude that mechanical allodynia is largely unaffected in *Runx1*$^{F/F}$*; Vglut3*$^{Cre/+}$ mutant mice.

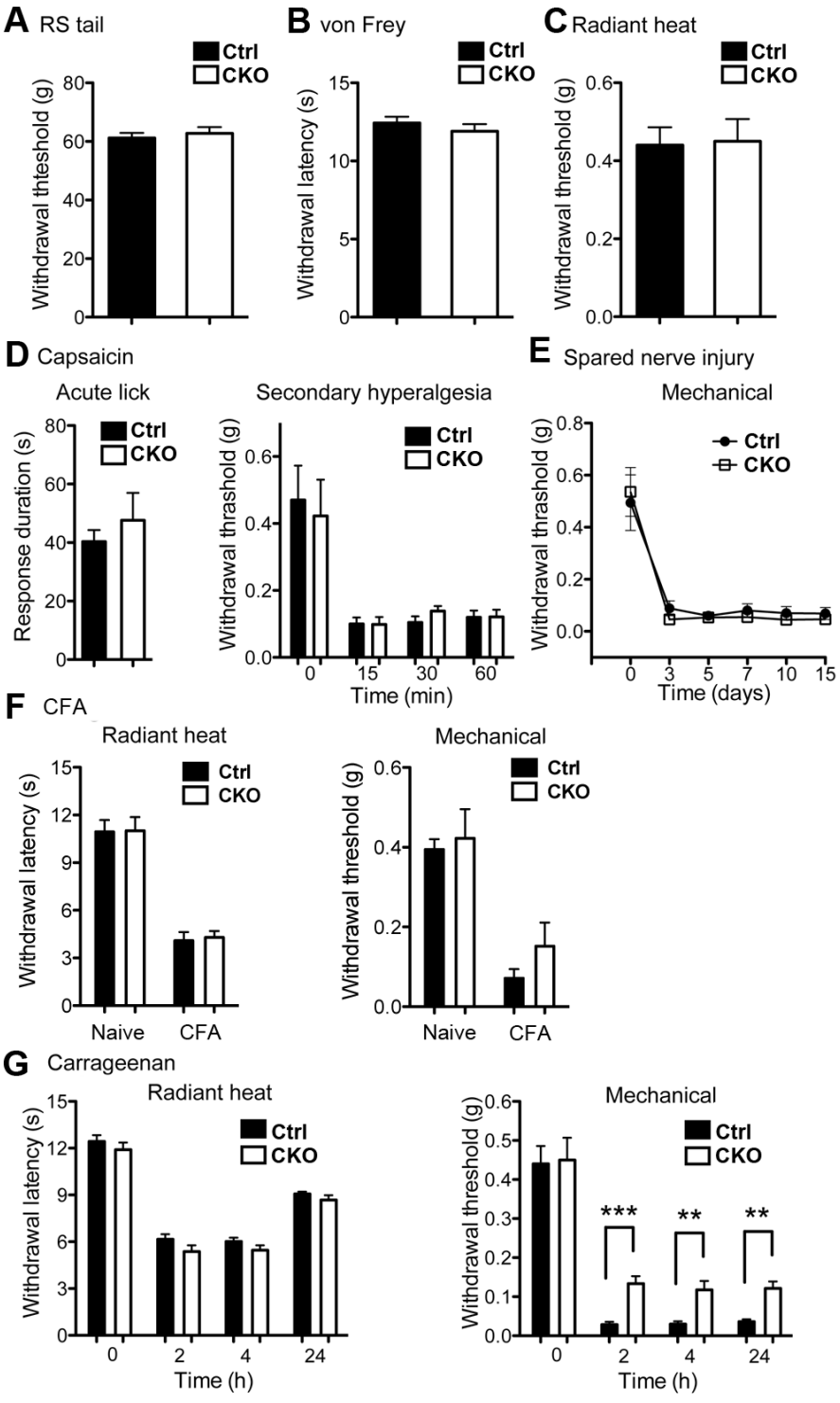

Figure 2. 7 Pain behavior analysis of *Runx1* conditional knockout mice

Figure 2.7 (Continued) Pain behavioral analyses. ***A***, The Randall-Selitto assay. *Runx1*$^{F/F}$*; Vglut3*$^{Cre/+}$ mutant ("CKO") and control (Ctrl) mice showed the same thresholds to tail withdrawal (Ctrl, n = 10, 61.2 ± 1.8 g; CKO, n = 8, 62.8 ± 2.2 g; $P > 0.05$, Student's unpaired *t* test). ***B***, The von Frey assays for acute mechanical pain measurement. No difference in withdrawal thresholds (Ctrl, n = 10, 0.44 ± 0.05 g; CKO, n = 8, 0.45 ± 0.06 g; $P > 0.05$, Student's unpaired *t* test). ***C***, The Hargreaves radiant heat test. No difference in withdrawal thresholds (Ctrl, n = 10, 12.4 ± 0.4 s; CKO, n = 8, 11.9 ± 0.5 s; $P > 0.05$, Student's unpaired *t* test). ***D***, In both Ctrl and CKO mice, capsaicin injection into the hindpaw produced similar licking response in the first 5 min (Ctrl, n = 6, 40.3 ± 4.0 s; CKO, n = 5, 47.6 ± 9.4 s; $P > 0.05$, Student's unpaired *t* test). Both CKO and Ctrl mice showed similar decrease in mechanical threshold at a distance from the injection site at 15, 30 and 60 min after injection (n = 7, p > 0.05, one-way ANOVA). ***E***, SNI-induced neuropathic pain. After SNI, a similar reduction in mechanical thresholds by von Frey assay was observed in Ctrl versus CKO mice (Ctrl, n = 7; CKO, n = 10; $P > 0.05$, by one-way ANOVA). ***F,*** CFA-induced inflammatory pain. Both Ctrl and CKO mice were injected with CFA in one hindpaw. Tested at before (naive) and 3 day after (CFA) injection (Ctrl, n = 7; CKO, n = 8; $P > 0.05$, Student's unpaired *t* test). ***G***, Carrageenan-induced inflammatory pain. Ctrl and CKO mice were injected with carrageenan in the hindpaw. Tested at 2, 4, 24 h after injection. Both genotypes show a similar withdrawal threshold to radiant heat at all times tested (Ctrl, n = 10; CKO, n = 8; $P > 0.05$, Student's unpaired *t* test). Both Ctrl and CKO mice showed significant reduction in mechanical thresholds (**, $P < 0.01$; #, $P < 0.05$), but CKO mice exhibited a small but significant increase in mechanical threshold at all times tested in comparison with Ctrl mice (Ctrl, n = 10; CKO, n = 8; *, $P < 0.05$, Ctrl vs. CKO, Student's unpaired *t* test).

Discussion

By investigating the ontogeny, mechanosensitivity, developmental control and physiological functions of VGLUT3 lineage sensory neurons, we have gained novel insight into several areas on mammalian mechanoreceptors. First, the genetic fate mapping shows that VGLUT3 lineage mechanoreceptors are composed of multiple subgroups, including 1) medium/large VGLUT3-transient myelinated A-mechanoreceptors forming the Merkel cell-neurite complex, and 2) small-diameter VGLUT3-persistent unmyelinated neurons that are further divided into two sub-populations: TH^+ C-LTMRs forming the lanceolate endings around hairs and TH^- neurons forming epidermal free nerve endings. Secondly, with great excitement generated from the recent identification of Piezo2 as a mechanically gated ion channel, we now show that Piezo2 is expressed in VGLUT3 lineage C-LTMRs, and Piezo2 mediates mechanosensitivity in these neurons. Thirdly, the runt domain transcription factor Runx1 plays a pivotal role in controlling C-LTMR development, including the formation of terminal morphologies, the expression of VGLUT3 and Piezo2, and the establishment of mechanosensitivity. Fourthly, with selective loss of VGLUT3 and mechanosensitivity in C-LTMRs, behavioral analyses in this new line of *Runx1* conditional knockouts allow us to revisit the roles of these neurons in sensing mechanical pain.

Distinct transcription factors control the formation of specialized mechanoreceptor terminal nerve endings

Most known low threshold mechanoreceptors form specialized nerve endings that allow them to respond to specific types of mechanical stimuli (Bautista and Lumpkin, 2011; Delmas, 2011; Johnson, 2001). Our studies consolidate the idea that distinct transcription factors control the formation of these nerve endings. The basic leucine-zipper transcription factor c-Maf and the ETS domain protein Er81 are required for the formation of the Pacinian corpuscles that are specialized to sense high-frequency vibrations (Hu, 2012; Sedý, 2006; Wende et al., 2012). Both c-Maf and the homeobox protein Shox2 are necessary for the formation of the Meissiner corpuscles that respond to skin motions and detect low-frequency vibration (Abdo et al., 2011; Scott et al., 2011; Wende et al., 2012). In the hairy skin, the longitudinal lanceolate endings respond to hair defection, and two recent studies reveal heterogeneity of mechanoreceptors forming these endings (Li et al., 2011; Wende et al., 2012). Formation of $NF200^{+}$ myelinated lanceolate endings is dependent on c-Maf (Wende et al., 2012). We demonstrate here that Runx1 is required for the TH^{+} subset of C-LTMRs to form unmyelinated lanceolate endings. In the absence of Runx1, prospective unmyelinated lanceolate endings are either lost or transformed to become circumferential endings. The Merkel cell-neurite complex is specialized for fine tactile discrimination, thereby the perception of form and texture (Bautista and Lumpkin, 2011; Delmas, 2011; Johnson, 2001). The basic helix-loop-helix protein Atoh1 controls the genesis of the Merkel cells (Maricich et al., 2012; Maricich et al., 2009). Among mechanoreceptors innervating the Merkel cells, Shox2 and the Runx1-related protein Runx3 appear to be required for proper

development of the $TrkB^+$ and $TrkC^+$ subsets, respectively (Abdo et al., 2011; Senzaki K, 2010). We show here that VGLUT3-transient myelinated mechanoreceptors innervate the Merkel cells, and we further found that among them 55% and 45% express the neurotrophin receptors TrkB and TrkC, respectively (Supplementary Figure 2.1). Further studies will be warranted to determine if Runx3 and Shox2 specify distinct subsets of VGLUT3-transient A-mechanoreceptor. All together, the emerging theme is that distinct transcription factors act alone or in combination to control the formation of distinct mechanoreceptor nerve endings and/or end organs.

Runx1-dependent Piezo2 mediates mechanosensitivity in C-LTMRs

Piezo proteins have been shown to be the long sought mechanically gated ion channels in mammals and in flies (Coste et al., 2010; Coste et al., 2012; Kim et al., 2012), a channel that is distinct from those found in *C.elegans* (Geffeney, 2012). In mice, elevated Piezo2 ($Piezo2^{high}$) expression is detected in ~20% of DRG neurons (Coste et al., 2010). Here we found that a large subset of $Piezo2^{high}$ neurons represent VGLUT3 lineage neurons, including small-diameter VGLUT3-persistent neurons and medium-diameter A-mechanoreceptors. Knock down of Piezo2 leads to a marked loss of rapidly adapting mechanical current in small VGLUT3-persistent neurons, and a concurrent increase of mechano-insensitive neurons (Fig. 2.6). The loss of Piezo2 expression should at least partly contribute to the marked loss of mechanosensitivity in VGLUT3-persistent neurons of *Runx1* mutants, although our data do not rule out that Runx1 may control other molecular components involved with mechanotransduction.

Notably, the adaption rates of mechanically evoked currents recorded from cultured neurons are different from those recorded from ex-vivo skin-nerve preparations. By ex-vivo skin-nerve preparations, C-LTMR neurons exhibit intermediate adaption rates in response to stationary mechanical stimuli (Li et al., 2011; Seal et al., 2009), and Merkel cells are innervated by type I slowly adapting Aβ-LTMRs, or SA1 Aβ-fibers (Bautista and Lumpkin, 2011; Delmas, 2011; Lumpkin, 2010). In contrast, mechanically evoked currents from cultured VGLUT3 lineage neurons mainly exhibit rapid or mixed adaption rates. The simplest interpretation is that adaption rates are modulated by specialized nerve endings/structures or the extracellular matrix molecules in the skin (Lumpkin, 2010). For example, laminin-332 released from keratinocytes is able to suppress the rapidly adapting mechanosensitive current (Chiang and Lewin, 2011). Similarly, Merkel cells themselves are mechanosensitive, and the SA1 current is selectively lost in mice lacking Merkel cells, despite the continuous innervation of Aβ-fibers to prospective touch domes (Maricich et al., 2009).

What are the physiological functions of VGLUT3-persistent DRG neurons?

Seal et al. reported that mechanical allodynia induced by inflammation, capsaicin, or nerve injury was all markedly impaired in mice lacking *Vglut3* (Seal et al., 2009). They further proposed that VGLUT3-persistent C-LTMRs are required for the execution, but not the induction, of mechanical allodynia (Seal et al., 2009). This interpretation is, however, complicated by the VGLUT3 expression in many parts of the nervous system (El Mestikawy, 2011) (Fig. 2.3). By using *Vglut3*-

Cre mice to knock out *Runx1*, we have now created a new line of mutant mice (*Runx1*$^{F/F}$; *Vglut3*$^{Cre/+}$) with a selective loss of VGLUT3 and mechanosensitivity in VGLUT3-persistent neurons, which offered a unique opportunity to reassess the physiological functions of these neurons.

We found that *Runx1*-dependent VGLUT3-persistent neurons do modestly contribute to the inflammatory mechanical hypersensitivity induced by carrageenan and measured from the hindpaw plantar. Among VGLUT3-persistent neurons, the TH$^+$ C-LTMRs innervates the hairy skin (Li et al., 2011), and only the TH$^-$ subset innervates the thick glabrous skin, forming the "D.P.E" endings that pass through the dermal papillae to enter the epidermis. Previous electrophysiological recording showed that most if, not all, VGLUT3-persistent neurons are C-LTMRs (Li et al., 2011). Thus, the TH$^-$ subset of VGLUT3-persistent neurons might also function as C-LTMRs, although further studies are needed to consolidate this hypothesis. Regardless, a defect in TH$^-$neurons could in principle contribute to the minor inflammatory pain deficit measured from the glabrous skin in *Runx1*$^{F/F}$; *Vglut3*$^{Cre/+}$ knockout mice.

Surprisingly, mechanical allodynia induced by nerve lesions, capsaicin and another inflammatory reagent CFA in *Runx1*$^{F/F}$; *Vglut3*$^{Cre/+}$ knockout mice is unaffected in *Runx1*$^{F/F}$; *Vglut3*$^{Cre/+}$ knockout mice. Even carrageenan-induced mechanical pain is only modestly impaired. How could we explain the marked loss of this type of pain in *Vglut3* complete null mice? Two possibilities are worthy for consideration.

Firstly, VGLUT3 may only play a developmental role in VGLUT3-persistent neurons. VGLUT3 expression was initiated at prenatal and neonatal stages (Fig. 2.1). In *Runx1*$^{F/F}$; *Vglut3*$^{Cre/+}$ knockout mice, a transient VGLUT3 expression was still preserved at neonatal stages

since *Vglut3-Cre* mice were used for *Runx1* knockout. Transient VGLUT3 expression has been shown to play a role in circuit maturation in the brain (Noh et al., 2010), and it is well known that spinal circuits also undergo maturation processes during postnatal development (Fitzgerald, 2005). Thus, if VGLUT3-dependent glutamate release from VGLUT3-persistent DRG neurons plays a role in circuit maturation and if this process only requires a transient VGLUT3 expression, maturation of sensory circuits would be impaired in *Vglut3* null mice, but not in $Runx1^{F/F}$; $Vglut3^{Cre/+}$ knockout mice.

Secondly, VGLUT3 activity in other parts of the nervous system may control mechanical hypersensitivity, such as neurons forming the Merkel cell-neurite complex, neurons located in the dorsal spinal cord, and hindbrain 5-HT neurons. Accordingly, the normal VGLUT3 expression in these neural cells in $Runx1^{F/F}$; $Vglut3^{Cre/+}$ knockout mice might explain why mechanical pain is unaffected. This interpretation is consistent with reports that VGLUT3 expression is confined to Nav1.8 lineage DRG neurons, and neuropathic mechanical pain is unaffected upon ablation of these neurons (Abrahamsen et al., 2008; Shields, 2012). Future conditional knockout of VGLUT3 in various parts of the nervous system will be needed to clarify where VGLUT3 operates to mediate mechanical pain.

Methods

Animals

The generation of mice carrying the floxed Runx1 allele and ROSA26-CAG-LSTOPL-tdTomato reporter mice have been described previously (Chen et al., 2006; Madisen et al., 2010). The generation of Vglut3-Cre mice will be described elsewhere by Vong L and Lowell BB. For histochemical studies, 2-3 pairs of control and mutant mice of 1-2 month old were used. For each behavioral analysis, 6-10 pairs of two-month-old mutant and control littermates were used. Animals were assigned in treatment groups in a blinded fashion and pain response was measured in a blinded manner. All behavioral test protocols were approved by the Institutional Animal Care and Use Committee at Dana-Farber Cancer Institute.

In situ hybridization (ISH) and immunohistochemistry (IHC)

In situ hybridization procedures have been described previously(Chen et al., 2006). Anti-sense Piezo2 probe (0.928 kb) was amplified from cDNA prepared from adult DRG, and was labeled with digoxigenin (Roche Dignostics). Immunohistochemistry on DRG sections was performed using rabbit anti-CGRP (1/1000, Santa Cruz), rabbit anti-NF200 (1/500, millipore), rabbit anti-VGLUT3 (1/100, Sys), mouse anti CK20 (1/20, Abcam), and rabbit anti-S100 (1/400, Dako), diluted in 0.1% of Triton X-100 plus 10% of goat serum in PBS. The binding of IB4-biotin (10 mg/ml, Sigma) was carried out as previously described33. The ISH/Tomato double staining was

performed as previously described46; the Tomato fluorescent signal was first photographed, followed by ISH. The pseudo fluorescent ISH signals (for VGLUT3, TH, Piezo2, and GFRa2) were converted from bright field images and then merged onto the Tomato images. For Tomato/IHC double staining (Tomato combined with anti-NF200, anti-S100, anti-VGLUT3, or anti CK20), different parts of skin (e.g. the dorsal hairy hindpaw, glabrous hindpaw and hairy back skin) were dissected in Zamboni's fixation solution, cryoprotected and embedded in OCT compound. 30 μm frozen sections were cut, washed with PBS, and made into floating sections. The floating sections were washed with PBS, blocked with 10% goat serum, and incubated with various antibodies overnight at 4^{o}C. Following incubation with the primary antibodies, sections were washed and incubated with the appropriate secondary antibodies.

Cell and innervation quantification

L4/L5 lumbar DRG from two to three mutant and control mice were dissected. For each marker, three mutant and/or control DRG were used to prepare six adjacent sections at 14-μm thickness. Each set was processed for immunostaining or used for ISH with the marker of interest, and positive cells with nuclei were counted. For the innervation quantification, 1.5X 1.5 cm2 back skin from two pairs of mutant and control mice were collected. Back skins were fixed in 4% PFA, cryoprotected in 20% sucrose, embedded in OCT, and cut into 30um thick sections. 30 hair follicles were randomly chosen from each animal, and the innervation pattern of Tomato+ nerve endings were documented to see if there are any longitudinal lanceolate endings.

DRG neuron culture and RNAi

Mice at P14-16 were killed by CO2 inhalation and DRGs from T10-L6 were collected in Ca2+ and Mg2+-free Hank's buffered salt solution (HBSS). DRGs were subsequently treated with papain (1.5 mg/ml, Roche) and collagenase/dispase (1 mg/ml, Roche) for 15 and 20 min, respectively, at 37 °C. Digested DRGs were washed twice with growth medium (Dulbecco's modified Eagle's medium (DMEM)-F12, Invitrogen) supplemented with GlutaMAX (Invitrogen) and 10% fetal bovine serum (HyClone), triturated using fire-polished Pasteur pipettes and plated in a droplet of growth medium on a glass coverslip pre-coated with poly-D-lysine (20 μg/ml, Sigma) and laminin (20 μg/ml, Sigma). To allow neurons to adhere, coverslips were kept for 2 h at 37 °C in a humidified 5% incubator before being flooded with fresh growth medium. To increase the survival of DRG neurons, recombinant human GDNF (2 ng/ml, R&D) was added in the growth medium. Cultures were used for patch-clamp experiments on the next day. Small interference RNA-mediated knockdown of Piezo2 was achieved by electroporation of a pool of 4 different siRNA (250 nM totally) purchased from Qiagen (Target sequences: GAATGTAATTGGACAGCGA, TCATGAAGGTGCTGGGTAA, GATTATCCATGGAGATTTA, GAAGAAAGGCATGAGGTAA) into freshly dissociated DRG neurons using the nucleofector kit with the nucleofector type II device (DRG, O-003 program; Lonza AG) based on the previous study9. A scrambled siRNA (250 nM, Qiagen) was transfected as control. To test the efficiency of electroporation, a 3'-Alexa Fluor 488-conjugated scramble siRNA (5 nM, Qiagen) was co-transfected. Further patch-clamp experiments were performed at 48-72 hours after electroporation.

Electrophysiology

The electrophysiological recordings were performed in the conventional whole-cell patch recording configuration under voltage clamp condition. Membrane currents were measured using Axoclamp 200B with Digidata 1320A and the pClamp 9 software (Molecular Devices). Patch pipettes (3-4 MΩ) were filled with (mM): 140 KCl, 1 CaCl2, 2 MgCl2, 10 EGTA, 2 MgATP and 10 HEPES, pH 7.2. The standard extracellular solution contained (mM): 150 NaCl, 5 KCl, 1 $MgCl_2$, 2 $CaCl_2$, 10 glucose, 10 HEPES, pH7.4. The membrane potential was voltage clamped at –60 mV throughout the experiments under voltage clamp conditions. All experiments were carried out at room temperature (22–25 °C).

Mechanical stimulation

For whole-cell recordings, mechanical stimulation was achieved using a fire-polished glass pipette (tip diameter ~2 μm) positioned at an angle of 40° to the surface of the dish. Downward movement of the probe toward the cell was driven by a Clampex-controlled piezoelectric stimulator (Corey and Hudspeth, 1980; Coste et al., 2010; Hao and Delmas, 2011). The stimulus was applied for 100 ms. To assess the mechanical sensitivity of a cell, a series of mechanical steps in 2 μm increments were applied every 20 s, which allowed full recovery of mechanosensitive currents. For recordings of mechanically evoked currents in DRG neurons, the inactivation kinetics of traces of currents reaching at least 75 % of the maximal amplitude of current elicited per cell were fitted with mono- or bi- (if mono-exponential function cannot fit

well) exponential functions (Drew et al., 2004) and classified as rapidly adapting-, mixed adapting- and slowly adapting-type currents according to their inactivation time constant.

Capsaicin-induced acute pain and secondary hyperalgesia

Capsaicin (3 μg/10 μl, Tocris) was injected into the plantar or hindpaw and the amount of time spent licking the hindpaw was counted for 5 minutes. To measure secondary hyperalgesia, mechanical thresholds in response to von Frey filaments were determined at a distance from the capsaicin injection site of the hindpaw 0, 15, 30 and 60 minutes after injection.

Neuropathic pain (spared nerve injury)

Unilateral spared nerve injury was done by exposing the sciatic nerve in the thigh region of the adult mouse (2 months), cutting and ligating the tibial and common peroneal nerves, and leaving the remaining sural nerve intact (Decosterd and Woolf, 2000a). Animals were subjected to testing at 3-15 days after lesion, in the plantar region of the left hind foot that was innervated by the sural nerve.

Inflammatory pain (carrageenan)

Carrageenan (20 μl, 1%, Sigma) was injected into the plantar of hindpaws, and both mechanical threshold and radiant heat sensitivity (paw withdrawal latency) were measured 2-24 hours later.

Pain behavioral test

All animals were acclimatized to the behavioral testing apparatus on three to five 'habituation' sessions. After habituation, two baseline measures were recorded on two consecutive days for each of the behavioral tests prior to the surgery or the CFA injection. After the surgical procedure or the chemical compounds injection (considered as day 0), the behavioral tests were performed at defined intervals (Fig. 2.7). The experimenter was blinded to the genotype of the animals. For tests using the Randall-Selitto device (IITC), mice were placed in a restraining plastic tube and allowed 5 min to acclimatize. Slowly ascending pressure was then applied to a point midway along the tail until the animal showed a clear sign of discomfort or tried to escape, and this pressure was taken as the pain threshold. For the von Frey test, we placed the animals on an elevated wire grid and the lateral plantar surface of the hindpaw was stimulated with calibrated von Frey monofilaments (0.008-1.4 g). The 50% paw withdrawal threshold for the von Frey assay was determined using Dixon's up-down method (Chaplan et al., 1994). To measure radiant heat pain, animals were put in plastic boxes and the plantar paw surface was exposed to a beam of radiant heat (IITC) according to the Hargreaves method (Hargreaves et al., 1988). Paw withdrawal latency was then recorded (beam intensity was adjusted to result in a latency of 8-12 seconds for control animals baselines). The heat stimulation was repeated 5 times at an interval of 10 min for each animal and the mean calculated. A cutoff time of 30 seconds was set to prevent tissue damage.

Statistics

Results are expressed as mean ± SE (s.e.m.). For acute pain and capsaicin-induced licking behavior, data were subjected to the Student's t test. For capsaicin-induced secondary hyperalgesia, carrageenan-induced inflammatory and SNI-induced neuropathic pain, time-course measurements were analyzed by both analyses of variance between groups (ANOVA), with $P < 0.05$ accepted as statistically significant.

Acknowledgement

We thank Dr. Nancy Speck and Dr. Gary Gilliland for the floxed Runx1 mice, Dr. David Corey for allowing us to use the recording setup in his lab, and Dr. Jing Hu and Dr. David Corey for advices on recording mechanically evoked currents on cultured DRG neurons. We thank Drs. Clifford Woolf, Ru-Rong Ji, Oliver Holmes and Fu-Chia Yang for helpful discussions and comments. Work done in Ma lab was supported by the NIH grants from NIDCR (R01 DE018025) and NINDS (P01 NS047572), and work done in Lowell lab was supported by the NIH grant from NIDDK (R01 DK075632). LL was supported by BNORC P&F (P30 DK046200).

Chapter III. Zfp521 acts downstream of RUNX1 to control C-LTMR development

Shan Lou, Mulin Xiong, Shu-Hsien Sheu, Bo Duan, Qiufu Ma

Chapter III. Abstract

Runx1 controls the development of multiple sensory neuron subtypes, such as nociceptors, thermal receptors, itch receptors, and C-LTMRs. Each Runx1 dependent subtype neuron has specific molecular and cellular identities. To find out how Runx1 specifies sensory neuron subtypes, I focused on one Runx1 dependent subtype, VGLUT3$^+$ C-LTMR, to answer this question. VGLUT3$^+$ C-LTMRs express TH, Ret signaling components, mechanical channel Piezo2, and form lanceolate endings around the hair shafts. In chapter III, I found that a Runx1-dependent transcriptional factor, zinc finger protein Zfp521, is predominantly expressed in TH$^+$ C-LTMRs in adult mice. Since Zfp521 has been shown to control bone development and neural stem cell differentiation, I hypothesized that Zfp521 also controls C-LTMR development. To test this hypothesis, I generated Zfp521 conditional knock out mice. Loss of Zfp521 led to partial loss of Runx1 dependent molecular markers, such as VGLUT3, while other phenotypes such as Piezo2 expression within C-LTMRs remain unchanged. Loss of Zfp521 also led to change of TH$^+$ C-LTMR skin innervations, disrupting the longitudinal lanceolate endings. Furthermore, we found that Runx1 and Zfp521 are required for suppressing alternative cell fates in VGLUT3$^+$ C-LTMRs. Loss of Runx1 led to expansion of MrgA3 and MrgB4, while loss of Zfp521 led to MrgD expression within VGLUT3$^+$ C-LTMR lineage.

In conclusion, my study reveals a new transcriptional factor Zfp521 that acts downstream of Runx1 to control TH$^+$ C-LTMR development. Runx1 might work through Zfp521-dependent and Zfp521-independent pathways to control VGLUT3$^+$ C-LTMR development. Both Runx1 and Zfp521 are required to suppress alternative cell fates.

Introduction

Introduction of C-LTMR (discovery, development and functions)

C-LTMR is a type of unmyelinated, C fiber, low threshold mechanoreceptor neuron that has been proposed to play a role in affiliative social touch in human (Björnsdotter et al., 2010; Löken et al., 2009; Olausson et al., 2010). Molecularly, there are two types of C-LTMRs found in mice so far: one is marked by VGLUT3, with the majority expressing TH (Li et al., 2011; Seal et al., 2009); the other is marked by MrgB4, which contribute to massage-like stroke feelings (Liu et al., 2007; Vrontou et al., 2013). Previous fate mapping studies showed that C-LTMRs also express GDNF and neurturin receptor RET and GFRα2, as well as mechanical channel Piezo2. Morphologically, TH^+ C-LTMRs form longitudinal lanceolate endings, while TH^- C-LTMRs form free nerve endings and innervate the epidermis (Li et al., 2011; Lou et al., 2013). Developmentally, $VGLUT3^+$ C-LTMR is Runx1-dependent. Loss of Runx1 led to loss of VGLUT3, TH, Ret, GFRa2, and Piezo2 expression. Furthermore, Runx1 controls the terminal morphologies of TH^+ C-LTMRs. In *Runx1* conditional knockout, TH^+ C-LTMRs still reach the hair shafts, but form circumferential endings instead of longitudinal lanceolate endings. Loss of Runx1 also led to loss of mechanical sensitivity in $VGLUT3^+$ C-LTMRs in *in vitro* cell culture environment, which is likely to be Piezo2-dependent. However, unlike VGLUT3 conventional knockout mice, no significant change of pain behavior was observed in Runx1 conditional knockout mice (Lou et al., 2013).

Runx1 controls development of multiple sensory neuron subtype

Runx1 controls development of a large cohort of nociceptors, thermal receptors and itch receptors. Loss of Runx1 led to loss of TRP receptors, Na^+-gated, ATP-gated, and H^+-gated channels, as well as Mrgpr class G protein coupled receptors (Chen et al., 2006). During the development, some of the Runx1 dependent neurons remain Runx1-persistent, such as $MrgD^+$, $TrpM8^+$, $TrpV1^{high}$ neuron, as well as $VGLUT3^+$ C-LTMRs, and are lost in *Runx1* late knockout; some of Runx1 dependent neurons extinguish Runx1 expression and become Runx1-transient neurons, such as $MrgC11^+$, $MrgA3^+$ and $MrgB4^+$ sensory neurons, which are expanded in *Runx1* late knockout (Lou et al., 2013; Samad et al., 2010).

MrgD expression starts as early as E16.5. Initially all $MrgD^+$ neurons co-express MrgC11. From E16.5 to P14, the MrgD lineage neurons segregate into Runx1-persistent $MrgD^+$ nociceptors, and Runx1-transient $MrgC11^+$ neurons, including both $MrgA3^+$ and $MrgB4^+$ neurons (Figure 1.3 B) (Liu et al., 2008; Samad et al., 2010). Mature MrgD and MrgA/B/C neurons innervate the cutaneous skin in the form of free nerve endings and occasionally circumferential endings in the hair follicles (Liu et al., 2007; Zylka and Anderson, 2004). Centrally they project to lamina II of the spinal cord. Functionally $MrgD^+$ neurons are necessary for mechanical pain and itch (Liu et al., 2012; Wang and Zylka, 2009), MrgA3 neurons are dedicated to itch and $MrgB4^+$ neurons play a role in sensing massage-like strokes in the hairy skin of mice (Han et al., 2012; Liu et al., 2007; Vrontou et al., 2013; Zylka and Anderson, 2004).

In chapter II, we learnt that VGLUT3$^+$ C-LTMRs are Runx1-dependent and Runx1-persistent, which is one of they many subtypes of sensory neurons that are Runx1-dependent. The question of how Runx1 controls the specification of the large varieties of sensory neuron subtypes remain unanswered. There are several hypotheses, of which I will mainly discuss two.

Firstly, that Runx1 could interact with different transcriptional factors or co-factors to directly activate or inhibit different promoters of the genes. This hypothesis is supported by the fact that in Runx1 Δ466 mouse line, of which the Runx1 repressor domain is mutated, there is an expansion of MrgB4 and MrgA3 expressions into the MrgD$^+$ neurons (Liu et al., 2008). This suggests that while Runx1 might be required to maintain MrgD expression, it switches from activator to repressor in regulating MrgA/B/C expressions. As a result, MrgD will persist in Runx1-persistent neurons but be transient in Runx1-transient neurons such as MrgA$^+$/B$^+$/C$^+$ neurons. Conversely, MrgA/B/C can only be maintained in Runx1-transient neurons.

The second hypothesis is that Runx1 could interact with target-derived signals, which leads to different functions of Runx1. This hypothesis is supported by the finding that BMP signaling is important for MrgB4 expression, that in BMP signaling component *Smad4* conditional knock out mice MrgB4 expression is selectively eliminated (Liu et al., 2008). Conceivably, Runx1 could interface with other factors to control downstream transcriptional factors and initiate a cascade to lead to sensory neuron specifications, although such transcriptional factors have not yet been identified.

Zfp521 plays a role in development in many tissues

In an *in situ* hybridization screen of transcriptional factors that work downstream of Runx1, Zinc Finger Protein 521 (Zfp521) turned out to be a possible candidate. Zfp521/evi3 gene locates to chromosome 18 and spans 284kb in mouse. The 3936nt long mRNA comprises 8 exons. The coding sequence of Zfp521 is highly identical to both its family member OAZ/Zfp423 and human orthologue EHZF/ZNF521. The Zfp521 protein is comprised of 1311 amino acids and contains 30 kruppel like zinc fingers. Zfp521 is highly expressed in haematopoietic cells, neural stem cells, cerebellar granule neuron precursors and developing striatum (Bond and Morrone, 2008). In bone development, studies showed that Zfp521 inhibits Runx2 (a family member of Runx1) activity by physically binding with Runx2 and HDAC3, which leads to delays of osteoblast differentiation (Wu et al., 2009). Recently, Zfp521 was found to work with co-activator p300 to promote embryonic stem cell (ES) differentiation into a neuroectodermal lineage in the absence of BMP signaling. A chromatin immunoprecipitation assay (CHIP) showed that Zfp521 directly binds with neuroectoderm-specific genes and functions as an activator, though it contains a NuRD (co-repressor complex) binding motif at its amino terminal. Overexpression of Zfp521 in ES could override BMP signaling in specifying neuronal cell fate differentiation, but it does not directly interact with BMP signaling as shown by luciferase assay (Kamiya et al., 2011).

In this chapter, I found that Zfp521 was expressed within Runx1-expressing sensory neurons and appeared to be Runx1 dependent. Zfp521 also colocalized well with TH^+ C-LTMR in adult mice. Loss of Zfp521 led to loss of VGLUT3 expression, as well as loss of lanceolate

endings, but did not affect RET, GFRa2, TH or Piezo2 expressions, which are lost in *Runx1* conditional knockouts, suggesting Zfp521 act downstream of Runx1 in regulating TH^+ C-LTMR development. Furthermore, I found that while in the *Runx1* conditional knock out there is expansion of MrgA3 and MrgB4 in $VGLUT3^+$ C-LTMR, upon loss of *Zfp521* there is, instead, an expansion of MrgD within $VGLUT3^+$ C-LTMR lineage neurons. This suggests that $VGLUT3^+$ C-LTMR specification could be a result of transcriptional cross-repression, in which Runx1 is needed for the segregation of MrgD and $VGLUT3^+$ C-LTMR cell identities from $MrgA3^+/B4^+$ neurons, while Zfp521 is needed for segregation of TH^+ C-LTMR cellular identities from $MrgD^+$ neurons. Our study reveals a new transcriptional factor that could regulate the specification of C-LTMRs and proposes a model of hierarchical control of sensory neuron lineage segregation.

Results

Zfp521 expression in the DRG neurons is Runx1 dependent

To characterize Zfp521 expression, I made a Zfp521 mRNA probe and did *in situ* hybridization on the DRG neurons of wild type mice. Using SCG10 as a pan neuronal marker in adjacent sections, it was found that Zfp521 was expressed in a subset of adult DRG neurons, 9.6%±0.8% in lumbar 1-3 levels. Since Zfp521 is a homolog of Zfp423, which is also expressed in DRG, I compared the expression pattern of Zfp521 with Zfp423, but saw no similarities since Zfp423 is expressed in almost all the DRG neurons (data not shown). It was also noticeable that the expression of Zfp521 was restricted in the small diameter neurons (Figure 3.1 A, red fluorescence). Since most small diameter sensory neurons are nociceptors, I hypothesized that Zfp521 is expressed within nociceptors. Because a big portion of non-peptidergic nociceptors express Runx1, I carried out double *in situ* hybridization with Runx1 (green) and Zfp521 (red) probes (Figure 3.1 A) and showed that almost all the Zfp521 (96.6%±4.7%) expressing neurons also express Runx1 in DRG, while about a third of $Runx1^{+}$ neurons express Zfp521 (34.5% ± 11%) in adult wild type mice (Figure 3.1A. arrows).

Since Runx1 controls the development of a large cohort of sensory neurons and that Zfp521 is exclusively expressed within $Runx1^{+}$ neurons, I asked the question of whether Zfp521 is also Runx1 dependent. To test this hypothesis, I used Runx1 conditional knock out mice in which *Runx1* with floxp cassete was crossed with Wnt1-Cre (*$Runx1^{f/f}$;Wnt1-Cre*), so that all the *Runx1* is deleted before any Runx1 expression. *In situ* hybridization showed that there was a significant loss

of Zfp521 in Runx1 conditional knock out mice (Figure 3.1B, right panel) compared to control DRG (Figure 3.1B, left panel). These data suggest that Zfp521 is expressed within Runx1 persistent DRG neurons and its expression is Runx1 dependent.

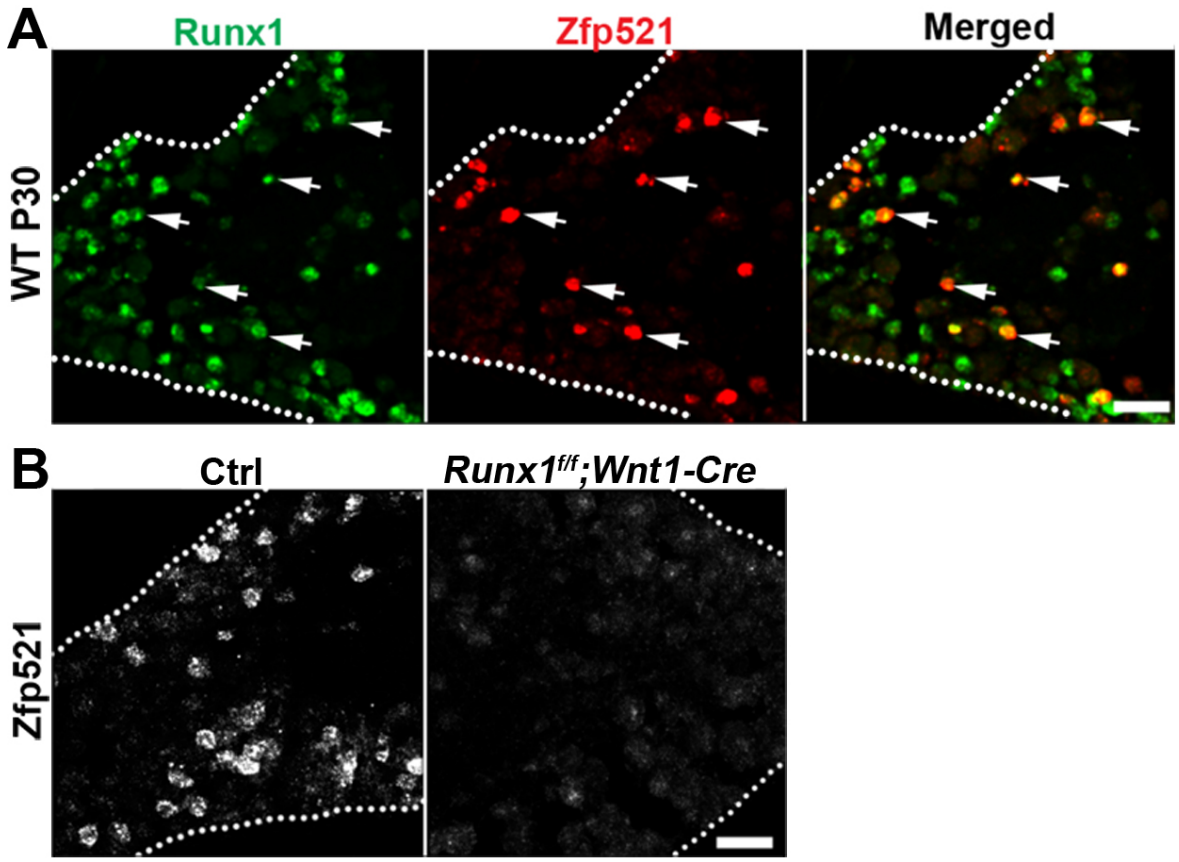

Figure 3. 1 Zfp521 expression is Runx1 dependent

Figure 3.1 Zfp521 expression in DRG is Runx1 dependent. A) Runx1 and Zfp521 double fluorescent *in situ* hybridization on P30 lumber 1-3 DRG neurons. Green fluorescence indicates Runx1. Red fluorescence indicates Zfp521. Arrows indicate the double fluorescent neurons that express both Runx1 and Zfp521. B) Zfp521 fluorescent *in situ* hybridization on adult DRG neurons in lumber 1-3 in control and Runx1 conditional knockout mice. Scale bar =50μm.

Zfp521 is predominantly expressed in adult Tyrosine Hydroxylase expressing (TH^+) C-LTMRs

Runx1-persistent neurons could be divided into several categories: $MrgD^+$ neurons, $TrpV1^{High}$ neurons, $TrpM8^+$ and $VGLUT3^+$ C-LTMRs. I asked whether Zfp521 is restricted in a specific subtype. Since Zfp521 was expressed in about 10% of DRG neurons in lumbar level, which is similar to C-LTMR, I hypothesized that Zfp521 colocalizes with C-LTMRs. To answer this question, I did Zfp521 *in situ* hybridization on C-LTMR reporter mice which used VGLUT3-Cre to drive tomato fluorescence expression ($ROSA^{Tomato/+};Vglut3^{Cre/+}$) (Figure 3.2). Previous studies had shown that there are three different populations of $Tomato^+$ neuron subtypes in Vglut3 reporter mouse DRG ($ROSA^{Tomato/+};Vglut3^{Cre/+}$): Vglut3 reporter line labels ~19% of all DRG neurons, of which 58% are TH^+ $VGLUT3^+$ neurons, 27% TH^- $VGLUT3^+$ neurons, and 15% $Tomato^+$ neurons that transiently express VGLUT3 (Lou et al., 2013) (As shown in chapter II). Most $Zfp521^+$ neurons (76.5%±4.4% of all $Zfp521^+$ neurons) were also $Tomato^+$, while 57.4%±3.4% of Vglut3-$Tomato^+$ neurons expressed Zfp521 mRNA. The percentage of Vglut3-$Tomato^+$ neurons that express Zfp521 coincides with that of TH^+ $VGLUT3^+$ C-LTMRs, suggesting that Zfp521 might be expressed within that population. To find out the relationship between Zfp521 and TH^+ C-LTMRs, I applied double *in situ* hybridization of Zfp521 and TH on $ROSA^{Tomato/+};Vglut3^{Cre/+}$ reporter line DRG neurons. It was found that the majority of Th^+/$Tomato^+$ neurons (90.8% 218/240) expressed Zfp521 (Figure 3.2, vertical arrows), while only a small portion (14.3% 19/133) of TH^-/$Tomato^+$ neurons expressed Zfp521 (Figure 3.2 arrow heads). In another way, 92% (218/237) $Zfp521^+$/$Tomato^+$ neurons expressed TH. Thus Zfp521 is mainly expressed in TH^+ C-LTMRs.

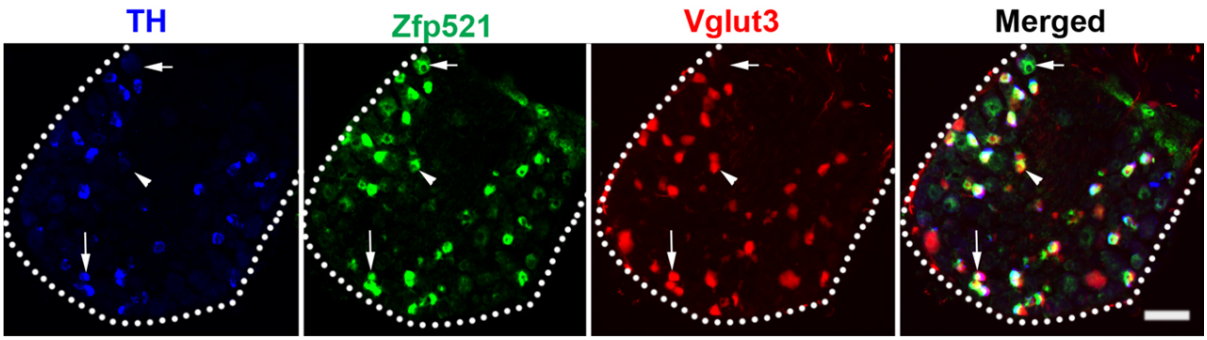

Figure 3.2 Zfp521 colocalizes with TH$^+$ C-LTMRs

Figure 3.2 Zfp521 colocalizes with TH$^+$ C-LTMR. TH, Zfp521 and Vglut3 triple staining on Vglut3-Tomato reporter DRG sections. Horizontal arrows indicating the Zfp521$^+$ (Green) neurons that are not within Vglut3-tomato$^+$ neurons. Arrowhead indicating a very small percentage of Zfp521$^+$/Vglut3$^+$/Th$^-$ neurons. Vertical arrow indicating Zfp521$^+$/Vglut3$^+$/Th$^+$ neurons. Scale bar=50 um.

Zfp521 acts downstream of Runx1 to control TH$^+$ C-LTMR cellular identities.

Zfp521 has been shown to play a role in development in multiple systems including bone formation as well as stem cell differentiation (Correa et al., 2010; Hesse et al., 2010; Kamiya et al., 2011; Seriwatanachai et al., 2011; Shen et al., 2011; Wu et al., 2009). Since Zfp521 colocalizes with TH$^+$ C-LTMRs, I hypothesized that Zfp521 also controls TH$^+$ C-LTMR development. To study the function of Zfp521 in C-LTMRs, I generated a *Zfp521$^{f/f}$* mouse line by inserting two floxp cassettes flanking the biggest exon (exon 4 455-3807bp) of *Zfp521* (Figure 3.3 A). By crossing *Zfp521$^{f/f}$* mouse line with *Vglut3$^{Cre/+}$* and *ROSA$^{Tomato/+}$* mouse line, I created a conditional knock out mouse that specifically deleted *Zfp521* exon2 (the longest exon, 455-3807 bp of cDNA)

within C-LTMRs, while labeling all the VGLUT3 lineage neurons. To verify the knock out of *Zfp521*, Zfp521 *in situ* hybridization was applied to the sections of *Zfp521* conditional knockout mouse DRG. While in control mouse DRG, there were clear Zfp521 mRNA signals (Figure 3.3B arrows left panel), the signals were greatly reduced in Zfp521 conditional knockout mice (Figure 3.3B arrows right panel). The leftover signals could be explained by the fact that 20% of Zfp521 expressing neurons were not within VGLUT$^+$ neurons by the fate mapping mentioned in the previous section. In conclusion, I successfully generated a *Zfp521* conditional knockout mouse line to study its function within C-LTMRs.

Firstly, I asked if Zfp521 contributes to neuronal survival for C-LTMRs. To answer this question, I quantified the Tomato$^+$ neurons in the lumbar level DRG in both control and mutant mice, while labeling all the neurons with pan-neuronal marker SCG10. I found no change of the percentage of Tomato$^+$ neurons in all DRG neurons (19.6%±1.2% in control, comparing with 19.1%±2.4%, $p>0.5$, $n=2$, Figure 3.3C).

Second, I did *in situ* hybridization using a Vglut3 mRNA probe on the DRG tissue, and found that there was a dramatic decrease of Vglut3$^+$ neurons comparing *Zfp521* CKO with control DRG (Figure 3.3 D). There were still some Vglut3$^+$ neurons in the mutant DRG, which is consistent with the fact that Zfp521 is only expressed within ~60% of C-LTMR. On the other hand, the number of Tomato$^+$ neurons that express molecular markers of C-LTMRs such as TH, GFRa2 or Piezo2 were not greatly changed.

A lot of transcriptional factors have feedback regulations (Alon, 2007). I asked the question if there is a feedback loop between Zfp521 and Runx1 interaction, in other words, if Zfp521 controls

VGLUT3 expression by regulating Runx1. To answer these questions, I applied Runx1 *in situ* hybridization and compared Runx1 expression within Tomato^{+} C-LTMR on the *Zfp521* mutant and control DRGs. It turned out that no significant change of Runx1 was observed, with 78.2%±4.1% of tomato^{+} neurons expressing Runx1 in controls, comparing to 67.7%±3.9% of tomato^{+} neurons expressing Runx1 in *Zfp521* mutant ($P>0.1$ Figure 3.3E). This suggests that the interaction of Runx1 and Zfp521 might be uni-directional, and that Zfp521 acts downstream of Runx1 to regulate the development of VGLUT3^{+} C-LTMR. However, it does not rule out the possibility that the expression level of Runx1 might have been changed, while the number of neurons expressing Runx1 has not. However, combined with the observation that there was no change of other Runx1 dependent gene expression, that scenario is unlikely to be the case.

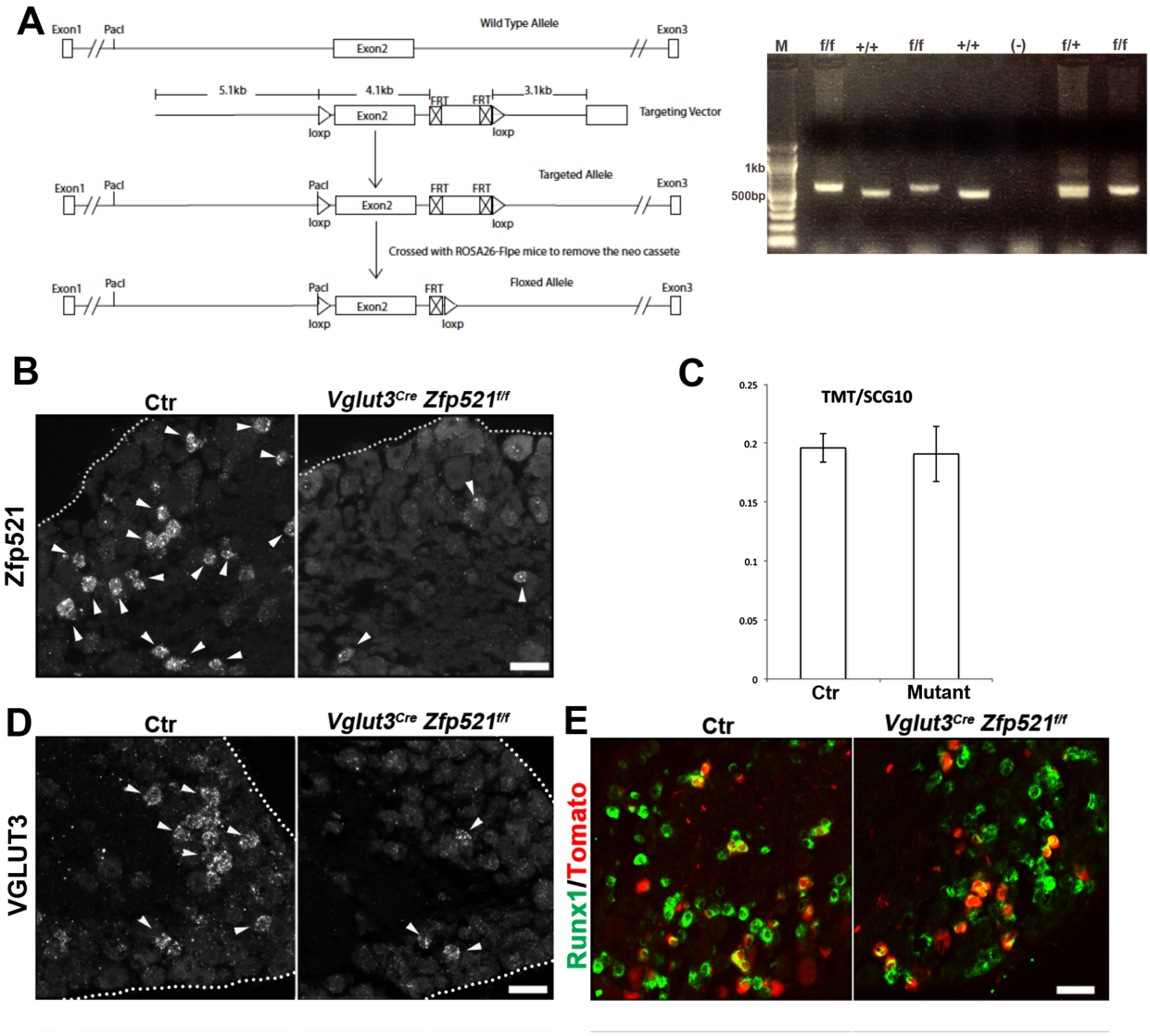

Figure 3.3 Zfp521 acts downstream of Runx1 to control C-LTMR development

Figure 3.3 (Continued)

Figure 3.3 Zfp521 acts downstream of Runx1 to control VGLUT3^{+} C-LTMR development. A) On the left panel is the scheme of Zfp521$^{f/f}$ mouse line. Floxp cassettes were inserted around the longest exon of Zfp521, the exon2. On the right side, genotyping results using Zfp521 primers, showing homozygous, heterozygous and wild type. B) Zfp521 fluorescence *in situ* hybridization on control and *Zfp521* CKO DRG sections, arrow heads indicating Zfp521 mRNA signals. C) Quantifications of *Vglut3*$^{Cre/+}$*; ROSA*$^{Tomato/+}$ neuron percentage in SCG10^{+} neurons in DRG. D) VGLUT3 fluorescence *in situ* hybridization on control and *Zfp521* CKO DRG sections, arrow heads indicating Vglut3 mRNA signals. E) Runx1 fluorescence *in situ* hybridization on control and mutant *Vglut3*$^{Cre/+}$*; ROSA*$^{Tomato/+}$ reporter line DRG neurons.

Zfp521 controls C-LTMR terminal morphologies

It was shown previously that Runx1 controls C-LTMR terminals (Lou et al., 2013). Since Zfp521 is expressed within the lanceolate ending innervating TH^+ C-LTMRs, I asked the question whether Zfp521 also controls the terminal morphology of C-LTMRs. Using fluorescence microscopy, I visualized the $Tomato^+$ nerve endings in cross sections of the back skin of the $Vglut3^{Cre/+}$; $ROSA^{Tomato/+}$ mice. It was observed that in both control and *Zfp521* conditional knock out mice, hair follicle number innervations by $Tomato^+$ nerve endings is comparable, with 66.8%±6.1% of control hair follicle innervated by $Tomato^+$ nerve endings, and 64.8%±8.9% of *Zfp521* conditional knockout ($p>0.7$, not significant different). While in control mice, there were clear lanceolate endings in most of the hair follicles that were innervated, with 68% of the innervated hair follicles having obvious longitudinal lanceolate endings; in *Zfp521* CKO mice, there were very few longitudinal lanceolate endings, with only 22% of the hair follicles that have obvious longitudinal lanceolate endings (Figure 3.4A, arrows indicating lanceolate endings, arrow head indicating innervations with out lanceolate endings, Figure 3B, n=6).

I then asked the question if the lanceolate endings in the *Zfp521* mutant mice are simply disorganized or systematically changed into other morphologies. To answer that question, we carried out 2-photon microscopy to visualize defined structures of the nerve terminals. It was found that the *Zfp521* mutant mouse hair follicle innervations resemble another specialized nerve terminal: circumferential (circular) endings (Fig 3.4B left panel shows lanceolate ending in controls, Fig 3.4B right panel and Fig 3.4C shows changed nerve terminal in mutant). This

observation was similar to *Runx1* conditional knockout nerve terminal morphology changes (Lou et al., 2013). Thus, it is possible that Runx1 controls the C-LTMR lanceolate ending through Zfp521. It does not exclude the possibility that Runx1 and Zfp521 control TH^+ C-LTMR lanceolate ending formation in parallel pathways and both are necessary for normal C-LTMRs lanceolate ending formations. Furthermore, it remained unclear whether the change of morphology is due to a switch of cell fates or loss of function, as there are other types of sensory neurons that form circumferential endings, such as $MrgD^+$ neurons and $MrgB4^+$ neurons.

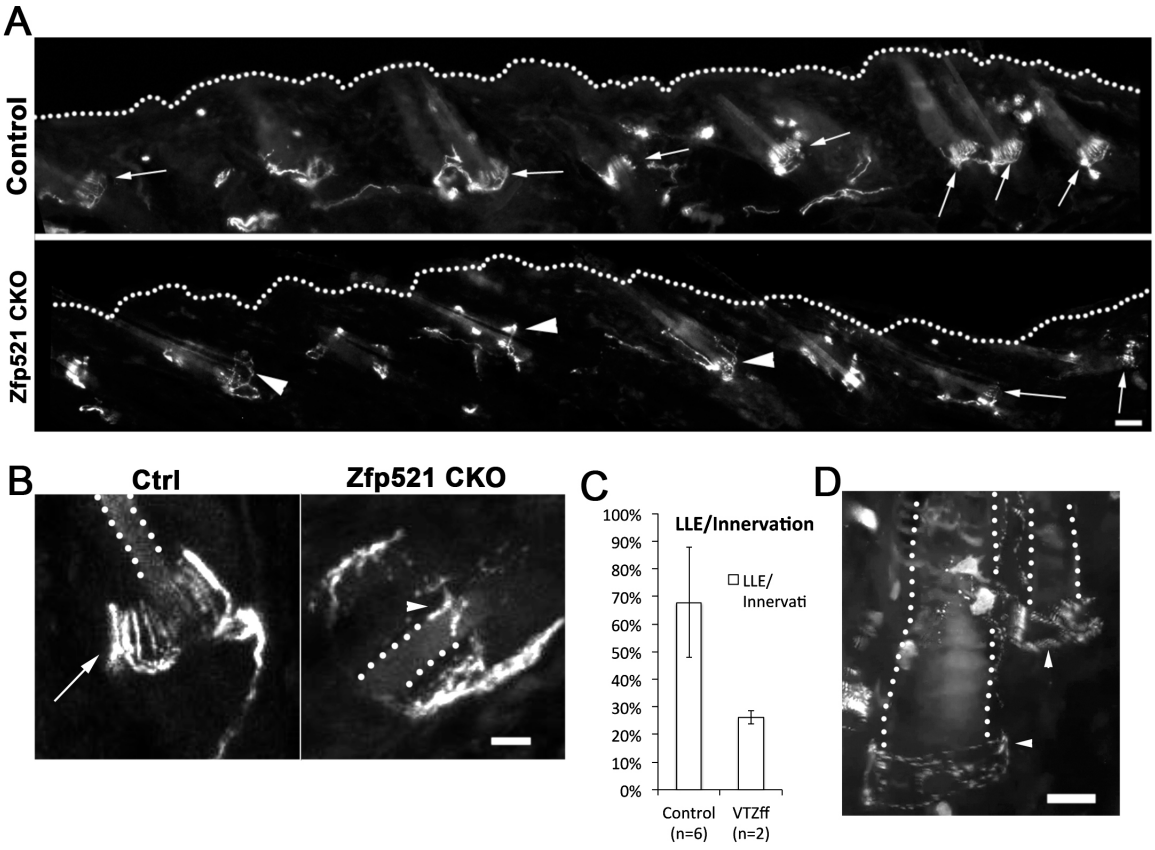

Figure 3.4 Zfp521 controls C-LTMR skin innervation morphologies

Figure 3.4 (Continued)

Figure 3.4 Zfp521 controls C-LTMR skin innervation morphologies A) Skin innervations of Vglut3-Tomato^{+} nerve fibers. Hairy skins taken from the back of control and the mutant mice. Arrows indicating lanceolate endings. Arrowheads indicating disrupted nerve endings. B) Higher magnification of a single hair follicle in control (left) and mutant (right). Arrows indicating lanceolate endings, while arrowheads indicating circumferential endings. C) Quantification of loss of lanceolate innervations. D) Confocal image showing a higher magnification of circumferential ending in the *Zfp521* CKO hair follicles. Arrowheads indicating circumferential endings. Scale bar=50μm in B, D, E and F; Scale bar=20μm in G and I

Runx1 and Zfp521 are required to suppress alternative cell fates

The transcriptional factor conditional knock out animal models, in which development has been interrupted, provided a unique opportunity to look into the lineage questions. For example, MrgA3 and MrgB4 lineage neurons are derived from MrgD lineage. Using the transgenic mice in which Runx1 lost its suppression domain, it was shown that MrgA3 and MrgB4 expanded in MrgD^{+} neurons in adult mouse DRG (Liu et al., 2008), suggesting the failure of lineage segregation.

Since both *Runx1* and *Zfp521* CKO mice show changes in the C-LTMRs terminal morphologies from longitudinal lanceolate endings to circumferential endings, which resemble the MrgD^{+} and/or MrgB4^{+} hair follicle innervations, I hypothesized that loss of Runx1 and Zfp521 could lead to switch of cell fate. To test this hypothesis, I applied MrgA3, MrgB4 and MrgD *in situ*

hybridizations on the *Runx1*$^{f/f}$*;Vglut3*$^{Cre/+}$ and *Zfp521*$^{f/f}$*;Vglut3*$^{Cre/+}$ mutant mouse DRG sections (Figure 3.5), followed by quantification and analysis of the *in situ* hybridization images.

Mrpgr family member MrgA3, is the receptor for anti-malaria drug chloroquine and mediates chloroquine induced scratch(Liu et al., 2009). MrgA3 was found in ~4% of all DRG neurons in control adult mice DRG (Han et al., 2012). In the control *Rosa*$^{Tomato/+}$*;Vglut3*$^{Cre/+}$ reporter line, there was little overlap between MrgA3 probe and Tomato^{+} neurons (only 2.4% Tomato^{+} neurons express MrgA3 (n=2, lumber DRG)) (Figure 3.5 A). However in *Runx1*$^{f/f}$*;Rosa*$^{Tomato/+}$*;Vglut3*$^{Cre/+}$ mice, there were 34.2% Tomato^{+} neurons that also express MrgA3, which is significantly higher than control ($p<0.05$, n=2, lumber DRG). This was not capitulated in *Zfp521*$^{f/f}$*;Rosa*$^{Tomato/+}$*;Vglut3*$^{Cre/+}$ mice, as there are only 2.5% of Tomato+ neurons that express MrgA3, similar to the control mice ($p>0.9$, Figure 3.5 A, arrows indicating colocalization).

MrgB4 is expressed within about 4% of all the DRG neurons (Liu, 2008). Recently MrgB4 expressing neurons were found to contribute to detecting massage-like stroking of hairy skin (Vrontou et al., 2013). In my experiments, there were 0.1% Tomato^{+} neurons that also express MrgB4 in control mice (Figure 3.5 B, first row). However, there were 51.3% of Tomato^{+} neurons that express MrgB4 in *Runx1*$^{f/f}$*;Rosa*$^{Tomato/+}$*;Vglut3*$^{Cre/+}$ mice, indicating an expansion of MrgB4 upon loss of Runx1, which was more significant than MrgA3 expansion ($p<0.001$, Figure 3.5 B, second row). In *Zfp521*$^{f/f}$*;Rosa*$^{Tomato/+}$*;Vglut3*$^{Cre/+}$ mice, there were only 1% of Tomato+ neurons that express MrgB4, which is not significantly different from the control (Figure 3.5 B, third row, arrows indicating MrgB4 expression within Tomato^{+} neurons).

Finally, I looked into the expression of MrgD. MrgD is the most abundant Mrgpr family member, which is expressed within 31% of the DRG neurons (Liu, 2008). MrgD expressing neurons are polymodal and respond to noxious thermal, mechanical and itch stimuli (Rau, 2009)(Liu et al., 2012). Ablation of $MrgD^{+}$ neurons produces selective deficits in behavioral responses to mechanical stimuli (Cavanaugh, 2009). There appeared to be 2.0% of $Tomato^{+}$ neurons that express MrgD in control DRG (Figure 3.5 C first row). There were 4.8% of $Tomato^{+}$ neurons that express MrgD in $Runx1^{f/f};Rosa^{Tomato/+};Vglut3^{Cre/+}$ mice, which is slightly higher but not significantly different from the control ($p>0.4$, Figure 3.5 C middle row). Surprisingly, there were about 34.2% (the number coincides with $MrgB4^{+}$ expression in $Runx1^{f/f};Rosa^{Tomato/+};Vglut3^{Cre/+}$ $Tomato^{+}$ neurons) of $Tomato^{+}$ neurons that express MrgD in $Zfp521^{f/f};Rosa^{Tomato/+};Vglut3^{Cre/+}$, *Zfp521* CKO mouse, DRG ($p<0.05$ Figure 3.5 C last row).

In summary, MrgA, MrgB and MrgD subfamily proteins have expression changes in C-LTMRs upon loss of Runx1 or Zfp521. MrgA and B tended to expand in C-LTMRs in absence of Runx1, while MrgD tended to expand in C-LTMRs in the absence of Zfp521. This suggests that in C-LTMRs, Runx1 controls C-LTMR identity by suppressing MrgA/B expression through Zfp521 independent manner, while Runx1 dependent Zfp521 acts to suppress MrgD identity (in an incoherent feed-forward loop (Alon, 2007)). Thus both Runx1 and Zfp521 are required for the normal development of C-LTMRs.

Figure 3.5 Runx1 and Zfp521 are required to suppress alternative cell identities in C-LTMRs

A) MrgA3 *in situ* hybridization on Runx1 and Zfp521 CKO mice DRG. B) MrgB4 *in situ* hybridization on *Runx1* and *Zfp521* CKO mice DRG. C) MrgD *in situ* hybridization on *Runx1* and

Figure 3.5 (Continued) *Zfp521* CKO mice DRG. Arrows indicating expression of indicating Mrgpr probe within Tomato^{+} neurons. Scale bar = 50μm.

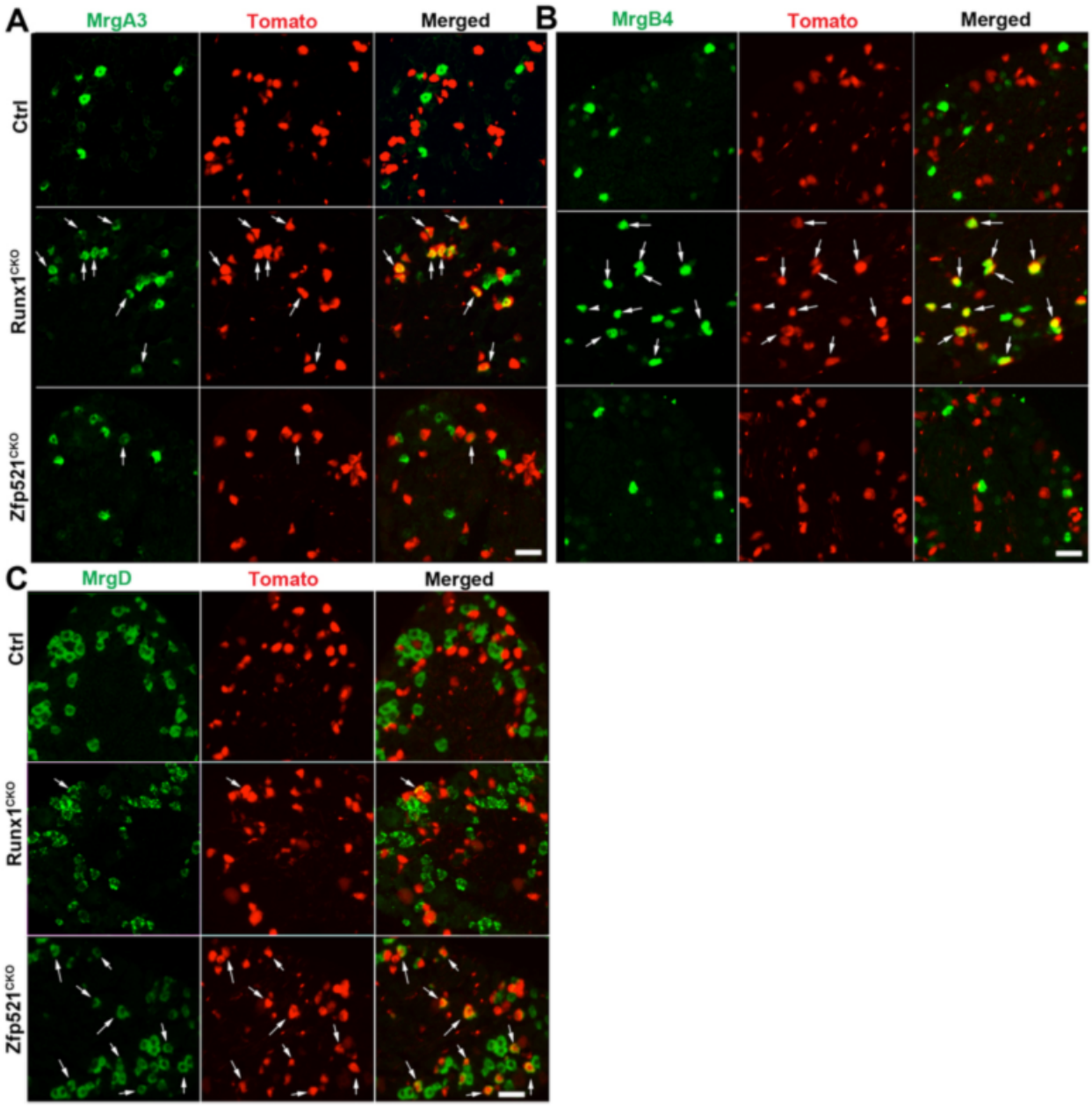

Figure 3.5 Runx1 and Zfp521 suppress alternative cell fates in C-LTMRs

Discussion

In this chapter, I focused on the development of VGLUT3$^+$ C-LTMR and found that a zinc finger protein transcriptional factor Zfp521 is specifically expressed within TH$^+$/ VGLUT3$^+$ C-LTMRs in adult murine DRG. I further found that Zfp521 acts downstream of Runx1 to control the VGLUT3 expression and cellular morphologies of VGLUT3$^+$ C-LTMRs. Finally I showed that Runx1 and Zfp521 are both required for alternative cell fates suppression and C-LTMR specification.

Runx1 controls C-LTMR development through Zfp521 dependent and independent pathways

Runx1 is known to control the development of most nociceptors, thermal receptors and itch receptors (Chen et al., 2006; Kramer et al., 2006). The mechanism of how Runx1 specifies each subtype is unknown, but it was suggested that Runx1 might interact with target-derived signals to specify subtypes. For example, it was found that Runx1 interacts with RET signaling and BMP signaling to regulate sensory channels and receptors. It was also suggested that Runx1 could activate a downstream transcription factor cascade to specify subtype differentiations. In accordance with that hypothesis, I show that Zfp521 is a downstream transcription factor of Runx1 to control proper development of C-LTMRs (Luo et al., 2007).

C-LTMRs co-express with Ret, GFRα2, as well as other molecular markers, such as Runx1, VGLUT3, TH, Piezo2, *etc.* C-LTMR development is Runx1-dependent. Loss of Runx1 affected almost all the C-LTMR expressing markers. Zfp521 is specifically expressed in VGLUT3$^+$/TH$^+$

CLTMRs. Loss of Zfp521 led to loss of only VGLUT3 and lanceolate ending morphologies, while GFRa2, RET, TH and Piezo2 expressions remain intact (Figure 3.3, 3.4, Supplementary Figure 3.1). This evidence suggests that the Runx1 controls C-LTMR development in both Zfp521 dependent and independent pathways (Figure 3.6).

The mechanism of how Runx1 activates Zfp521 expression specifically in C-LTMRs is unknown. But the studies in other Zfp521 expressing systems might shed some light on this question. During bone development, parathyroid hormone-related peptide PTHrP increases the expression of Zfp521 through parathyroid hormone receptor 1 (PthR1)(Correa et al., 2010; Seriwatanachai et al., 2011). PTHrP has been found in normal skin and overexpression of PTHrP in mouse skin showed disturbance of hair follicle development (Wysolmerski et al., 1994). Could the skin-expressing PTHrP retrogradely induce and activates Zfp521? It is a hypothesis worth exploring. Another possibility is that the RET signaling contributes to Zfp521 expression. However RET is not specifically expressed in VGLUT3^{+} C-LTMRs but also in some other Runx1 dependent subtypes, so it is unlikely to play such a role.

Molecular segregation of different sensory subtypes through cross-repression

I have shown that Runx1 and Zfp521 are not only required to establish C-LTMR features, but also required to suppress alternative cellular fates. Surprisingly, loss of Runx1 and Zfp521 unmasked different cellular competence in C-LTMR lineage neurons: loss of Runx1 led to expansion of MrgA3 and MrgB4, while loss of Zfp521 led to expansion of MrgD.

Yet the fate switch was not complete in either *Runx1* or *Zfp521* CKO. In *Runx1* CKO, the new MrgA3$^+$ and MrgB4$^+$ neurons do not express RET or GFRa2, which is different from the normal MrgA3$^+$/B4$^+$ neurons. This suggests that though Ret signaling might be required to establish MrgA3 and B4 expression (Luo et al., 2007) it is not necessary to maintain their expression. Meanwhile, in *Zfp521* CKO, the new MrgD expressing neurons in C-LTMR lineage now co-express with TH, which is not normally found in the wild type MrgD$^+$ neurons.

The ensuing question is to what extent did fate switch happen upon loss of Runx1 and Zfp521? Did other molecular features of MrgA3/B4$^+$ neurons expand in to C-LTMR lineage, including TrpV1, TrpA1 *etc.*? Did the central projection of C-LTMRs change upon loss of Runx1 and Zfp521, so that they now project to the alternative pathway? Did the lanceolate endings of C-LTMR turn to MrgA/B/D like nerve ending structures? And furthermore, did MrgA3 and MrgB4 expansion in C-LTMR in Runx1 CKO happen in the same population of C-LTMR lineage neurons? If yes, what leads to a different extent of expansions of the two molecular markers (less MrgA3 expansion than MrgB4 expansion)? These are all interesting questions, and will be looked at in future experiments.

Conclusion

In conclusion, we identified a new transcriptional factor Zfp521 that acts downstream of Runx1 to regulate the development of VGLUT3$^+$/TH$^+$ C-LTMRs. Runx1 controls all features of VGLUT3$^+$ C-LTMRs including molecular identities, terminal morphologies as well as electrophysiology, while Zfp521 controls part of the molecular identities and the terminal morphology. Thus Runx1

functions through Zfp521-dependent and Zfp521-independent pathways. Both Runx1 and Zfp521 are required to suppress alternative cell fates in VGLUT3^{+} C-LTMRs, while Runx1 supresses MrgA3/B4 expression, Zfp521 supresses MrgD expression in VGLUT3^{+} C-LTMRs. As a result, we identified a new cross-repression mechanism for a subtype segregation in sensory neuron development (summarized in Figure 3.6).

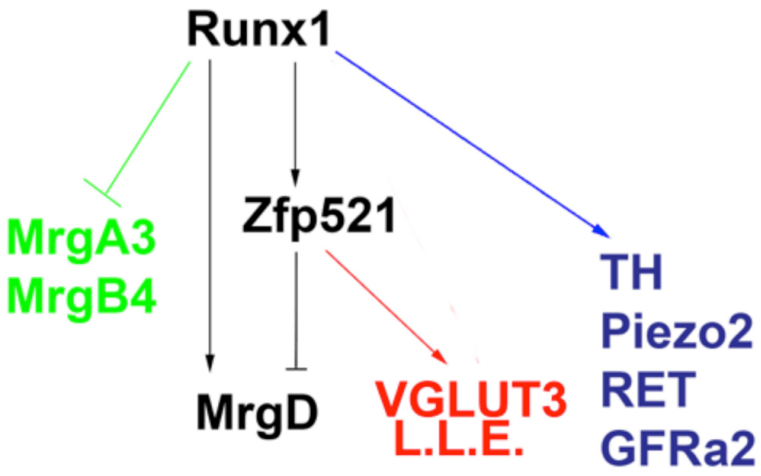

Figure 3.6 Molecular Control of TH^+ C-LTMR identities

Figure 3.6 Scheme of molecular control of TH^+ C-LTMR identity. Runx1 promotes MrgD identities while suppressing MrgA3/B4 identities. Runx1 is also required for Zfp521 expression as well as all the known features of $VGLUT3^+$ CLTMRs. Zfp521 is required for VGLUT3 expression and longitudinal lanceolate ending (L.L.E.) formations within $TH^+/VGLUT3^+$ C-LTMRs, but it is not required for TH, RET, GFRα2, Piezo2 expressions. Zfp521 inhibits MrgD expression, which forms an incoherent feedforward loop with Runx1 (black pathway).

Methods

Gene targeting in ES cells and generation of knock-in mice

The floxp knock in mouse line was generated following the protocol of a highly efficient recombineering-based method for generating conditional knock out mutations, published in 2003 (Liu et al., 2003). In brief, using homologous recombination mediated by the phage Red proteins, DNA from BACs was sub-cloned into high-copy plasmids by gap repair, and together with Cre or Flpe recombinases, loxP sites were inserted into sub-cloned DNA in the upstream and downstream of Zfp521 exon2. The conditional knockout vector was verified and sent to transgenic core laboratory in Children's Hospital in Boston for gene targeting in embryonic stem cells. ES cells were genotyped and positive ES cell clones were injected into 129J/v blastocysts to obtain chimeric mice following standard procedures. Chimeric founder mice were bred with C57BL/6 mice at least two generations to obtain germline transmission for characterization.

Animals

The generation of mice carrying the floxed Runx1 allele and ROSA26-CAG-LSTOPL-tdTomato reporter mice have been described previously (Chen et al., 2006; Growney, 2005; Madisen et al., 2010). The generation of Vglut3-Cre mice will be described elsewhere by Vong L and Lowell BB. PCR-based genotyping for conditional null mice has been described previously (Chen et al., 2006; Liu et al., 2008). The following primers were used for the Runx1 mutant and wild type

allele, 5'-GAG TCC CAG CTG TCA ATT CC-3' and 5'-GGT GAT GGT CAG AGT GAA GC-3', with floxed allele showing a larger size of DNA band after gel electrophoresis; for the VGLUT3-Cre allele, 5'-TAT CTC ACG TAC TGA CGG TG-3' and 5'-AGA CTA ATC GCC ATC TTC CAG C-3'; for the ROSA26-CAG-LSTOPL-tdTomato allele, 5'- GGC ATT AAA GCA GCG TAT CC -3' and 5'- CTG TTC CTG TAC GGC ATG G -3'; and for the mutant and wild type Zfp521 allele, 5'- AGT GAG CAT CGC AGA TCT GA -3' and 5'- TGA GGA AAA CCT GGT TGT CT -3', with floxed allele showing a larger size of DNA band after gel electrophoresis. The morning that vaginal plugs were observed was considered as E0.5. For histochemical studies, 2-3 pairs of control and mutant mice of 1-2 month old were used.

In situ hybridization (ISH) and immunohistochemistry (IHC)

Detailed *In situ* hybridization procedures are attached in the appendix. Anti-sense Zfp521 probe (1.001kb), Runx1 probe (0.858 kb), VGLUT3 probe (0.771 kb), TH probe (0.788 kb), Piezo2 probe (0.977 kb), GFRa2 probe (0.941 kb), TrkA probe (0.7kb), MrgA3 probe (1.15kb), MrgB4 (0.888 kb) and MrgD probes (1.058kb) were amplified from cDNA prepared from adult DRG, and was labeled with digoxigenin (Roche Dignostics). Ret probe, CGRP probe, SCG10 probe were digested from prepared plasmid and labeled with digoxigenin (Chen et al., 2006). The pseudo fluorescent ISH signals (for Zfp521 and TH) were converted from bright field images and then merged onto the Tomato images. For Tomato skin innervation imaging, back skins of corresponding adult mice (males and females) were dissected, fixed in Zamboni's fixation overnight and cryoprotected in 20% sucrose overnight and embedded in OCT compound. 30 μm

frozen sections were cut, washed with PBS for 10 min and PBS with DAPI for 5min to counterstain nuclei, then mounted in glycerol and photographed within 1 hour after sectioning (Lou et al., 2013).

Cell and innervation quantification

L1-L3 lumbar DRG from two to three mutant and control mice were dissected, fixed, and embedded. For each marker, three mutant and/or control DRG were used to prepare six adjacent sections at 14-μm thickness. Each set was processed for immunostaining or used for ISH with the marker of interest, and positive cells with nuclei were counted.

For the innervation quantification, after imaging, all visible hair follicles by DAPI staining were counted, and total number of $Tomato^{+}$ nerve endings innervated hair follicles, the obvious lanceolate ending ones and obvious circumferential endings ones were documented and analyzed. 2 controls and 2 mutant animals were used. The quantification was double blinded.

Statistics

Results are expressed as mean ± SE (s.e.m.). For acute pain and capsaicin-induced licking behavior, data were subjected to the Student's t test. For capsaicin-induced secondary hyperalgesia, carrageenan-induced inflammatory and SNI-induced neuropathic pain, time-course measurements were analyzed by both analyses of variance between groups (ANOVA), with $P < 0.05$ accepted as statistically significant.

Chapter IV General Discussion

Varieties of C-LTMRS

There are at least two subtypes within VGLUT3$^+$ C-LTMRs: TH$^+$ and TH$^-$ subtypes. Anatomical analysis showed that these two subtypes have distinct nerve terminal morphologies: 1) TH$^+$ C-LTMRs predominantly form longitudinal lanceolate endings innervating Awl/Auchene and Zigzag hairs; 2) TH$^-$ C-LTMRs form free nerve endings that innervate the epidermis in both hairy and glabrous skin, of which VGLUT3$^+$ free nerve endings in the glabrous skin are further specialized to be D. P. E. endings.

Developmentally, though both TH$^+$ and TH$^-$ C-LTMRs are Runx1-dependent and Runx1-persistent, they are slightly different during specification: while TH$^+$ C-LTMRs development is controlled by Runx1-dependent transcription factor Zfp521, TH$^-$/VGLUT3$^+$ C-LTMRs lack Zfp521 expression, thus are likely to be Zfp521 independent. Meanwhile, Runx1 controls TH$^+$ C-LTMR longitudinal lanceolate ending morphologies, though TH$^-$/VGLUT3$^+$ C-LTMR free nerve endings do not seem to change much in *Runx1* CKO.

in vitro whole cell patch recordings also showed variance in mechanosensitivities in VGLUT3$^+$ neurons. It was shown that not all VGLUT3$^+$ neurons are mechanically sensitive. Three types exist within the mechanically sensitive population, including fast-adapting, slow-adapting and mixed-adapting (Lou et al., 2013). Do different channel expression levels contribute to variations in adaptation patterns? Piezo2 *in situ* hybridization showed that Piezo2 mRNA is enriched in VGLUT3$^+$ C-LTMRs, though with uneven expression levels from cell to cell. Furthermore, Piezo2 knock down experiment showed a significant increase of mechanically insensitive VGLUT3$^+$ neurons upon loss of Piezo2 comparing to controls, as well as a decrease of

rapid-adapting mechanical neurons, while the mixed adapting and slow-adapting neurons number remain unchanged. As a result, it is likely that Piezo2 might contribute to the rapid-adapting components, and that other mechanical channels might exist within VGLUT3$^+$ C-LTMRs.

In conclusion, VGLUT3$^+$ C-LTMRs have multiple subtypes that have different molecular identities, morphologies, developmental ontogenies, as well as electrophysiology properties. The variations within the VGLUT3$^+$ neurons call for further investigation and characterization of subtypes within C-LTMRs. Gene profiling using a *VGLUT3^{Cre}; Rosa^{Tomato}* reporter line will be useful to identify the molecular markers as well as different subtypes.

A second large population of C-LTMRs, which are MrgB4$^+$, has recently been identified (Vrontou et al., 2013). While 19% of DRGs belong to VGLUT3$^+$ C-LTMRs, only 4% of DRGs are MrgB4$^+$ C-LTMRs. VGLUT3$^+$ and MrgB4$^+$ sensory neurons are different molecularly, morphologically, electro-physiologically and developmentally. Morphologically, TH$^+$ VGLUT3$^+$ sensory neurons form longitudinal lanceolate endings in zigzag and Awl/Auchene hair follicles while MrgB4$^+$ neurons for free nerve endings in the hairy skin epidermis and circular nerve endings in the neck of hair follicles. Centrally, while MrgB4$^+$ neurons innervate the outer layer of Lamina II, VGLUT3$^+$ C-LTMRs innervate the inner Lamina II (Li et al., 2011; Vrontou et al., 2013). Ex-vivo electrophysiological recordings showed that mouse VGLUT3$^+$ neurons are extremely sensitive to mechanical stimuli, which is similar with human C-LTMRs, while MrgB4$^+$ neurons failed to do so in ex vivo preparations (Liu et al., 2007). Developmentally, though both VGLUT3$^+$ and MrgB4$^+$ neurons are Runx1 dependent, VGLUT3$^+$ neurons are Runx1 persistent, while MrgB4$^+$ neurons are Runx1-transient (Chen et al., 2006; Liu et al., 2008; Lou et al., 2013).

In human beings, there is no MrgB4 homolog. The human Mrg genes are more similar to murine MrgA subfamily than MrgB subfamily in the phylogenic tree and are referred to as MrgX genes. (Choi and Lahn, 2003; Lembo et al., 2002). Ectopic expression of hMrgX genes in HEK cells showed that like mMrgAs and mMrgC11 (Han et al., 2002; Lembo et al., 2002), they respond to Bam22, a peptide-evoking itch. As of now, the molecular identities of human C-LTMRs remain unknown.

Logic of sensory neuron diversification

It was shown in Chapter I that there is a large cohort of sensory subtypes, defined by different channels and receptor expressions, and thus different modalities. The diversification of sensory neuron subtypes is achieved by hierarchical developmental controls. The timing of neurogenesis determines the general modalities of the sensory neurons, so that the NGN2-dependent first wave of sensory neurons become proprioceptors and mechanoreceptors, while the NGN1-dependent second wave of sensory neurons become nociceptors, itch receptors and thermal receptors, as well as C-LTMRs (Figure 1.3 A).

After the first wave of sensory neurogenesis, Runx3 is required for differentiation of proprioceptors. Shox2 and MafA/c-Maf are required for the differentiation of $TrkB^+$ and RET^+ mechanoreceptors. For the specializations of each individual mechanoreceptors and proprioceptor organs, the basic leucine-zipper transcription factor c-Maf and the ETS domain protein Er81 are required for the formation of the Pacinian corpuscles that are specialized to sense high-frequency vibrations (Hu, 2012; Sedý, 2006; Wende et al., 2012). And c-Maf and Shox2 are necessary for the

formation of the Meissner's corpuscles that respond to skin motions and detect low-frequency vibration (Abdo et al., 2011; Scott et al., 2011; Wende et al., 2012) (Figure 1.3 A).

Within the NGN1-dependent second wave of sensory neurons, Runx1-dependent neurons become non-peptidergic neurons that mostly innervate the skin, while Runx1 independent neurons become peptidergic neurons that innervate throughout the body. Within Runx1-dependent neurons, persistent Runx1 is associated with $MrgD^{+}$ polymodal nociceptors for mechanical pain and itch sensations, $TrpM8^{+}$ neurons for cold sensations, $TrpV1^{High}$ neurons for warm and mild heat, as well as $VGLUT3^{+}$ C-LTMRs that are suggested to be involved with pleasant touch, while transient Runx1 expression is associated with $MrgA3^{+}$ and $MrgC11^{+}$ pruritic neurons for itch, and $MrgB4^{+}$ neurons for massage-like strokes (Figure 1.3 B).

How exactly subtype specification is achieved within Runx1-dependent neurons is unknown. There are several hypotheses: 1) Runx1 activates different transcriptional factors in the downstream to trigger the programs for subtype specialization; 2) Runx1 interacts with the target-derived signals to initiate the subtype specification. The two hypotheses are not necessarily exclusive. Previously, it was found that BMP4 signaling is required for RUNX1 dependent $MrgB4^{+}$ neuron development. Now I have shown that Zfp521 acts downstream of Runx1 to regulate $VGLUT3^{+}/TH^{+}$ C-LTMR development, and Runx1 works through Zfp521 dependent and independent pathways to specialize $VGLUT3^{+}/TH^{+}$ C-LTMRs. These two examples suggest that the both mechanisms are likely.

Cross-repression is another mechanism that has been widely used in sensory neuron specializations. It was found in the specification of mechanoreceptors, loss of Shox2 causes a

switch from $TrkB^+$ to $TrkC^+$ neurons. Loss of Runx1 in the early stages was shown to cause a switch from non-peptidergic RET^+ neurons to $TrkA^+$ peptidergic neurons. Loss of Runx1 within $VGLUT3^+$ neurons leads to depression of MrgA3 and MrgB4. Here, I further showed that Zfp521 is required to suppress MrgD-like cell fate in $VGLUT3^+$ C-LTMRs, with a loss of Zfp521 leading to de-repression of MrgD as well as MrgD like terminal morphologies. Thus, Runx1 and Zfp521 are not only required to establish identities belonging to C-LTMRs, but are also required to suppress features that belong to other neurons, thereby providing an effective way for the emergence of molecularly distinct sensory neuron subtypes.

Meanwhile, it is notable that the emotion-related sensory modalities (negative and annoying stimuli, such as pain, itch, and pleasant stimuli, such as massage, stroke and social affiliated behavior) are predominantly transduced by Runx1-dependent, late-wave, sensory subtypes (so far). As animal body plans emerged during the half billion years evolution, the role of individual development scheme and evolutionary events were apparently sometimes closely intertwined in phylogenic, comparative and functional biology. The late emergence of emotional-related sensory subtypes during developmental stages suggests that they could have appeared in later and higher intelligence forms of species during evolution.

Physiological functions of C-LTMRs

Human studies showed that C-LTMR exhibit bell-shape responses to the speed of moving stimuli, whose peak activity correlates well with the perception of touch-evoked pleasantness (Löken et al., 2009). Furthermore, human patients lacking myelinated A-fibers were still able to sense pleasant

touch, but this sensation was impaired upon a loss of C-fibers (Björnsdotter et al., 2010; Löken et al., 2009; Morrison et al., 2011). These evidences suggested that they could signal pleasant touch associated with affiliative social body contact (Björnsdotter et al., 2010; Olausson et al., 2010).

In mice, VGLUT3^{+} C-LTMR were suggested to play a role in mechanical allodynia (pain evoked by innocuous mechanical stimuli) induced by inflammation, tissue injury, chemicals (capsaicin), and nerve injury, based on behavioral analyses in *VGLUT3* complete null mice (Seal et al., 2009). However, the mechanical pain defects were measured from the glabrous skin in the hindpaw plantar, while VGLUT3^{+} C-LTMRs mostly innervate the hairy skin (with the exception of scarce VGLTU3^{+} free nerve endings called D.P.E.). Furthermore, VGLUT3 expression has been found in the spinal cord as well as the brain, where the somatosensory circuitry is closely related. Conventional knockout of VGLUT3 will lead to disruption of the central parts of the sensory circuitry. Thus the cellular basis of mechanical allodynia deficits in VGLUT3 null mice is not clear. In other words, the functions of VGLUT3^{+} C-LTMR remain unknown.

Using *Runx1*$^{F/F}$*; Vglut3*$^{Cre/+}$ conditional knock out mice, I showed that VGLUT3^{+} C-LTMR development is greatly disrupted (loss of molecular identities, change of terminal morphologies, loss of mechanical sensitivities in vitro). Behaviorally, this conditional knockout mouse line showed little phenotype in inflammatory or neuropathic mechanical pain assays. Only a mild impairment in carrageenan induced mechanical allodynia was observed, suggesting VGLUT3^{+} C-LTMRs might play a minor role in mechanical allodynia in pathological conditions.

However, the *Runx1* conditional knockout mouse line has its own disadvantages, since there is not only disruption of the C-LTMR development, but also gain of function of alternative cell

types. Loss of Runx1 led to de-repression of MrgA3 and MrgB4 expression. Even though there is a loss of mechanical channel Piezo2, as well as loss of mechanical sensitivity *in vitro*, it does not exclude the possibility that VGLUT3$^+$ C-LTMRs are switched to MrgB4-like C-LTMRs, which do not respond to mechanical stimuli in vitro or ex vivo, but are mechanosensitive in vivo. Since the mechanisms of mechanical sensitivity in MrgB4$^+$ C-LTMRs are unknown, it is hard to test if the whole mechanical sensitive machineries are also expanded into VGLUT3$^+$ C-LTMRs in *Runx1* mutants. *In vivo* calcium imaging of VGLUT3$^+$ neurons in *Runx1* conditional knockout mice might be necessary to find out if the VGLUT3$^+$ C-LTMRs indeed lost mechanical sensitivities in physiological conditions. Alternatively, future experiments using ablation of VGLUT3$^+$ C-LTMRs would be needed to find out if VGLUT3$^+$ C-LTMRs actually contribute to mechanical allodynia or not.

Remaining questions and future directions

One important unsolved issue concerns central nerve projections. I was also very interested in learning if the central nerve projections of VGLUT3$^+$ C-LTMRs are changed upon loss of Runx1 and Zfp521. In this thesis, due to the fact that VGLUT3 is also expressed in the spinal cord, VGLUT3 reporter line exhibits VGLUT3-Tomato positive signals also in the spinal cord neurons. As a result, I could not analyze the central projections in detail. To resolve this problem, we have imported TH^{CreER} mice in which we can induce Th expression spatially and temporally. Using TH^{CreER} mice I can investigate if Runx1 and Zfp521 can regulate the central nerve innervations,

and furthermore, which subset of C-LTMR (TH^+ or TH^-) still maintains the competence to be switched to MrgA3/B4 or MrgD.

Equally interesting are the longitudinal lanceolate endings that TH^+ C-LTMRs have, which are a highly organized structure seen in most of the hair follicles, or the zigzag hairs. Though dramatically different from a developmental point of view, the Aδ and Aβ LTMRs also form identical structures around Awl/Auchene and guard hair. It will be interesting to determine if there is a common signal shared by Aδ, Aβ and C fiber neurons that controls the formation of lanceolate endings.

Though $VGLUT3^+$ C-LTMRs were suggested to be similar to the C-LTMRs found in human beings due to their electrophysiological similarities (low threshold, slow conduction, cool sensing, *etc*.), there is a lack of direct evidence to show that $VGLUT3^+$ C-LTMRs do contribute to light touch sensation, and light touch induced pleasant feelings. Even for the electrophysiology carried out in $VGLUT3^+$ C-LTMRs, no neuronal activation correlation with the stroke speed has been examined, while the preference firing of C-LTMRs to the optimum slow stoking speed is a signature of the human C-LTMRs. There are several criteria to consider the C-LTMR as pleasant touch neurons: 1) light touch could evoke their neuronal activities; 2) the loss of function of C-LTMRs leads to loss of light touch induced pleasant sensation; 3) the activation of C-LTMRs will leads to pleasant touch pathway activation, thus pleasant sensation. So far, we are unable to test these criteria in our *Runx1* conditional knock out mice due to lack of efficient behavioral assays. As a result, it is still an open question whether $VGLUT3^+$ C-LTMR contribute to pleasant touch.

Several experiments carried out in humans as well as mice could enlighten our behavioral assay designs. The human brain fMRI is one example. fMRI has been carried out in normal volunteers comparing to the patients who specifically lost myelinated fibers, while their forearms were being stroked with various speeds and intensity settings. Mice fMRI could be challenging as fMRI has limited resolution, and the mice generally need anesthetizations. Recently, several studies have been using awake mice and achieved high resolution of fMRI images (Ahrens and Dubowitz, 2001; Desai et al., 2011; Jonckers et al., 2011; Lee et al., 2010; Pautler, 2004). It remains to see if rodent fMRI will be as efficient as human fMRI and if the brain regions are the same areas.

To test the mechanical sensitivities of mice, a sand paper assay has been reported before (Maricich et al., 2012). With rough and smooth sand papers on each side of a chamber where mice could move freely, it was found that female C57 mice always prefer the rough side, while male C57 mice don't have this preference. And the female mice preference is lost in the mutant mice that lack Merkel cells. However, it was also found that the mice could compensate the loss of Merkel cells and mechanical sensitivities with whiskers, introducing some complications to this assay.

The MrgB4^{+} neuron activation assays set a good example for potential behavioral assays (Vrontou et al., 2013). To generate a mouse model whose C-LTMR neurons could be drug induced, we will use VGLUT3-Cre mice and inject the mice with AAV virus that carries Cre dependent DREADD vectors (DREADD standing for designer receptors exclusively activated by designer drugs) (Alexander et al., 2009; Dong et al., 2010; Vrontou et al., 2013). The DREADD vector

carries the coding of a GRPR sequence that is mutated (hM3Dq) and can only be activated by exogenous drug clozapine-N-oxide (CNO). The vector also includes a stop cassette that is flanked by floxp and mCherry, so that the expression of hM3Dq could be monitored. When hM3Dq is properly expressed and activated by CNO, the neurons with the expression will be activated and fire action potentials.

The mice will then be put into conditioned place preference (CPP) chambers combined with CNO activation of the C-LTMRs. CPP was a behavior assay developed more than forty years ago to test the rewarding effects of environmental factors, such as drugs, water, food or sex. The principle of CPP is to create a coupling between contextual stimuli and primary reinforcement (Bardo et al., 1995). So far, CPP assays were shown to be significant in multiple addictive drug applications, including dopaminergic drugs, amphetamine, morphine, cocaine, opioids *etc.* (Tzschentke, 2007). If $VGLUT3^+$ C-LTMRs indeed contribute to pleasant touch and positive emotions, activation of C-LTMRs should be able to reflect a positive coupling of the conditioned chamber. As a result, the mice will bias toward the chamber cues where their C-LTMRs are activated, just as what $MrgB4^+$ neuron activated mice do (Vrontou et al., 2013).

Meanwhile, though functional C-LTMR studies were mostly from human being (Löken et al., 2009; McGlone et al., 2007; Morrison et al., 2011; Olausson et al., 2008; Olausson et al., 2002; Olausson et al., 2010; Vallbo and Kakuda, 2005; Vallbo et al., 1999; Vallbo and Wessberg, 1999; Wessberg et al., 2003), the molecular identities of human C-LTMRs are largely unknown. VGLUT3 and Zfp521 both have human homologs (Bond et al., 2004; Hesse et al., 2010). It will be interesting to find if VGLUT3 and Zfp521 are expressed and functional in human C-LTMRs. But

so far, VGLUT3 has been suggested to link to nonsyndromic hearing impairments (Smith et al., 1993), no Zfp521 natural mutations have been reported.

As more and better genetic and behavioral assays become available, we will expect to have better tools to decipher the somatosensory circuitry, to understand how environmental stimuli could be converted to cognitions, emotions and corresponding responses.

Appendix

Supplementary Figures:

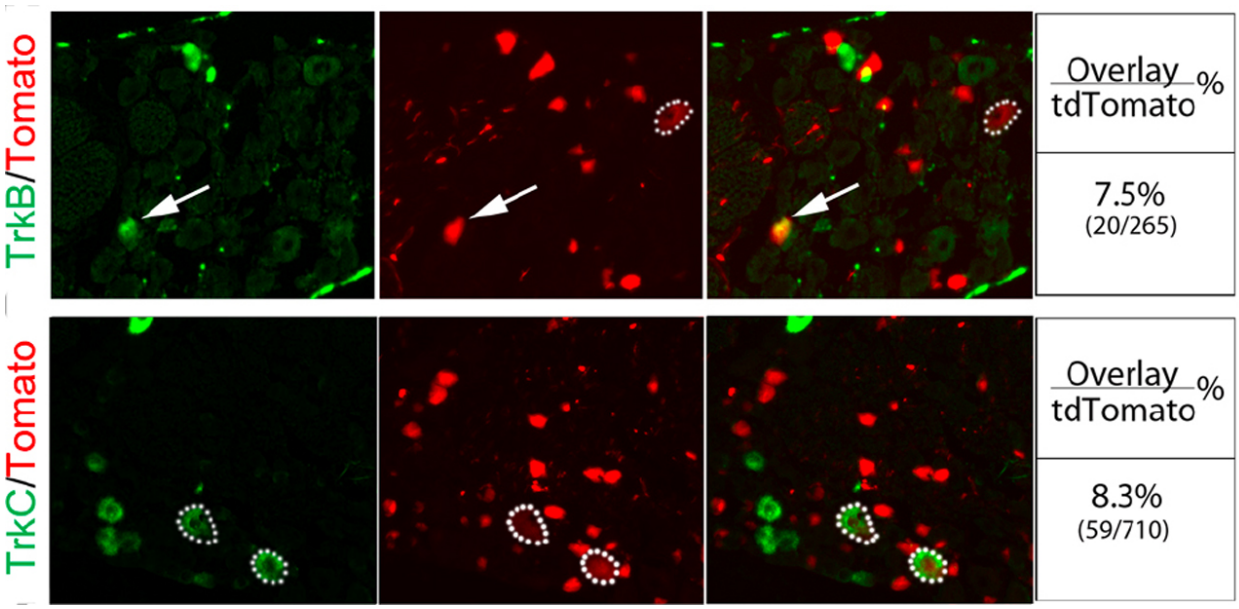

Supplementary Figure 2.1 TrkA and TrkB are expressed in VGLUT3 transient DRG neurons

Supplementary Figure 2.1 The VGLUT3 transient DRG neurons express TrkA and/or TrkB. Arrows indicating medium Tomato^{+} neurons overlapping with TrkB. Dotted circle indicating large and dim Tomato^{+} neurons, which are also TrkC^{+}.

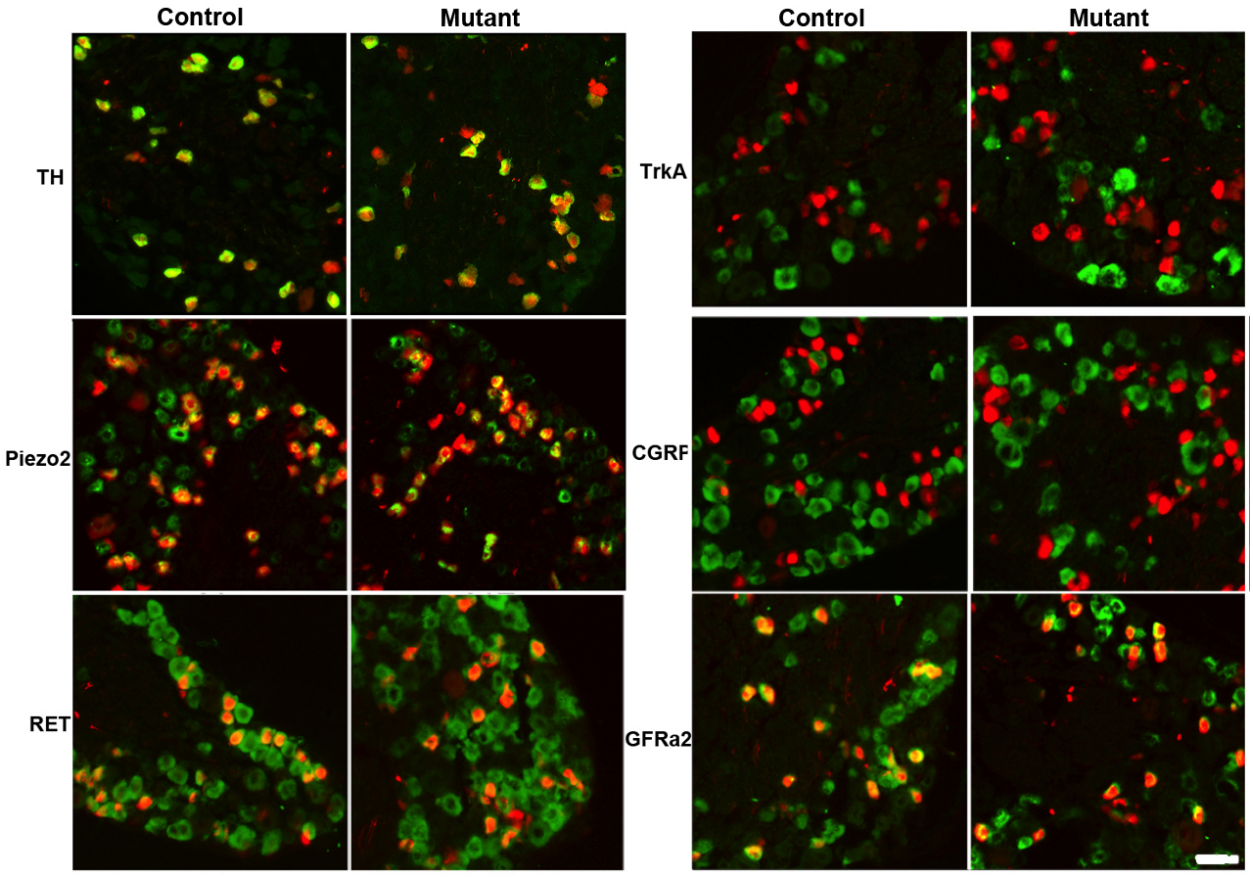

Supplementary Figure 3.1 C-LTMR molecular markers that are not Zfp521 dependent

Supplementary Figure 3.1 Other molecular markers that are expressed in VGLUT3^{+} sensory neurons that do not change in Zfp521 CKO by *in situ* hybridizations. Controls were using wild type animals. Mutants are Zfp521$^{f/f}$;Vglut3$^{Cre/+}$; ROSA$^{Tomato/+}$ mice. Scale bar 50μm.

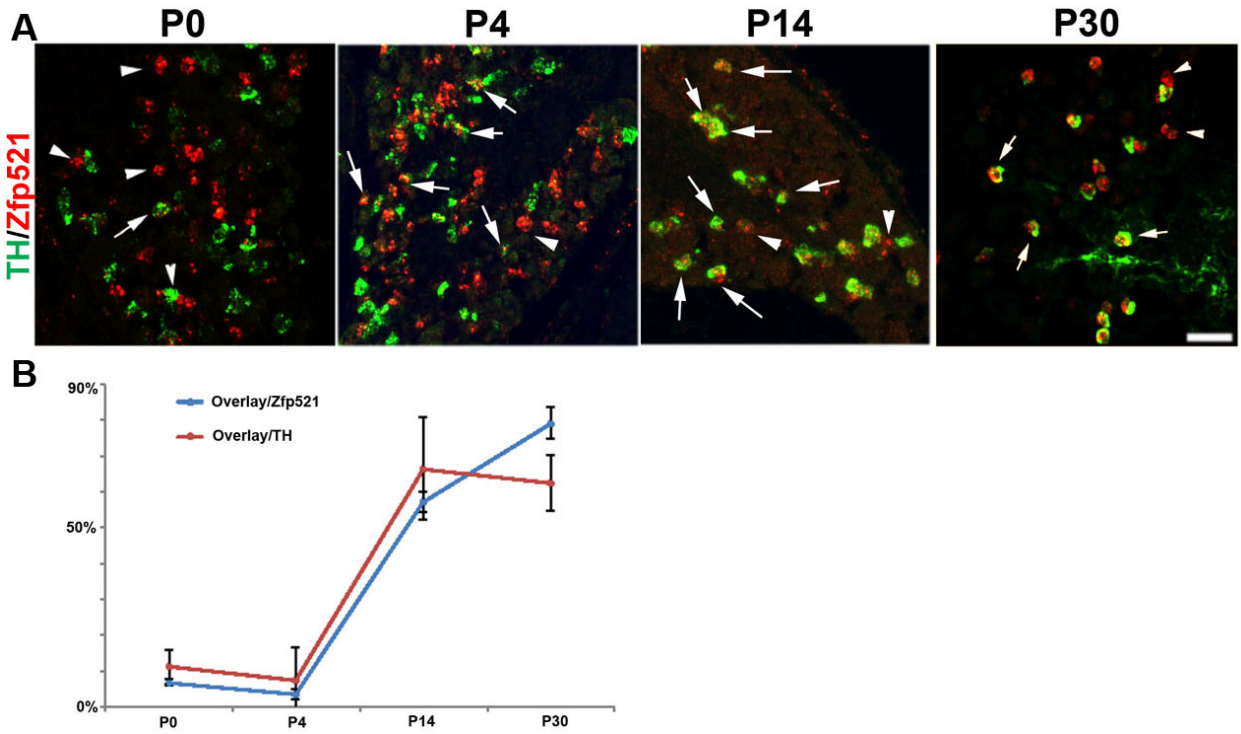

Supplementary Figure 3.2 TH and Zfp521 colocalization increases during postnatal stages

Supplementary Figure 3.2 TH^{+}/ $Zfp521^{+}$ neurons increase during first several postnatal week development. A. Double fluorescence *in situ* hybridization of TH (green) and Zfp521 (red). Arrows indicating overlapping neurons, while arrowheads indicating non-overlapping neurons. B. The trends of overlay over the first several weeks. Scale 50μm

Probe sequences:

MrgB4

Gtcctgcatggctctctgaagaagtagcttcagagactgccatcgcaacctgtgttgtctaatggagccaacaaggaagtaaatgatgggattg
gcacagctgttaacacaggacaggaattctattatttcataaacattgttaaagaaaatgctatcaaactccataatccttgataagaggaaccagc
agataccaaagggcatgccaaagtatatgaagaccaccactgtgagagcaatggtcacaaagaacctggtcacaggaatcctgtgtgacccc

cacacaatcttcaccaacagggccaggctagatacagaaagaaccacagataacactattaaaaatgcagcagtgataaaattcaaagtaata
cagaaataataatcataataactgaacagaaaaccacagcctagccctaccacgaggctcaacaatagagaggaaacccagaccagagcac
acatgatggctgatgtgtgtcttggtctttggcagtgataccagataggccacataacagataggcagcgttcagcactgatggctgcaatcata
cacaaacctgcaaggtaagcaaacattgttacaatgaggagaatataaaaggagttattatctaactgaaggacacattccagggaatgcacaa
cttgagtgaaaaggtacaagaaatcagcaccagccagattgaggacatagacagagaaggcattcctatgcaggtggaaggctagaagcca
tagcactatgccgtttcctgccaggccaaccacagctatgatgacagtaagaaaattcagggtattgaacttggtgatacaggagaacatttcag
tgtaacttccattttcagcggtgttgttaatgttccaggccagggt

MrgA3

Gtgttggtggaccagtgaggcatgtcaagtcagtaagctgagaggagagtggacagtggtcaagtgcagcagggcagtgctcactccaaat
ccacctctgaagtctaggcagaggctcttcatcacggctctgctttgtttcttgacatctccaccatgttttcaggtgtctcaggagtgtcctgcagg
gctttctggagaaccattttgagggtctgtttattcaaccgttgcctgaaggagcccacgaagaagtaaataatggggttggcacagctgttaata
gcagttaggaccagaagagggctataatctagtacaaacacaccaggtgcaatccagaataacaggaaccaggtgatgccccagggcaacc
cacagagaagaaaaaccaaaacggtcagcatgatggtcacgaataatctggtaaatttcatattcctagcaccacagaacaacctggccagta
gagccagggtggacagacagaggactacaaacaaaaacatcaggtatgctccgataaagatgtcccatgcctgacacacagagtaattgaaa
taatggttatctaagtaaccgcagaaataaccatccagaatgcagatcaacagggacaggacccagatcacagcacacatgacagttgatgtg
tgttctgggcggcggcagtgataccagatggggcacaggacagacaggcagcgctcagtgctgatggcactgagcatgctcaggcctgtga
tatagagaaccctttgatagtgtgaaaacaaaaggcaaaaattcctttgggtagggtaaacttgagaagatccactgtggaatttatgatgtgac
agagaaggaagaggaagtcagccagggccaagtttaggatgtagactaagaaggcagtcctgtgcatgcggaagccaaggagccagaac
acaatcgcatttcctgtcagcccgaccagtccgaagatgatgatcatcaagtctgggatcagggtctcgatgtcaatacttccagggatggtttc
gttcattgaatttgttgttgtgggtgtcattgtcgaggctgaggtgtttcgggccagaaaccctgcactggtgttgctttctcccattcctcttgctgg
atgtagcttgctggcttgtgtagaag

MrgD

gaggatggtgctggtcaggatcatgaccggcatgaagatccccaggataagactgttgaaaacaatgtccaccttgaagcactggtgtttgttg
ggatgccagaattggacgcagaagaaagaagccaggaagttcatcaggaaggccagtgcccagagtgcaccagataccactgatgacagg
tgccggggccggtggcacttataccagatggggaaaagcacggagaggcagcgctgggtgctgatggctgtcagcaggctcaggcctgct
gtataggcaaagtacttgattctcctcatcccttcatagattttggcagaaatgttgactatgagcaggggccctgtttccaggctgagcatggag
gccatgcagaataagaagaggaagtcagccaccgccaggttgagcacatagacacagaagggagacctctgcatgccattgcagctcagg
agccaaatcaccaatgagttgcctgccatccccccccacacacgtggccatggcgaggaatgtcactgaaaagtagatccaggtcacaaggtc

catggtgggactgatggtcagacctggagctgggctgctgtcaagagtggagttcattcctgctcctgagtgtgccaatctgtccttccgcaaag
atggtgatccctcttggctgtgatccctagaagtgtttccagcagcaccgtgaggcctgggcttctcagctgcttctgcaggtcctgactcagtgt
ctcttccactaagcaaggatggtcctgtctgtctctactgctcccagccacatagaacccttgatttgggggacccccctcaaggaccttggcttc
ctttcagaagtgtgagaaggaatcctagatataagtgccggaaagatgcccgtccaccctgtggagacctgcgcccacaggagcctagctga
agactaatgggcctccccagtatggccctctcctgccccacccagattcctttgatactgggggcttttgaggattctagcaaggaccactccttc
tggcatcatcctggtagcctctcccttctca

VGLUT3

Tgagaggacgaccttgggtagaccaacctattgtaaaacaggtataactgtattagggtgtgagtgttaaataatgttcacaaagcacctggca
caaccaagggcccccatgagtgattcccttcattaggtttaggaaactcctctacatgagtatcctaagagatgtgatggcaaccaccatgtactc
ttctccagaacaaagagggatttcttccagtgtttatttgagcaacatgctactccttattcttctcaccattaattcctgaataactagttcttttgagag
aaggctcaacggccaatgcccaatccacaccccaaccccaaatatgatcaactattttatcaactgagaccaaggtccatattcccatctttgtaa
gaaggcgtgtttcttttctctgttgttaatttaatctcccccttcccacgatttggcccctggcaagacgcagtatgggaaaggcgatgggtgcg
atacttccagttgtaagctgaggtgaagccagacatttaggatgtttctgagaagtctccttcggcctggtaggataatggctcctccccgtcgaa
ggcagattctctctgttgtctccactccgtcttctggacctcacaattctgggtggtggctccataagacatcttctttctgggacttacgaaagtctc
gtggttgagttctgtctcctcagctaactcatcttggtcaatgattccacatttgtcctcagagagattctctgggtcagcccag

GFRα2

Gggttggagtccacatagttcggtgtcatatcaaacccaatcatgccagcataggagcccagacatgcctggtagttgtccgcagggcagctg
gtgattgtccggtaggaggctcgacagttggcgtggaagtctgccaggcgggaccggcacaagtggtctgtacgacacaggctgcgcaggt
ccaagcagttgggcttctccttgtcctcataggaacagctgggcaggatggtttgccggcgacgctcggcgcatgcctggtcctgacaggagc
agaagagcatgcggtaggtatactcgctgggcacacggtcgaagaactggcgcagggccttgtggcacttgcggcggttgcagcgttcagt
gggagagatctcgcggttgcagatggagatgtaggaggagcggagcttcttgcagttgtcgttcaggttgcaggccttggcggcatccaggc
agtggttgctcttggcactgaccaccgggtctgcccctgtccctgagaagattgaagcgagcctgaagatgtccgagaggcgggaggtcaca
ggctcatagggcgaagcttcgtagaactcctcaccctccgtcagccccagatggatgctccaatagatctgcagacactgcagctccttcttcat
gccccgcttgcagcggcagtcatacaatgggctttcctgcaagacctccagggccgcctggcactccttattggccagcatggtattgcgatcc
cggccggccaggcactgccgaagggtgcggtacctggagctgcagttggattcagccgcacacagctcattggcccggacacagtccactt
gggggcgccagccgtggagctcagagccctgcggagaggaagggctggccaaagagcggagggtttcgtctaaaaagaagaagaggca
gaaggcgtttgccaagatcat

Piezo2

Taccggaacgcacatgctactgccaggcagatgggaagcagcagcctgaagatcagcccgcacaccacttccgaagccatcgtgtcgtgg
gaccttgctagtccgagcagtagggcgacgctcaggggttcctagagctgggatgtcaggcccatgtctacctagggcctcgtgcgcccggc
tgctcgtagccaccctggcatcgcgtcggctggcgcggcgctctctgccccgagggcgcgctcgacgggcgggagccgctcagctcacgg
ggctccaggcagccacctaaccaggcgcccgagcccctgtggcccgcccatgaagtgtggaatcggaatccagcggcagcggctccagg
ggtcgcctgggaaggagccaagggagggacactctgggagtggagaagaatgggggcggtgaggagaggggatggaggaggatagct
gtcctctgcctgctctggaggcggcgttccgggatggccgagagtttctagctgaacccttccgaagtaagtgagtctgggcggcgcagccc
gggctccgagtccacgcggactgaggcgctcccggtgcgctaaagacccgccgggcgccctggaagccgcgtcctggagccccagcctc
cgggcggatcgctgaattgctgctccgctcagcctcagcgcccccaagcttcaggccagggagagccgggcgccagttgcagggcgcgg
agaaacattcccgacccggcggggtcgcgctgccagcccgcggggatgcgagtccagtcctccccgtgaggagctgtgcgagtctgggcc
ggaaccaagacccagacgcggagcgcgcggcgctaccaccgcgactttagtgagaaaagaaagcccaggagccctgcagaggtccccg
cgtccccaacggagcagcctctcccgagccaagcagcccgggctccccggagggcgcgagctcctccaccttcaatgaaac

Runx1

Ttgggattcctcacgaccacatctaacacttgccacatgtgtgggcagtagctggaggctggagaactgcattttctgaggtgtgttttttttttttttt
tttacccccaatacatgtgttttactgctatttcaatttggaagtttgttttttgttttttgttttccattgatctttttccatccagagtaacagaaataccca
acagttcatttgaagattgatttttttttttgcacattcatttctcctagaacataaggtgaacttaaaaaaaaacccattggaaccatgcttgtttattatgt
ttataaaagtgagtaagaagtagcttggttttttaaaatctaaaataaacaagttaagagaagcatttttcttctacaatatttagcgaacataagaaa
aagtccttagaaacacacacaaaatgtgaaaaaagttattacaggcattaacaatattttataatgaagcatgaaatctatttacatacataaataca
attgagtttgtggatacaactcttctgaggaaaaaaaagaaaaaacagacaaatgatcagctttggctataccgacctggctgaaagagggaag
gcatttccgaccaacagccaaacccaccaaataaaggtgtactgtagagtaaacaaaacagtactttgttcaaataaggaaaaaatatattctga
gattgctgtcaaactatttattttcatgtatgaaagaccctcaacatctcatgccttctcctacaaagaaaatgagaagaaccaaaaaaaccaaaac
aaaacaaaacccatcaaaaccaaaaaatccctaagaccgaatgtccctgggggaaagttatttca

Zfp521

Acagctgtaggtgactttcgcctgcttactagaggggccagtcatatcggaggtctgctgagcagctcgcttcctcccgcggctctttggaatc
ggtggtgcagcctctaccatggtcgagctgtccactgagaggttcgagtctggagtcgtgctggacactgaggtgtaacccacagtgaccagg

gaagggctgttgctgtgattgcaggactctggctgctggtgactgtccatgtggctatacagctcctcgaccgtgaggaagctctctgagcaaat
gctgcaagagttcttcttctcacccccgtgtacctgctcgatgtggttcatgagggacgtctcctccacaaacagctcgtggcagtacatgcactg
gagggctgctcggtcctcattaggggagcactcggggtggcattctgcaatgtgcttctggaggtcttccgggaagtcaaagccttcctcgcac
tggctgcacttctgagtgtccttcatcttccagtcctccatcctggagccagactgggagccgtccttgttccgctcatgaacctgcatatgtccgt
gcaaggagctagaggagaggaaccctctgcggcagacggcacatttatatggcttgttggaggtgtgagtctttaagtggatcttgagatgatc
gctccgggagaaggctgcgtcacactcgctacagtgatacttcttatccccagtgtggagctttatgtggcggtcacggctccgcttgtgtttgaa
cagccgactgcagtaggtgcacttgaagggcagcttgtcactgtggctctgttcatggtgctttaggtagctgaggcggctaaaggacttgtcac
agaactggcatgggtaaggcagtccagggccaccttcttcctctccgaaatcacacccttctccatggctgggggaagtctggtccttactgga
aggcgaggaggctggccaagagcagctggggtcgtcctcaacgtcaacgccat

TH

Tctctgacacgaagtacaccggctggtaggtttgatcttggtagggctgcacggctgctgtgtctgggtcaaaggcccggacctcgggctcct
ctgacagggagtgcaggagctctccataggaagacagcagccctgcaccgtaagccttcagctccccattctgtttacacagcccaaactcca
cagtgaaccagtacaccgtggagagtttttcaatttcttcatctgaagcccccagagatgcaagtccaatgtcctgggagaactgggcaaatgtg
cggtcagccaacatgggtacgtgtcccagcagctcgtggcagcagtctggctcgggtgagtgcataggtgaggaggcatgacggatgtact
gtgtgcactgaaacacacggaaggccagactggccagaaaatcacgggcagacagtagaccggccacgggtcgcagctggaagccagtc
cgttccttcaagaagtgagacacatcctccagctgtggaatgctgtcctctcggtagccacagtaccgttccagaagctggaaagcctccaggt
gttcccggcaggcatgggtagcatagaggcccttcagcgtggcgtatacctccttccaggtagcaatttcctcctttgtgtattccacgtgggga
attggctcaccctgcttgtattggaaggcaatctctgcaatcagcttccggcgctggcgatacgcctggtcagagaagcccggatggtccaggt
ccaggtcagggtcaaacttggtgaccaggtggtgacacttatcc

***In situ* hybridization protocols:**

Day 1
Reagents:
4% PFA in PBS (30 ml/mailer)
DEPC-PBS (60 ml/mailer)
10μg/ml protein K in PK buffer (15 ml/mailer)
DEPC dH_2O (30 ml/mailer)

0.1 M TEA/0.25% acetic anhydride (15 ml/mailer), add acetic anhydride just before use
Pre-hybridization buffer (15 ml/mailer)
1-2 μg/ml probes in hybridization buffer (10-15 ml/mailer)
2X SSC (30 ml/mailer + 600 ml/large trough + 400 ml/small trough)

Method:
1. Warm slides to RT and dry at 50°C for 15 minutes.
2. Fix in PFA for 20 minutes.
3. Wash in DEPC-PBS for 5 minutes 2X.
4. Treat with protein K.
   8 minutes for E9.5 – E11.5
   12 minutes for ≥ E12.5
   11 minutes for mixed sections
5. Wash in DEPC-PBS for 5 minutes.
6. Fix in PFA for 15 minutes.
7. Rinse in DEPC-dH_2O twice.
8. Add TEA/acetic anhydride for 10 minutes.
9. Wash in DEPC-PBS for 5 minutes.
10. Pre-hybridization at Room Temperature for 1 hour.
11. Heat water bath to 80 degree. Prepare the hybridization cocktail, 250ul for each slide:
    a. Dilute the probe into the final concentration of 1ng/ml
    b. Add 4% Dextran Sulfate from 50% stock solution
12. Heat probe cocktail for 5min at 80 degree, cool down in ice for 5 min
13. Cut the paraffin and apply the cocktail, put into the humid chamber, sealed. Incubate at 68 degree overnight.
14. Meanwhile, warm up 30 ml/mailer, 300 ml/large trough, and 200 ml/small trough 2X SSC to 64°C and 300 ml/large trough and 200 ml/small trough to 37°C.

Day 2
Reagents:
2X SSC (see reagents under Day 1)
RNase A
0.2X SSC (900 ml/large trough + 600 ml/small trough)
TNT: 100mM Tris pH7.5, 150mM NaCl, 0.05% Tween 20
TNB: TNT without Tween, with 0.5% blocking powder
DIG Ab solution (15 ml/mailer)

Method:
1. Prewarm 0.2X SSC at 64°C.
2. Pour the probes into the original tubes. Rinse mailers with prewarmed 2X SSC twice.
3. Transfer slides to troughs containing 2X SSC. Incubate at 64°C for 15 minutes.
4. Add RNaseA to a concentration of 1.5 μg/ml to 37 °C 2X SSC and incubate slides at 37°C for 30 minutes.
5. Wash slides in 0.2X SSC at 64°C briefly once, then for 30 minutes 2X.
6. Transfer slides to mailers and equilibrate in TNT for 5min.

7. Block in TNB solution for 30 minutes.
8. Incubate in antibody solution overnight at 4°C or 2 hours at RT.

Day 3
Reagents:
AP buffer (45 ml/mailer)
Levamisole
NBT/BCIP
PBS (45 ml/mailer)
4% PFA in PBS (15 ml/mailer)
Glycerol
Clear nail polish

Method:
1. In new mailers, wash in TNT for 30 minutes 3X.
2. Wash in AP buffer for 5 minutes. The second time, add levamisole to the concentration of 1.2 g/L.
3. Add 1µl NBT and 3.5 µl BCIP per ml AP buffer and levamisole. Incubate slides in NBT/BCIP solution in the dark for up to 3 days. First check after 2 hours, then every day thereafter. Replace the NBT/BCIP solution daily.
4. In new mailers, wash in PBS 3X.
5. Fix in PFA for ≥ 15 minutes at 4°C.
6. Coverslip with glycerol. Let dry for at least an hour standing upright on paper towels.
7. Quickly rinse in dH_2O.
8. Seal with clear nail polish.

Making probe

Probe preparation
1. PCR amplify template from cDNA or plasmid in a 50-µl reaction.
2. Run 10 µl on a gel to check that only one band is present.
3. DIG labeling reaction:
    15 µl DNA
    10 µl 5X transcription buffer
    5 µl 0.1 M DTT
    4.5 µl T7 polymerase (20 U/µl)
    0.5 µl RNase Inhibitor (40 U/µl)
    3 µl DIG labeling mix (10X)
    12 µl dH2O
    50 µl
    Incubate at 37°C for 2 h.
4. Add 2 µl DNase I (20 U). Incubate at 37°C for 10 min.
5. Save 2 µl to run on a gel.
6. Add 52 µl stop buffer (8 % SDS, 20 mM EDTA, 20 mM Tris, pH 7.5, 100 mM NaCl).

7. Spin through a Sephadex G50 column.
8. Add 1/10 volume 3 M NaOAc, pH 4.8 and 2.5 volume 100 % EtOH.
9. Precipitate at -80°C for 30 min.
10. Spin 15 min at 4°C.
11. Wash with 2.5 volume 75 % EtOH.
12. Air dry for 5 min.
13. Resuspend in 50 µl DEPC dH2O.
14. Dilute to 1-2 µg/ml in 10-15 ml hybrdization solution.
15. Store at -20°C.

Reagents:

Name	Company	Catolog
100X Denhardt's Solution	Amresco	E257-50ML
Strapavidin 488	invitrogen	S32354, 748200
Anti-DIG_AP	Roche	11093274910
1X Plus amplification diluent	Perkin Elmer	511196
Biotinyl tyramide reagent	Perkin Elmer	560549
BCIP	Roche	11383221001
NBT	Roche	11383213001
DIG RNA labeling mix 10x	Roche	11277073910
T7 RNA Polymerase	Roche	10881775001
Fluorescein RNA labeling mix 10x	Roche	1675619
RNase inhibitor	Roche	3335339001
Dextran sulfate 50%	Amresco	E516-100ML
Acetic anhydride	Sigma	A6404-200ML
Formamide	Sigma	47671-1L-F
Triethanolamine	Sigma	90279-500ML
Tween 20	Sigma	P9416-50ML
Ribonucleic Acid	Ambion	AM7118
Heparin sodium salt	Sigma	H3393-250KU
CHAPS	Fisher	986734-36
5 Place Slide holder with flip	Globe	513062
Blocking reagent	Perkin Elmer	FP 1020
Tetramisole hydrochloride	Sigma	L95975610G
Biotinyl tyramide reagent	Perkin Elmer	560549
Fluorescein RNA labeling mix 10x	Roche	1675619
DIG RNA labeling mix 10x	Roche	11277073910
Anti DIG POD	Roche	11207733910
Anti FLU POD	Roche	11426346910
Streptavidin, Rhodamine Red™-X conjugate	invitrogen	S-6366
Alexa Fluor® 488 tyramide	invitrogen	T-20922
1X Plus amplification diluent	Perkin Elmer	511196

References

Abdo, H., Li, L., Lallemend, F., Bachy, I., Xu, X., Rice, F., and Ernfors, P. (2011). Dependence on the transcription factor Shox2 for specification of sensory neurons conveying discriminative touch. European Journal of Neuroscience *34*, 1529-1541.

Abrahamsen, B., Zhao, J., Asante, C., Cendan, C., Marsh, S., Martinez-Barbera, J., Nassar, M., Dickenson, A., and Wood, J. (2008). The Cell and Molecular Basis of Mechanical, Cold, and Inflammatory Pain. Science *321*, 702-705.

Agarwal, N., Offermanns, S., and Kuner, R. (2004). Conditional gene deletion in primary nociceptive neurons of trigeminal ganglia and dorsal root ganglia. genesis *38*, 122-129.

Aguayo, L.G., and White, G. (1992). Effects of nerve growth factor on TTX- and capsaicin-sensitivity in adult rat sensory neurons. Brain Research *570*, 61-67.

Ahrens, E., and Dubowitz, D. (2001). Peripheral somatosensory fMRI in mouse at 11.7 T. NMR in Biomedicine *14*, 318-324.

Alexander, G., Rogan, S., Abbas, A., Armbruster, B., Pei, Y., Allen, J., Nonneman, R., Hartmann, J., Moy, S., Nicolelis, M.*, et al*. (2009). Remote Control of Neuronal Activity in Transgenic Mice Expressing Evolved G Protein-Coupled Receptors. Neuron *63*, 27-39.

Allan, D.W., St Pierre, S.E., Miguel-Aliaga, I., and Thor, S. (2003). Specification of neuropeptide cell identity by the integration of retrograde BMP signaling and a combinatorial transcription factor code. Cell *113*, 73-86.

Alon, U. (2007). Network motifs: theory and experimental approaches. Nature Reviews Genetics *8*, 450-461.

Anakopian, Abson, N., and Wood, J. (1997). Molecular genetic approaches to nociceptor development and function. TINS *19*, 240.

Arber, S., Ladle, D.R., Lin, J.H., Frank, E., and Jessell, T.M. (2000). ETS gene Er81 controls the formation of functional connections between group Ia sensory afferents and motor neurons. Cell *101*, 485-498.

Árnadóttir, J., and Chalfie, M. (2010). Eukaryotic Mechanosensitive Channels. Annual review of biophysics *39*, 111-137.

Bardo, M.T., Rowlett, J.K., and Harris, M.J. (1995). Conditioned place preference using opiate and stimulant drugs: a meta-analysis. Neuroscience and biobehavioral reviews *19*, 39-51.

Bartels, A., and Zeki, S. (2000). The neural basis of romantic love. NeuroReport *11*, 3829-3834.

Bassilana, F., Champigny, G., Waldmann, R., de Weille, J.R., Heurteaux, C., and Lazdunski, M. (1997). The acid-sensitive ionic channel subunit ASIC and the mammalian degenerin MDEG form a heteromultimeric H+-gated Na+ channel with novel properties. The Journal of Biological Chemistry *272*, 28819-28822.

Bautista, D., and Lumpkin, E. (2011). Perspectives on: Information and coding in mammalian sensory physiology: Probing mammalian touch transduction. The Journal of General Physiology *138*, 291-301.

Bautista, D., Siemens, J., Glazer, J., Tsuruda, P., Basbaum, A., Stucky, C., Jordt, S., and Julius, D. (2007). The menthol receptor TRPM8 is the principal detector of environmental cold. Nature *448*, 204-208.

Behar, O., Golden, J.A., Mashimo, H., Schoen, F.J., and Fishman, M.C. (1996). Semaphorin III is needed for normal patterning and growth of nerves, bones and heart. Nature *383*, 525-528.

Bell, J., Bolanowski, S., and Holmes, M.H. (1994). The structure and function of Pacinian corpuscles: a review. Progress in neurobiology *42*, 79-128.

Bertrand, N., Castro, D.S., and Guillemot, F. (2002). Proneural genes and the specification of neural cell types. Nature reviews Neuroscience *3*, 517-530.

Bessou, P., and Taylor, C.B. (2003). Dynamic Properties of Mechanoreceptors with Unmyelinated (C) Fibers. J Neurophysiol *34*, 116.

Björnsdotter, M., Morrison, I., and Olausson, H. (2010). Feeling good: on the role of C fiber mediated touch in interoception. Experimental Brain Research *207*, 149-155.

Bond, H.M., Mesuraca, M., Carbone, E., Bonelli, P., Agosti, V., Amodio, N., De Rosa, G., Di Nicola, M., Gianni, A.M., Moore, M.A., *et al*. (2004). Early hematopoietic zinc finger protein (EHZF), the human homolog to mouse Evi3, is highly expressed in primitive human hematopoietic cells. Blood *103*, 2062-2070.

Bond, H.M., and Morrone, G. (2008). Earlyhematopoieticzincfingerprotein—zincfingerprotein521: Acandidateregulatorofdiverseimmaturecells. The International Journal of Biochemistry and Cell Biology *40*, 848.

Boulais, N., and Misery, L. (2008). The epidermis: a sensory tissue. Eur J Dermatol.

Boulland, J., Qureshi, T., Seal, R., Rafiki, A., Gundersen, V., Bergersen, L., Fremeau, R., Edwards, R., Storm-Mathisen, J., and Chaudhry, F. (2004). Expression of the vesicular glutamate transporters during development indicates the widespread corelease of multiple neurotransmitters. The Journal of Comparative Neurology *480*, 264-280.

Bourane, S., Garces, A., Venteo, S., Pattyn, A., Hubert, T., Fichard, A., Puech, S., Boukhaddaoui, H., Baudet, C., Takahashi, S., *et al*. (2009). Low-Threshold Mechanoreceptor Subtypes Selectively Express MafA and Are Specified by Ret Signaling. Neuron *64*, 857-870.

Bradbury, E.J., Burnstock, G., and McMahon, S.B. (1998). The expression of P2X3 purinoreceptors in sensory neurons: effects of axotomy and glial-derived neurotrophic factor. Molecular and cellular neurosciences *12*, 256-268.

Brierley, S., Castro, J., Harrington, A., Hughes, P., Page, A., Rychkov, G., and Blackshaw, L. (2011). TRPA1 contributes to specific mechanically activated currents and sensory neuron mechanical hypersensitivity. The Journal of Physiology *589*, 3575-3593.

Bron, R., Eickholt, B.J., Vermeren, M., Fragale, N., and Cohen, J. (2004). Functional knockdown of neuropilin-1 in the developing chick nervous system by siRNA hairpins phenocopies genetic ablation in the mouse. Developmental dynamics : an official publication of the American Association of Anatomists *230*, 299-308.

Brooks, J.C., Nurmikko, T.J., Bimson, W.E., Singh, K.D., and Roberts, N. (2002). fMRI of thermal pain: effects of stimulus laterality and attention. NeuroImage *15*, 293-301.

Brown, A.G., and Hayden, R.E. (1971). The distribution of cutaneous receptors in the rabbit's hind limb and differential electrical stimulation of their axons. The Journal of Physiology *213*, 495-506.

Brown, A.G., and Iggo, A. (1967). A quantitative study of cutaneous receptors and afferent fibres in the cat and rabbit. The Journal of Physiology *193*, 707-733.

Campbell, J.N., and Meyer, R.A. (2006). Mechanisms of neuropathic pain. Neuron *52*, 77-92.

Cao, E., Cordero-Morales, J.F., Liu, B., Qin, F., and Julius, D. (2013). TRPV1 Channels Are Intrinsically Heat Sensitive and Negatively Regulated by Phosphoinositide Lipids. Neuron *77*, 667-679.

Caterina, M.J., Rosen, T.A., Tominaga, M., Brake, A.J., and Julius, D. (1999). A capsaicin-receptor homologue with a high threshold for noxious heat. Nature *398*, 436-441.

Caterina, M.J., Schumacher, M.A., Tominaga, M., Rosen, T.A., Levine, J.D., and Julius, D. (1997). The capsaicin receptor: a heat-activated ion channel in the pain pathway. Nature *389*, 816-824.

Cavanaugh, D.J., Lee, H., Lo, L., Shields, S.D., Zylka, M.J., Basbaum, A.I., and Anderson, D. (2009). Distinct subsets of unmyelinated primary sensory fibers mediate behavioral responses to noxious thermal and mechanical stimuli. Proceedings of the National Academy of Sciences of the United States of America *106*, 9075-9080.

Chalfie, M. (2009). Neurosensory mechanotransduction. Nature reviews Molecular cell biology *10*, 44-52.

Chang, H., and Nathans, J. (2013). PNAS Plus: Responses of hair follicle-associated structures to loss of planar cell polarity signaling. Proceedings of the National Academy of Sciences, 1-10.

Chaplan, S.R., Bach, F.W., Pogrel, J.W., Chung, J.M., and Yaksh, T.L. (1994). Quantitative assessment of tactile allodynia in the rat paw. Journal of neuroscience methods *53*, 55-63.

Chen, C., Broom, D.C., Liu, Y., Nooij, J., Li, Z., Cen, C., Samad, O.A., Jessell, T.M., Woolf, C.J., and Ma, Q. (2006). Runx1 Determines Nociceptive Sensory Neuron Phenotype and Is Required for Thermal and Neuropathic Pain. Neuron *49*, 365.

Chen, C.C., Akopian, A.N., Sivilotti, L., Colquhoun, D., Burnstock, G., and Wood, J.N. (1995). A P2X purinoceptor expressed by a subset of sensory neurons. Nature *377*, 428-431.

Chiang, L., and Lewin, G.R. (2011). Laminin-332 coordinates mechanotransdution and growth cone bifurcation in sensory neurons. Nat Neurosci *14*, 993.

Choi, S.S., and Lahn, B.T. (2003). Adaptive Evolution of MRG, a Neuron-Specific Gene Family Implicated in Nociception. Genome Research *13*, 2252-2259.

Christensen, A.P., and Corey, D.P. (2007). TRP channels in mechanosensation: direct or indirect activation? Nature Reviews Neuroscience *8*, 510-521.

Christianson, J.A., and Davis, B.M. (2006). Transient Receptor Potential Vanilloid 1-Immunopositive Neurons in the Mouse are More Prevalent within Colon afferents Compared to Skin and Muscle Afferents. neuroscience *140*, 247-257.

Cojen Ho, M.E.O.L. (2011). Single-cell analysis of sodium channel expression in dorsal root ganglion neurons. Molecular and cellular biology *46*, 159.

Corey, D.P., and Hudspeth, A.J. (1980). Mechanical stimulation and micromanipulation with piezoelectric bimorph elements. Journal of neuroscience methods *3*, 183-202.

Correa, D., Hesse, E., Seriwatanachai, D., Kiviranta, R., Saito, H., Yamana, K., Neff, L., Atfi, A., Coillard, L., Sitara, D., *et al*. (2010). Zfp521 is a target gene and key effector of parathyroid hormone-related peptide signaling in growth plate chondrocytes. Developmental cell *19*, 533-546.

Coste, B., Mathur, J., Schmidt, M., Earley, T., Ranade, S., Petrus, M., Dubin, A., and Patapoutian, A. (2010). Piezo1 and Piezo2 Are Essential Components of Distinct Mechanically Activated Cation Channels. Science *330*, 55-60.

Coste, B., Xiao, B., Santos, J.S., Syeda, R., Grandl, J., Spencer, K.S., Kim, S.E., Schmidt, M., Mathur, J., Dubin, A.E., *et al*. (2012). Piezo proteins are pore-forming subunits of mechanically activated channels. Nature, 1-8.

Craig, A.D., Chen, K., Bandy, D., and Reiman, E.M. (2000). Thermosensory activation of insular cortex. Nature Neuroscience *3*, 184-190.

Crozier, R.A., Ajit, S.K., Kaftan, E.J., and Pausch, M.H. (2007). MrgD activation inhibits KCNQ/M-currents and contributes to enhanced neuronal excitability. J Neurosci *27*, 4492-4496.

da Silva, S., Hasegawa, H., Scott, A., Zhou, X., Wagner, A.K., Han, B.X., and Wang, F. (2011). Proper formation of whisker barrelettes requires periphery-derived Smad4-dependent TGF-beta signaling. Proceedings of the National Academy of Sciences of the United States of America *108*, 3395-3400.

da Silva, S., and Wang, F. (2011). Retrograde neural circuit specification by target-derived neurotrophins and growth factors. Current opinion in neurobiology *21*, 61-67.

Davis, J.B., Gray, J., Gunthorpe, M.J., Hatcher, J.P., Davey, P.T., Overend, P., Harries, M.H., Latcham, J., Clapham, C., Atkinson, K., *et al*. (2000). Vanilloid receptor-1 is essential for inflammatory thermal hyperalgesia. Nature *405*, 183-187.

Decosterd, I., and Woolf, C.J. (2000a). Spared nerve injury: an animal model of persistent peripheral neuropathic pain. PAIN *87*, 149-158.

Decosterd, I., and Woolf, C.J. (2000b). Spared Nerve Injury: an animal model of persistent peripheral neuropathic pain. PAIN *87*, 149-158.

Delmas, P., Hao, J., and Rodat-Despoix, L. (2011). Molecular mechanisms of mechanotransduction in mammalian sensory neurons. . Nature reviews Neuroscience *12*, 139-153.

Desai, M., Kahn, I., Knoblich, U., Bernstein, J., Atallah, H., Yang, A., Kopell, N., Buckner, R., Graybiel, A., Moore, C., *et al*. (2011). Mapping brain networks in awake mice using combined optical neural control and fMRI. Journal of Neurophysiology *105*, 1393-1405.

Dhaka, A., Earley, T., Watson, J., and Patapoutian, A. (2008). Visualizing Cold Spots: TRPM8-Expressing Sensory Neurons and Their Projections. Journal of Neuroscience *28*, 566-575.

Dhaka, A., Viswanath, V., and Patapoutian, A. (2006). TRP Ion Channels and Temperature Sensation. Annual Review of Neuroscience *29*, 135-161.

Dib-Hajj, S.D., Tyrrell, L., Black, J.A., and Waxman, S.G. (1998). NaN, a novel voltage-gated Na channel, is expressed preferentially in peripheral sensory neurons and down-regulated after axotomy. Proceedings of the National Academy of Sciences of the United States of America *95*, 8963-8968.

Djouhri, L., Newton, R., Levinson, S.R., Berry, C.M., Carruthers, B., and Lawson, S.N. (2003). Sensory and electrophysiological properties of guinea-pig sensory neurones expressing Nav 1.7 (PN1) Na+ channel alpha subunit protein. The Journal of Physiology *546*, 565-576.

Dong, S., Rogan, S.C., and Roth, B.L. (2010). Directed molecular evolution of DREADDs: a generic approach to creating next-generation RASSLs. Nature Protocols *5*, 561-573.

Dong, X., and Anderson, D.J. (2001). A Diverse Family of GPCRs Expressed in Specific Subsets of Nociceptive Sensory Neurons. Cell *106*, 619-632.

Drew, L.J., Rohrer, D.K., Price, M.P., Blaver, K.E., Cockayne, D.A., Cesare, P., and Wood, J.N. (2004). Acid-sensing ion channels ASIC2 and ASIC3 do not contribute to mechanically activated currents in mammalian sensory neurones. The Journal of Physiology *556*, 691-710.

Drew, L.J., Rohrer, D.K., Price, M.P., Blaver, K.E., Cockayne, D.A., Cesare, P., and Wood, J.N. (2004). Acid-sensing ion channels ASIC2 and ASIC3 do not contribute to mechanically activated currents in mammalian sensory neurones. . Journal de physiologie *556*, 691-710.

Drew, L.J., Wood, J.N., and Cesare, P. (2002). Distinct mechanosensitive properties of capsaicin-sensitive and -insensitive sensory neurons. . J Neurosci *22*, RC228.

Driskell, R., Giangreco, A., Jensen, K., Mulder, K., and Watt, F. (2009). Sox2-positive dermal papilla cells specify hair follicle type in mammalian epidermis. Development *136*, 2815-2823.

Driskell, R.R., Clavel, C., Rendl, M., and Watt, F.M. (2011). Hair follicle dermal papilla cells at a glance. Journal of cell science.

Dubin, A., Schmidt, M., Mathur, J., Petrus, M., Xiao, B., Coste, B., and Patapoutian, A. (2012). Inflammatory Signals Enhance Piezo2-Mediated Mechanosensitive Currents. Cell Reports *2*, 511-517.

Dykes, I.M., Tempest, L., Lee, S.I., and Turner, E.E. (2011). Brn3a and Islet1 act epistatically to regulate the gene expression program of sensory differentiation. J Neurosci *31*, 9789-9799.

Eade, K.T., and Allan, D.W. (2009). Neuronal phenotype in the mature nervous system is maintained by persistent retrograde bone morphogenetic protein signaling. The Journal of neuroscience : the official journal of the Society for Neuroscience *29*, 3852-3864.

El Mestikawy, S., Wallén-Mackenzie, A., Fortin, G.M., Descarries, L., and Trudeau, L.E. (2011). From glutamate co-release to vesicular synergy: vesicular glutamate transporters. . Nature reviews Neuroscience *12*, 204-216.

El-oteify, M., and Mubarak, W. (2011). Sensory nerve endings in the human female umbilical skin: light and electron microscopic study. The Egyptian Journal of Histology *34*, 57-68.

Ernfors, P., Kucera, J., Lee, K.F., Loring, J., and Jaenisch, R. (1995). Studies on the physiological role of brain-derived neurotrophic factor and neurotrophin-3 in knockout mice. The International journal of developmental biology *39*, 799-807.

Ernfors, P., Lee, K.F., Kucera, J., and Jaenisch, R. (1994). Lack of neurotrophin-3 leads to deficiencies in the peripheral nervous system and loss of limb proprioceptive afferents. Cell *77*, 503-512.

Fitzgerald, M. (2005). The development of nociceptive circuits. . Nature reviews Neuroscience *6*, 507-520.

Gascon, E., Gaillard, S., Malapert, P., Liu, Y., Rodat-Despoix, L., Samokhvalov, I.M., Delmas, P., Helmbacher, F., Maina, F., and Moqrich, A. (2010). Hepatocyte Growth Factor-Met Signaling Is Required for Runx1 Extinction and Peptidergic Differentiation in Primary Nociceptive Neurons. Journal of Neuroscience *30*, 12424-12423.

Geffeney, S.L., and Goodman, M.B. (2012). How We Feel: Ion Channel Partnerships that Detect Mechanical Inputs and Give Rise to Touch and Pain Perception. . Neuron *74*, 609-619.

Ginty, D. (2002). Retrograde neurotrophin signaling: Trk-ing along the axon. Current Opinion in Neurobiology *12*, 268-274.

Gonzalez-Martinez, T., Farinas, I., Del Valle, M.E., Feito, J., Germana, G., Cobo, J., and Vega, J.A. (2005). BDNF, but not NT-4, is necessary for normal development of Meissner corpuscles. Neurosci Lett *377*, 12-15.

Gonzalez-Martinez, T., Germana, G.P., Monjil, D.F., Silos-Santiago, I., de Carlos, F., Germana, G., Cobo, J., and Vega, J.A. (2004). Absence of Meissner corpuscles in the digital pads of mice lacking functional TrkB. Brain Res *1002*, 120-128.

Growney, J. (2005). Loss of Runx1 perturbs adult hematopoiesis and is associated with a myeloproliferative phenotype. Blood *106*, 494-504.

Gu, C., Rodriguez, E.R., Reimert, D.V., Shu, T., Fritzsch, B., Richards, L.J., Kolodkin, A.L., and Ginty, D.D. (2003). Neuropilin-1 conveys semaphorin and VEGF signaling during neural and cardiovascular development. Dev Cell *5*, 45-57.

Guillemot, F., Lo, L.C., Johnson, J.E., Auerbach, A., Anderson, D.J., and Joyner, A.L. (1993). Mammalian achaete-scute homolog 1 is required for the early development of olfactory and autonomic neurons. Cell *75*, 463-476.

Haeberle, H., and Lumpkin, E.A. (2004). Molecular profiling reveals synaptic release machinery in Merkel cells. PNAS *101*, 14503.

Hamalainen, H.A., Warren, S., and Gardner, E.P. (1985). Differential sensitivity to airpuffs on human hairy and glabrous skin. Somatosensory research *2*, 281-302.

Han, L., Ma, C., Liu, Q., Weng, H., Cui, Y., Tang, Z., Kim, Y., Nie, H., Qu, L., Patel, K., *et al*. (2012). A subpopulation of nociceptors specifically linked to itch. Nature Neuroscience, 1-11.

Han, S., Dong, X., Hwang, J., Zylka, M., Anderson, D., and Simon, M.I. (2002). Orphan G protein-coupled receptors MrgA1 and MrgC11 are distinctively activated by RF-amide- related peptides through the Gaq/11 pathway. PNAS *99*, 14740.

Hao, J., and Delmas, P. (2011). Recording of mechanosensitive currents using piezoelectrically driven mechanostimulator. Nature Protocols *6*, 979-989.

Hao, J., Padilla, F., Dandonneau, M., Lavebratt, C., Lesage, F., Noël, J., and Delmas, P. (2013). Kv1.1 Channels Act as Mechanical Brake in the Senses of Touch and Pain. Neuron *77*, 899-914.

Hargreaves, K., Dubner, R., Brown, F., Flores, C., and Joris, J. (1988). A new and sensitive method for measuring thermal nociception in cutaneous hyperalgesia. PAIN *32*, 77-88.

Hesse, E., Saito, H., Kiviranta, R., Correa, D., Yamana, K., Neff, L., Toben, D., Duda, G., Atfi, A., Geoffroy, V., *et al*. (2010). Zfp521 controls bone mass by HDAC3-dependent attenuation of Runx2 activity. The Journal of cell biology *191*, 1271-1283.

Hippenmeyer, S., Kramer, I., and Arber, S. (2004). Control of neuronal phenotype: what targets tell the cell bodies. Trends in Neuroscience *27*, 482.

Hjerling-Leffler, J., Alqatari, M., Ernfors, P., and Koltzenburg, M. (2007). Emergence of Functional Sensory Subtypes as Defined by Transient Receptor Potential Channel Expression. Journal of Neuroscience *27*, 2435-2443.

Hu, J., and Lewin, G.R. (2006). Mechanosensitive currents in the neurites of cultured mouse sensory neurones. . J Physiol *577*, 815-822.

Hu, J., Huang, T., Li, T., Guo, Z., and L., C. (2012). c-Maf is required for the development of dorsal horn laminae III/IV neurons and mechanoreceptive DRG axon projections. J Neurosci *32*, 5362-5373.

Huang, S.M., Lee, H., Chung, M., Park, U., Yu, Y.Y., Bradshaw, H.B., Coulombe, P.A., Walker, J.M., and Caterina, M.J. (2008). Overexpressed Transient Receptor Potential Vanilloid 3 Ion Channels in Skin Keratinocytes Modulate Pain Sensitivity via Prostaglandin E2. The Journal of Neuroscience *28*, 13727.

Iannetti, G., and Mouraux, A. (2010). From the neuromatrix to the pain matrix (and back). Experimental Brain Research *205*, 1-12.

Iggo, A. (1960). Cutaneous mechanoreceptors with afferent C fibres. The Journal of Physiology *152*, 337-353.

Inoue, K., Ozaki, S., Ito, K., Iseda, T., Kawaguchi, S., Ogawa, M., Bae, S.C., Yamashita, N., Itohara, S., Kudo, N., *et al*. (2003). Runx3 is essential for the target-specific axon pathfinding of trkc-expressing dorsal root ganglion neurons. Blood cells, molecules & diseases *30*, 157-160.

Inoue, K., Ozaki, S., Shiga, T., Ito, K., Masuda, T., Okado, N., Iseda, T., Kawaguchi, S., Ogawa, M., Bae, S.C., *et al*. (2002). Runx3 controls the axonal projection of proprioceptive dorsal root ganglion neurons. Nat Neurosci *5*, 946-954.

Ivanavicius, S., Blake, D., Chessell, I., and Mapp, P. (2004). Isolectin b4 binding neurons are not present in the rat knee joint. Neuroscience *128*, 555.

Jessell, E.R.K.J.H.S.T.M. (2000). Principles of Neuroscience, 4th edn (McGraw-Hill).

Ji, S., and Jaffrey, S.R. (2012). Intra-axonal Translation of SMAD1/5/8 Mediates Retrograde Regulation of Trigeminal Ganglia Subtype Specification. Neuron *74*, 95-107.

Johnson, K.O. (2001). The roles and functions of cutaneous mechanoreceptors. Curr Opin Neurobiol *11*, 455-461.

Jonckers, E., Van Audekerke, J., De Visscher, G., Van Der Linden, A., and Verhoye, M. (2011). Functional Connectivity fMRI of the Rodent Brain: Comparison of Functional Connectivity Networks in Rat and Mouse. PLoS ONE *6*, e18876.

Jones, A. (1998). The pain matrix and neuropathic pain. Brain, 1-2.

Kakuda, N. (1992). Conduction velocity of low-threshold mechanoreceptive afferent fibers in the glabrous and hairy skin of human hands measured with microneurography and spike-triggered averaging. Neuroscience research *15*, 179-188.

Kamiya, D., Banno, S., Sasai, N., Ohgushi, M., Inomata, H., Watanabe, K., Kawada, M., Yakura, R., Kiyonari, H., Nakao, K., *et al*. (2011). Intrinsic transition of embryonic stem-cell differentiation into neural progenitors. Nature *470*, 503-509.

Kandel, E. (2006). Principles of Neural Science. 1-1230.

Kang, L., Gao, J., Schafer, W., Xie, Z., and Xu, X. (2010). C. elegans TRP Family Protein TRP-4 Is a Pore-Forming Subunit of a Native Mechanotransduction Channel. Neuron *67*, 381-391.

Kasemeier-Kulesa, J. (2005). Imaging neural crest cell dynamics during formation of dorsal root ganglia and sympathetic ganglia. Development *132*, 235-245.

Kayser, V., and Guilbaud, G. (1987). Local and remote modifications of nociceptive sensitivity during carrageenin-induced inflammation in the rat. Pain *28*, 99-107.

Kim, S.E., Coste, B., Chadha, A., Cook, B., and Patapoutian, A. (2012). The role of Drosophila Piezo in mechanical nociception. Nature, 1-5.

Knowlton, W.M., Bifolck-Fisher, A., Bautista, D., and McKemy, D.D. (2010). TRPM8, but not TRPA1, is required for neural and behavioral responses to acute noxious cold temperatures and cold-mimetics in vivo. PAIN *150*, 340-350.

Kramer, I., Sigrist, M., Nooij, J., taniuchi, i., Jessell, T.M., and Arber, S. (2006). A Role for Runx Transcription Factor Signaling in Dorsal Root Ganglion Sensory Neuron Diversification. Neuron *49*, 1-15.

Kucera, J., Cooney, W., Que, A., Szeder, V., Stancz-Szeder, H., and Walro, J. (2002). Formation of supernumerary muscle spindles at the expense of Golgi tendon organs in ER81-deficient mice. Developmental dynamics : an official publication of the American Association of Anatomists *223*, 389-401.

Kwan, K.Y., Glazer, J., Corey, D.P., Rice, F., and Stucky, C. (2009). TRPA1 modulates mechanotransduction in cutaneous sensory neurons. Journal of Neuroscience *29*, 4808-4819.

Lallemend, F., and Ernfors, P. (2012). Molecular interactions underlying the specification of sensory neurons. Trends Neurosci *35*, 373-381.

LaMotte, R.H., Shain, C.N., Simone, D.A., and Tsai, E.F. (1991). Neurogenic hyperalgesia: psychophysical studies of underlying mechanisms. J Neurophysiol *66*, 190-211.

Lanier, J., Dykes, I.M., Nissen, S., Eng, S.R., and Turner, E.E. (2009). Brn3a regulates the transition from neurogenesis to terminal differentiation and represses non-neural gene expression in the trigeminal ganglion. Developmental dynamics : an official publication of the American Association of Anatomists *238*, 3065-3079.

Lee, J.H., Durand, R., Gradinaru, V., Zhang, F., Goshen, I., Kim, D., Fenno, L.E., Ramakrishnan, C., and Deisseroth, K. (2010). Global and local fMRI signals driven by neurons defined optogenetically by type and wiring. Nature *465*, 788-792.

Lembo, P., Grazzini, E., Groblewski, T., O'Donnell, D., Roy, M., Zhang, J., Hoffert, C., Cao, J., Schmidt, R., Pelletier, M.*, et al*. (2002). Proenkephalin A gene products activate a new family of sensory neuron–specific GPCRs. Nature Neuroscience *5*, 201-209.

Levanon, D., and Groner, Y. (2002). The Runx3 transcription factor regulates development and survival of TrkC dorsal root ganglia neurons. The EMBO Journal *21*, 3454.

Li, J.L., Ding, Y.Q., Li, Y.Q., Li, J.S., Nomura, S., Kaneko, T., and Mizuno, N. (1998). Immunocytochemical localization of mu-opioid receptor in primary afferent neurons containing substance P or calcitonin gene-related peptide. A light and electron microscope study in the rat. Brain Research *794*, 347-352.

Li, L., Rutlin, M., Abraira, V., Cassidy, C., Kus, L., Gong, S., Jankowski, M., Luo, W., Heintz, N., Koerber, H.*, et al*. (2011). The Functional Organization of Cutaneous Low-Threshold Mechanosensory Neurons. Cell *147*, 1615-1627.

Li, W., Feng, Z., Sternberg, P.W., and Xu, X.Z. (2006). A C. elegans stretch receptor neuron revealed by a mechanosensitive TRP channel homologue. Nature *440*, 684-687.

Liberty K. Hodge, M.P.K., Bao-Xia Han, Glenn Yiu, Joanna Hurrell, Audrey Howell, Guy Rousseau, Frederic Lemaigre, Marc Tessier-Lavigne, Fan Wang (2007). Retrograde BMP Signaling Regulates Trigeminal Sensory Neuron Identities and the Formation of Precise Face Maps. Cell *55*, 572.

Lin, J.H., Saito, T., Anderson, D.J., Lance-Jones, C., Jessell, T.M., and Arber, S. (1998). Functionally related motor neuron pool and muscle sensory afferent subtypes defined by coordinate ETS gene expression. Cell *95*, 393-407.

Liu, P., Jenkins, N.A., and Copeland, N.G. (2003). A Highly Efficient Recombineering-Based Method for Generating Conditional Knockout Mutations. Genome Research *13*, 476-484.

Liu, Q., Sikand, P., Ma, C., Tang, Z., Han, L., Li, Z., Sun, S., LaMotte, R.H., and Dong, X. (2012). Mechanisms of itch evoked by beta-alanine. J Neurosci *32*, 14532-14537.

Liu, Q., Tang, Z., Surdenikova, L., Kim, S., Patel, K.N., Kim, A., Ru, F., Guan, Y., Weng, H., Geng, Y., *et al*. (2009). Sensory Neuron-Specific GPCR Mrgprs Are Itch Receptors Mediating Chloroquine-Induced Pruritus. Cell *139*, 1353-1365.

Liu, Q., Vrontou, S., Rice, F., Zylka, M., Dong, X., and Anderson, D. (2007). Molecular genetic visualization of a rare subset of unmyelinated sensory neurons that may detect gentle touch. Nature Neuroscience *10*, 946-948.

Liu, X., Liu, Z., Sun, Y., Ross, M., Kim, S., Tsai, F., Li, Q., Jeffry, J., Kim, J., Loh, H., *et al*. (2011). Unidirectional Cross-Activation of GRPR by MOR1D Uncouples Itch and Analgesia Induced by Opioids. Cell *147*, 447-458.

Liu, Y., and Ma, Q. (2011). Generation of somatic sensory neuron diversity and implications on sensory coding. Current Opinion in Neurobiology *21*, 52-60.

Liu, Y., Yang, F., Okuda, T., Dong, X., Zylka, M., Chen, C., Anderson, D., Kuner, R., and Ma, Q. (2008). Mechanisms of Compartmentalized Expression of Mrg Class G-Protein-Coupled Sensory Receptors. Journal of Neuroscience *28*, 125-132.

Lo, L., Dormand, E., Greenwood, A., and Anderson, D.J. (2002). Comparison of the generic neuronal differentiation and neuron subtype specification functions of mammalian achaete-scute and atonal homologs in cultured neural progenitor cells. Development *129*, 1553-1567.

Loewenstein, W.R., and Mendelson, M. (1965). COMPONENTS OF RECEPTOR ADAPTATION IN A PACINIAN CORPUSCLE. The Journal of Physiology *177*, 377-397.

Löken, L., Wessberg, J., Morrison, I., McGlone, F., and Olausson, H. (2009). Coding of pleasant touch by unmyelinated afferents in humans. Nature Neuroscience *12*, 547-548.

Lopes, C., Liu, Z., Xu, Y., and Ma, Q. (2012). Tlx3 and Runx1 act in combination to coordinate the development of a cohort of nociceptors, thermoceptors, and pruriceptors. Journal of Neuroscience *32*, 9706-9715.

Lou, S., Duan, B., Vong, L., Lowell, B., and Ma, Q. (2013). Runx1 Controls Terminal Morphology and Mechanosensitivity of VGLUT3-expressing C-Mechanoreceptors. Journal of Neuroscience *33*, 870-882.

Lumpkin, E.A., Marshall, K.L., and Nelson, A.M. (2010). The cell biology of touch. J Cell Biol *191*, 237-248.

Luo, W., Enomoto, H., Rice, F., Milbrandt, J., and Ginty, D.D. (2009). Molecular Identification of Rapidly Adapting Mechanoreceptors and Their Developmental Dependence on Ret Signaling. Neuron *64*, 841-856.

Luo, W., Wickramasinghe, S., Savitt, J., Griffin, J., Dawson, T., and Ginty, D. (2007). A Hierarchical NGF Signaling Cascade Controls Ret-Dependent and Ret-Independent Events during Development of Nonpeptidergic DRG Neurons_supplementary. Neuron *54*, 739-754.

Ma, Q. (2010). Labeled lines meet and talk: population coding of somatic sensations. The Journal of clinical investigation *120*, 3773-3778.

Ma, Q. (2012). Population coding of somatic sensations. Neuroscience bulletin *28*, 91-99.

Ma, Q., Chen, Z., del Barco Barrantes, I., de la Pompa, J.L., and Anderson, D.J. (1998). neurogenin1 is essential for the determination of neuronal precursors for proximal cranial sensory ganglia. Neuron *20*, 469-482.

Ma, Q., Fode, C., Guillemot, F., and Anderson, D.J. (1999). Neurogenin1 and neurogenin2 control two distinct waves of neurogenesis in developing dorsal root ganglia. Genes Dev *13*, 1717-1728.

Ma, Q., Kintner, C., and Anderson, D.J. (1996). Identification of neurogenin, a vertebrate neuronal determination gene. Cell *87*, 43-52.

Mach, D.B., and Mantyh, P.W. (2002). Origins of Skeletal Pain: Sensory and Sympathetic Innervation of the Mouse Femur. neuroscience *113*, 155-166.

Madisen, L., Zwingman, T., Sunkin, S., Oh, S., Zariwala, H., Gu, H., Ng, L., Palmiter, R., Hawrylycz, M., Jones, A., *et al*. (2010). A robust and high-throughput Cre reporting and characterization system for the whole mouse brain. Nature Neuroscience *13*, 133-140.

Maricich, S., Morrison, K., Mathes, E., and Brewer, B. (2012). Rodents Rely on Merkel Cells for Texture Discrimination Tasks. Journal of Neuroscience *32*, 3296-3300.

Maricich, S.M., Wellnitz, S.A., Nelson, A.M., and Zoghbi, H.Y. (2009). Merkel Cells are essential for light touch reponses. Science *324*, 1580.

Marmigère, F., and Ernfors, P. (2007). Specification and connectivity of neuronal subtypes in the sensory lineage. Nature Reviews Neuroscience *8*, 114-127.

Marmigere, F., Montelius, A., Wegner, M., Groner, Y., Reichardt, L.F., and Ernfors, P. (2006). The Runx1/AML1 transcription factor selectively regulates development and survival of TrkA nociceptive sensory neurons. Nat Neurosci *9*, 180-187.

Maro, G.S., Vermeren, M., Voiculescu, O., Melton, L., Cohen, J., Charnay, P., and Topilko, P. (2004). Neural crest boundary cap cells constitute a source of neuronal and glial cells of the PNS. Nat Neurosci *7*, 930-938.

Marqués, G., Haerry, T.E., Crotty, M.L., Xue, M., Zhang, B., and O'Connor, M.B. (2003). Retrograde Gbb signaling through the Bmp type 2 receptor wishful thinking regulates systemic FMRFa expression in Drosophila. Development (Cambridge, England) *130*, 5457-5470.

May, A. (2009). New insights into headache: an update on functional and structural imaging findings. Nature Reviews Neurology *5*, 199-209.

McCarter, G.C., Reichling, D.B., and Levine, J.D. (1999). Mechanical transduction by rat dorsal root ganglion neurons in vitro. Neurosci Lett *273*, 179-182.

McGlone, F., Vallbo, A.B., Olausson, H., Loken, L., and Wessberg, J. (2007). Discriminative touch and emotional touch. Canadian journal of experimental psychology = Revue canadienne de psychologie experimentale *61*, 173-183.

Messersmith, E.K., Leonardo, E.D., Shatz, C.J., Tessier-Lavigne, M., Goodman, C.S., and Kolodkin, A.L. (1995). Semaphorin III can function as a selective chemorepellent to pattern sensory projections in the spinal cord. Neuron *14*, 949-959.

Miguel-Aliaga, I., Allan, D.W., and Thor, S. (2004). Independent roles of the dachshund and eyes absent genes in BMP signaling, axon pathfinding and neuronal specification. Development (Cambridge, England) *131*, 5837-5848.

Mishra, S.K., Tisel, S.M., Orestes, P., Bhangoo, S.K., and Hoon, M.A. (2010). TRPV1-lineage neurons are required for thermal sensation. The EMBO Journal *30*, 582-593.

Molliver, D.C., and Snider, W.D. (1997). IB4-Binding DRG Neurons Switch from NGF to GDNF Dependence in Early Postnatal Life. Neuron *19*, 849-861.

Montelius, A., Marmigere, F., Baudet, C., Aquino, J.B., Enerback, S., and Ernfors, P. (2007). Emergence of the sensory nervous system as defined by Foxs1 expression. Differentiation; research in biological diversity *75*, 404-417.

Moqrich, A., Earley, T.J., Watson, J., Andahazy, M., Backus, C., Martin-Zanca, D., Wright, D.E., Reichardt, L.F., and Patapoutian, A. (2004). Expressing TrkC from the TrkA locus causes a subset of dorsal root ganglia neurons to switch fate. Nat Neurosci *7*, 812-818.

Morrison, I., Loken, L.S., Minde, J., Wessberg, J., Perini, I., Nennesmo, I., and Olausson, H. (2011). Reduced C-afferent fibre density affects perceived pleasantness and empathy for touch. Brain *134*, 1116-1126.

Morrison, K., and Maricich, S. (2009). Mammalian Merkel cells are descended from the epidermal lineage. Dev Biol *336*, 76.

Muraki, K., Iwata, Y., Katanosaka, Y., Ito, T., Ohya, S., Shigekawa, M., and Imaizumi, Y. (2003). TRPV2 is a component of osmotically sensitive cation channels in murine aortic myocytes. Circulation research *93*, 829-838.

Nassar, M.A., and Wood, J.N. (2004). Nociceptor-specific gene deletion reveals a major role for Nav1.7 (PN1) in acute and inflammatory pain. PNAS *101*, 12706.

Noh, J., Seal, R.P., Garver, J.A., Edwards, R.H., and Kandler, K. (2010). Glutamate co-release at GABA/glycinergic synapses is crucial for the refinement of an inhibitory map. Nature Neuroscience *13*, 232.

Nolte, J. (2002). The Human Brain: An introduction to its functional anatomy, 5th edn (Mosby Inc.).

Nunzi, M.G., Pisarek, A., and Mugnaini, E. (2004). Merkel cells, corpuscular nerve endings and free nerve endings in the mouse palatine mucosa express three subtypes of vesicular glutamate transporters. Journal of neurocytology *33*, 359-376.

O'Hagan, R., Chalfie, M., and Goodman, M.B. (2005). The MEC-4 DEG/ENaC channel of Caenorhabditis elegans touch receptor neurons transduces mechanical signals. Nat Neurosci *8*, 43-50.

Olausson, H., Cole, J., Rylander, K., McGlone, F., Lamarre, Y., Wallin, B.G., Kramer, H., Wessberg, J., Elam, M., Bushnell, M.C., *et al*. (2008). Functional role of unmyelinated tactile afferents in human hairy skin: sympathetic response and perceptual localization. Experimental brain research Experimentelle Hirnforschung Experimentation cerebrale *184*, 135-140.

Olausson, H., Lamarre, Y., Backlund, H., Morin, C., Wallin, B., Starck, G., Ekholm, S., Strigo, I., Worsley, K., Vallbo, Å., *et al*. (2002). Unmyelinated tactile afferents signal touch and project to insular cortex. Nature Neuroscience *5*, 900-904.

Olausson, H., Wessberg, J., Morrison, I., McGlone, F., and Vallbo, A. (2010). The neurophysiology of unmyelinated tactile afferents. Neurosci Biobehav Rev *34*, 185-191.

Parisi, I., and Collinson, J.M. (2012). Regulation of Merkel cell development by Pax6. The International journal of developmental ….

Patel, T.D., Kramer, I., Kucera, J., Niederkofler, V., Jessell, T.M., Arber, S., and Snider, W.D. (2003). Peripheral NT3 signaling is required for ETS protein expression and central patterning of proprioceptive sensory afferents. Neuron *38*, 403-416.

Pattyn, A., Morin, X., Cremer, H., Goridis, C., and Brunet, J.F. (1999). The homeobox gene Phox2b is essential for the development of autonomic neural crest derivatives. Nature *399*, 366-370.

Pautler, R. (2004). Mouse MRI: Concepts and Applications in Physiology. Physiology *19*, 168-175.

Perez, S.E., Rebelo, S., and Anderson, D.J. (1999). Early specification of sensory neuron fate revealed by expression and function of neurogenins in the chick embryo. Development *126*, 1715-1728.

Perez-Pinera, P., Garcia-Suarez, O., Germana, A., Diaz-Esnal, B., de Carlos, F., Silos-Santiago, I., del Valle, M.E., Cobo, J., and Vega, J.A. (2008). Characterization of sensory deficits in TrkB knockout mice. Neurosci Lett *433*, 43-47.

Perrin, F.E., Rathjen, F.G., and Stoeckli, E.T. (2001). Distinct subpopulations of sensory afferents require F11 or axonin-1 for growth to their target layers within the spinal cord of the chick. Neuron *30*, 707-723.

Pezet, S., and McMahon, S. (2006). NEUROTROPHINS: Mediators and Modulators of Pain. Annu Rev Neurosci *29*, 507.

Philips, H., and Armanini, M.P. (2008). Expression of the trk Family of Neurotrophic receptors in developing and adult dorsal root ganglion neurons. Phil Trans R Soc Lond B *351*, 413.

Postigo, A. (2002). Distinct requirements for TrkB and TrkC signaling in target innervation by sensory neurons. Genes & Development *16*, 633-645.

Price, M.P., McIlwrath, S.L., Xie, J., Cheng, C., Qiao, J., Tarr, D.E., Sluka, K.A., Brennan, T.J., Lewin, G.R., and Welsh, M.J. (2001). The DRASIC cation channel contributes to the detection of cutaneous touch and acid stimuli in mice. Neuron *32*, 1071-1083.

Quick, K., Zhao, J., Eijkelkamp, N., Linley, J.E., Rugiero, F., Cox, J.J., Raouf, R., Gringhuis, M., Sexton, J.E., Abramowitz, J., *et al*. (2012). TRPC3 and TRPC6 are essential for normal mechanotransduction in subsets of sensory neurons and cochlear hair cells. Open Biology *2*, 120068.

Rahman, F., Harada, F., Saito, I., Suzuki, A., and Kawano…, Y. (2011). Detection of acid-sensing ion channel 3 (ASIC3) in periodontal Ruffini endings of mouse incisors. Neuroscience ….

Rainville, P., Duncan, G.H., Price, D.D., Carrier, B., and Bushnell, M.C. (1997). Pain Affect Encoded in Human Anterior Cingulate But Not Somatosensory Cortex. Science *277*, 968-971.

Rice, F.L., Albers, K.M., Davis, B.M., Silos-Santiago, I., Wilkinson, G.A., LeMaster, A.M., Ernfors, P., Smeyne, R.J., Aldskogius, H., Phillips, H.S., *et al*. (1998). Differential dependency of unmyelinated and A delta epidermal and upper dermal innervation on neurotrophins, trk receptors, and p75LNGFR. Developmental biology *198*, 57-81.

Ridley, A. (1969). Silver staining of nerve endings in human digital glabrous skin. J Anat *104*, 41.

Samad, O.A., Liu, Y., Yang, F., Kramer, I., Arber, S., and Ma, Q. (2010). Characterization of two Runx1-dependent nociceptor differentiation programs necessary for inflammatory versus neuropathic pain. Molecular Pain, 1-12.

Schlake, T. (2007). Determination of hair structure and shape. Seminars in cell & developmental biology.

Schneider, C., Wicht, H., Enderich, J., Wegner, M., and Rohrer, H. (1999). Bone morphogenetic proteins are required in vivo for the generation of sympathetic neurons. Neuron *24*, 861-870.

Scott, A., Hasegawa, H., Sakurai, K., Yaron, A., Cobb, J., and Wang, F. (2011). Transcription Factor Short Stature Homeobox 2 Is Required for Proper Development of Tropomyosin-Related Kinase B-Expressing Mechanosensory Neurons. Journal of Neuroscience *31*, 6741-6749.

Seal, R.P., Wang, X., Guan, Y., Raja, S.N., Woodbury, C.J., Basbaum, A.I., and Edwards, R.H. (2009). Injury-induced mechanical hypersensitivity requires C-low threshold mechanoreceptors. Nature, 1-5.

Sedý, J., Tseng, S., Walro, J.M., Grim, M., and Kucera, J. (2006). ETS transcription factor ER81 is required for the Pacinian corpuscle development. Developmental dynamics : an official publication of the American Association of Anatomists *235*, 1081-1089.

Senzaki K, O.S., Yoshikawa M, Ito Y, Shiga T. (2010). Runx3 is required for the specification of TrkC-expressing mechanoreceptive trigeminal ganglion neurons. Mol Cell Neurosci *43*, 296-307.

Serbedzija, G.N., and Bronner-Fraser, M. (2005). Pathways of trunk neural crest cell migration in the mouse embryo as revealed by vital dye labelling. Development *108*, 605-612.

Seriwatanachai, D., Densmore, M.J., Sato, T., Correa, D., Neff, L., Baron, R., and Lanske, B. (2011). Deletion of Zfp521 rescues the growth plate phenotype in a mouse model of Jansen metaphyseal chondrodysplasia. FASEB journal : official publication of the Federation of American Societies for Experimental Biology *25*, 3057-3067.

Shen, S., Pu, J., Lang, B., and McCaig, C.D. (2011). A zinc finger protein Zfp521 directs neural differentiation and beyond. Stem cell research & therapy *2*, 20.

Shields, S.D., Ahn, H., Yang, Y., Han, C., Seal, R.P., Wood, J.N., Waxman, S.G., and Dib-Hajj, S.D. (2012). Nav1.8 expression is not restricted to nociceptors in mouse peripheral nervous system. PAIN *153*, 2017-2030.

Shields, S.D., Ahn, H.S., Yang, Y., Han, C., Seal, R.P., Wood, J.N., Waxman, S.G., and Dib-Hajj, S.D. (2012). Na(v)1.8 expression is not restricted to nociceptors in mouse peripheral nervous system. . Pain *153*, 2017-2030.

Shinohara, T. (2004). Identification of a G Protein-coupled Receptor Specifically Responsive to -Alanine. Journal of Biological Chemistry *279*, 23559-23564.

Smith, E.S., and Lewin, G.R. (2009). Nociceptors: a phylogenetic view. Journal of comparative physiology A, Neuroethology, sensory, neural, and behavioral physiology *195*, 1089-1106.

Smith, R.J., Shearer, A.E., Hildebrand, M.S., and Camp, G.V. (1993). Deafness and Hereditary Hearing Loss Overview. Gene Reviews.

Snider, W.D., and McMahon, S.B. (1998). Tackling Pain at the Source: New Ideas about Nociceptors. Neuron *20*, 629-632.

Spiegel I, A.K., Eshed Y, Milo R, Sabanay H, Sarig-Nadir O, Horresh I, Scherer SS, Rasband MN, Peles E. (2007). A central role for Necl4 (SynCAM4) in Schwann cell-axon interaction and myelination. Nat Neurosci *10*, 861.

Stanke, M., Junghans, D., Geissen, M., Goridis, C., Ernsberger, U., and Rohrer, H. (1999). The Phox2 homeodomain proteins are sufficient to promote the development of sympathetic neurons. Development *126*, 4087-4094.

Stoleru, S., Gregoire, M., Gerard, D., Decety, J., Lafarge, E., Cinotti, L., Lavenne, F., Bars, D.L., Vernet-Maury, E., Rada, H., *et al*. (2000). Neuroanatomical Correlates of Visually Evoked Sexual Arousal in Human Males. Archives of Sexual Behavior *28*, 1-21.

Story, G.M., and Patapoutian, A. (2003). ANKTM1, a TRP-like Channel Expressed in Nociceptive Neuron, is activated by Cold Temperatures. Cell *112*, 819-829.

Sukharev, S.I., Blount, P., Martinac, B., Blattner, F.R., and Kung, C. (1994). A large-conductance mechanosensitive channel in E. coli encoded by mscL alone. Nature *368*, 265-268.

Sun, Y., Dykes, I.M., Liang, X., Eng, S.R., Evans, S.M., and Turner, E.E. (2008). A central role for Islet1 in sensory neuron development linking sensory and spinal gene regulatory programs. Nat Neurosci *11*, 1283-1293.

Suzuki, M., Watanabe, Y., Oyama, Y., and Mizuno…, A. (2003). Localization of mechanosensitive channel TRPV4 in mouse skin. Neuroscience ….

Takahashi-Iwanaga, H., and Shimoda, H. (2004). The three-dimensional microanatomy of Meissner corpuscles in monkey palmar skin. Journal of neurocytology *32*, 363.

Takatoh, J., and Wang, F. (2012). Axonally translated SMADs link up BDNF and retrograde BMP signaling. Neuron *74*, 3-5.

Talbot, J.D., Marrett, S., Evans, A.C., Meyer, E., Bushnell, M.C., and Duncan, G.H. (2008). Multiple Representations of Pain in Human Cerebral Cortex. Science *251*, 1355-1358.

Toledo-Aral, J.J., Moss, B.L., He, Z.J., Koszowski, A.G., Whisenand, T., Levinson, S.R., Wolf, J.J., Silos-Santiago, I., Halegoua, S., and Mandel, G. (1997). Identification of PN1, a predominant voltage-dependent sodium channel expressed principally in peripheral neurons. Proceedings of the National Academy of Sciences of the United States of America *94*, 1527-1532.

Tominaga, M., Caterina, M.J., Malmberg, A.B., Rosen, T.A., Gilbert, H., Skinner, K., Raumann, B.E., Basbaum, A.I., and Julius, D. (1998). The cloned capsaicin receptor integrates multiple pain-producing stimuli. Neuron *21*, 531-543.

Torebjörk, H.E., Lundberg, L.E., and LaMotte, R.H. (1992). Central changes in processing of mechanoreceptive input in capsaicin-induced secondary hyperalgesia in humans. J Physiol *448*, 765-780.

Tzschentke, T.M. (2007). Measuring reward with the conditioned place preference (CPP) paradigm: update of the last decade. Addiction biology *12*, 227-462.

Vallbo, A., Olausson, H., Wessberg, J., and Norrsell, U. (1993). A system of unmyelinated afferents for innocuous mechanoreception in the human skin. Brain Res *628*, 301-304.

Vallbo, A.B., and Kakuda, N. (2005). Receptive field characteristics of tactile units with myelinated afferents in hairy skin of human subjects. Journal of Physiology *483*, 783.

Vallbo, A.B., Olausson, H., and Wessberg, J. (1999). Unmyelinated afferents constitute a second system coding tactile stimuli of the human hairy skin. J Neurophysiol *81*, 2753-2763.

Vallbo, A.B., Olausson, H., Wessberg, J., and Kakuda, N. (1995). Receptive field characteristics of tactile units with myelinated afferents in hairy skin of human subjects. J Physiol *483 (Pt 3)*, 783-795.

Vallbo, V.B., and Wessberg, J. (1999). Unmyelinaed Afferents Constitute a Second System coding tactile stimuli of the human Hairy skin. J Neurophysiol *81*, 2753.

Verrillo, R.T., and Bolanowski, S.J., Jr. (1986). The effects of skin temperature on the psychophysical responses to vibration on glabrous and hairy skin. The Journal of the Acoustical Society of America *80*, 528-532.

Vielkind, U., Sebzda, M., and Hardy, M. (2010). Dynamics of merkel cell patterns in developing hair follicles in the dorsal skin of mice, demonstrated by a monoclonal antibody to mouse keratin 8. Acta Anat *152*, 93-109.

Vilceanu, D., and Stucky, C. (2010). TRPA1 Mediates Mechanical Currents in the Plasma Membrane of Mouse Sensory Neurons. PLoS ONE *5*, e12177.

Vrontou, S., Wong, A.M., Rau, K.K., Koerber, H.R., and Anderson, D. (2013). Genetic identification of C fibres that detect massage-like stroking of hairy skin in vivo. Nature *493*, 669-673.

Waldmann, R., Bassilana, F., de Weille, J., Champigny, G., Heurteaux, C., and Lazdunski, M. (1997a). Molecular cloning of a non-inactivating proton-gated Na+ channel specific for sensory neurons. The Journal of Biological Chemistry *272*, 20975-20978.

Waldmann, R., Champigny, G., Bassilana, F., Heurteaux, C., and Lazdunski, M. (1997b). A proton-gated cation channel involved in acid-sensing. Nature *386*, 173-177.

Waldmann, R., and Lazdunski, M. (1998). H(+)-gated cation channels: neuronal acid sensors in the NaC/DEG family of ion channels. Current Opinion in Neurobiology *8*, 418-424.

Walker, R.G., Willingham, A.T., and Zuker, C.S. (2000). A Drosophila mechanosensory transduction channel. Science *287*, 2229-2234.

Wang, H., and Zylka, M. (2009). Mrgprd-Expressing Polymodal Nociceptive Neurons Innervate Most Known Classes of Substantia Gelatinosa Neurons. Journal of Neuroscience *29*, 13202-13209.

Wende, H., Lechner, S.G., Cheret, C., Bourane, S., Kolanczyk, M.E., Pattyn, A., Reuter, K., Munier, F.L., Carroll, P., Lewin, G.R., *et al*. (2012). The Transcription Factor c-Maf Controls Touch Receptor Development and Function. Science *335*, 1373.

Wessberg, J., Olausson, H., Fernstrom, K.W., and Vallbo, A.B. (2003). Receptive field properties of unmyelinated tactile afferents in the human skin. J Neurophysiol *89*, 1567-1575.

Westling, G., and Johansson, R.S. (1987). Responses in glabrous skin mechanoreceptors during precision grip in humans. Experimental brain research Experimentelle Hirnforschung Experimentation cerebrale *66*, 128-140.

Wilson, S.R., Gerhold, K.A., Bifolck-Fisher, A., Liu, Q., Patel, K.N., Dong, X., and Bautista, D. (2011). TRPA1 is required for histamine-independent, Mas-related G protein-coupled receptor-mediated itch_supplement. Nature Neuroscience *14*, 595-602.

Wu, M., Hesse, E., Morvan, F., Zhang, J.P., Correa, D., Rowe, G.C., Kiviranta, R., Neff, L., Philbrick, W.M., Horne, W.C., *et al*. (2009). Zfp521 antagonizes Runx2, delays osteoblast differentiation in vitro, and promotes bone formation in vivo. Bone *44*, 528-536.

Wysolmerski, J., Broadus, A., Zhou, J., Fuchs, E., Milstone, L., and Philbrick, W. (1994). Overexpression of parathyroid hormone-related protein in the skin of transgenic mice interferes with hair follicle development. Proceedings of the National Academy of Sciences *91*, 1133-1137.

Yan, Z., Zhang, W., He, Y., Gorczyca, D., Xiang, Y., Cheng, L.E., Meltzer, S., Jan, L.Y., and Jan, Y.N. (2012). Drosophila NOMPC is a mechanotransduction channel subunit for gentle-touch sensation. Nature, 1-5.

Yang, Y., Wang, Y., Li, S., Xu, Z., Li, H., Ma, L., Fan, J., Bu, D., Liu, B., Fan, Z., *et al*. (2004). Mutations in SCN9A, encoding a sodium channel alpha subunit, in patients with primary erythermalgia. Journal of medical genetics *41*, 171-174.

Yoshikawa, M., Senzaki, K., Yokomizo, T., Takahashi, S., Ozaki, S., and Shiga, T. (2007). Runx1 selectively regulates cell fate specification and axonal projections of dorsal root ganglion neurons. Dev Biol *303*, 663-674.

Zagami, C.J., and Stifani, S. (2010). Molecular characterization of the mouse superior lateral parabrachial nucleus through expression of the transcription factor Runx1. PLoS One *5*, e13944.

Zelená, J. (1976). The role of sensory innervation in the development of mechanoreceptors. Progress in brain research *43*, 59-64.

Zhong, L., Hwang, R.Y., and Tracey, W.D. (2010). Pickpocket is a DEG/ENaC protein required for mechanical nociception in Drosophila larvae. Current biology : CB *20*, 429-434.

Zimmermann, K., Leffler, A., Babes, A., Cendan, C., Carr, R., Kobayashi, J., Nau, C., Wood, J., and Reeh, P. (2007). Sensory neuron sodium channel Nav1.8 is essential for pain at low temperatures. Nature *447*, 856-859.

Zirlinger, M., Lo, L., McMahon, J., McMahon, A.P., and Anderson, D.J. (2002). Transient expression of the bHLH factor neurogenin-2 marks a subpopulation of neural crest cells biased for a sensory but not a neuronal fate. Proc Natl Acad Sci U S A *99*, 8084-8089.

Zotterman, Y. (1939). Touch, pain and tickling: an electro-physiological investigation on cutaneous sensory nerves. The Journal of Physiology *95*, 1-28.

Zylka, M.J., and Anderson, D.J. (2003). Atypical Expansion in Mice of the sensory neuron-specific Mrg G protein-coupled receptor family. PNAS *100*, 10043.

Zylka, M.J., and Anderson, D.J. (2004). Topographically Distinct Epidermal Nociceptive Circuits Revealed by Axonal Tracer Targeted to Mrgprd. Neuron *45*, 17-25.

Zylka, M.J., Rice, F., and Anderson, D.J. (2005). Topographically Distinct Epidermal Nociceptive Circuits Revealed by Axonal Tracers Targeted to Mrgprd. Neuron *45*, 17-25.